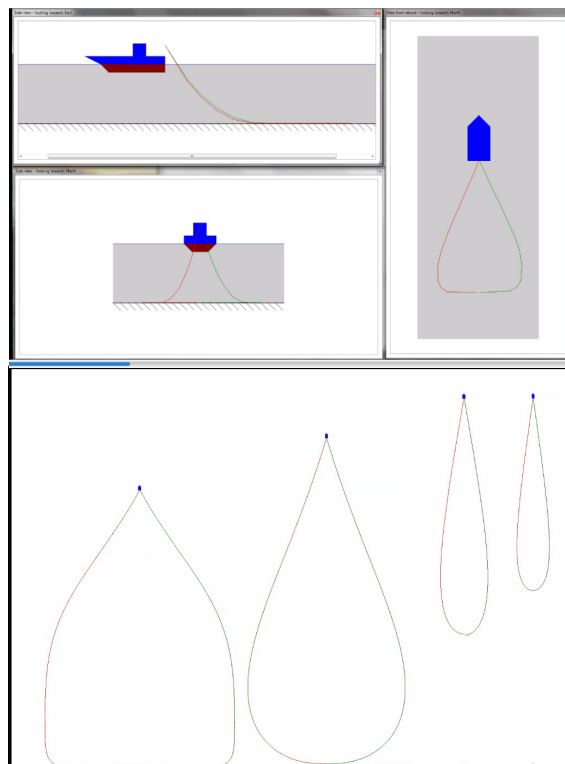


# Report

## Simulation of Seine Rope Behaviour: Model, Software Tools and Validation

### Author(s)

Nina A. H. Madsen  
Karl Gunnar Aarsæther  
Bent Herrmann



# Report

## Simulation of Seine Rope Behaviour: Model, Software Tools and Validation

**KEYWORDS:**Demersal seining  
Simulation  
Software tools  
Seine ropes  
Model validation**VERSION**

1.0

**DATE**

2015-08-12

**AUTHOR(S)**Nina A. H. Madsen  
Karl Gunnar Aarsæther  
Bent Herrmann**CLIENT(S)**

RCN / FHF

**CLIENT'S REF.**

225193 (MAROFF-2) / 900861 (FHF)

**PROJECT NO.**

6020699 (SFH)

**NUMBER OF PAGES/APPENDICES:**

75 + Appendices

**ABSTRACT**

Demersal Seining is an active fishing method applying two seine ropes and a seine net. The seine ropes and net are laid out on the fishing ground in a way that they encircle an aggregation of fish. During the fishing operation, the fish is gradually herded by the seine ropes into the path of the net. Knowledge about how the size and shape of the area encircled by the seine ropes gradually change during the fishing process is important for an efficient fishery. The purpose of the project "Danish Seine: Computer based Development and Operation" (MAROFF-2 project no. 225193 / FHF 900861), funded by Research Council of Norway (RCN) and Norwegian Seafood Research Fund (FHF), is to develop software tools to investigate Demersal Seine fishing. An important aspect of the research is to be able to simulate the physical behaviour of the seine ropes during the fishing process. Therefore this report: i) formulates a model for the physical behaviour of seine ropes for demersal seining; ii) describes the implementation of the model into a set of software tools that together enable simulation of seine rope kinematics for demersal fishing operations; iii) validates predictions made using the simulation toolbox against flume tank experiments.

**PREPARED BY**

Nina A. H. Madsen

**SIGNATURE****CHECKED BY**

Manu Sistiaga

**SIGNATURE****APPROVED BY**

Hanne Digre

**SIGNATURE****REPORT NO.**

A27110

**ISBN**

978-82-14-05887-1

**CLASSIFICATION**

Unrestricted

**CLASSIFICATION THIS PAGE**

Unrestricted

# Document history

---

VERSION	DATE	VERSION DESCRIPTION
1.0	2015-08-12	

# Table of contents

<b>1</b>	<b>Introduction .....</b>	<b>5</b>
1.1	Background and Objectives .....	5
1.2	The Demersal Seine Fishing Process .....	5
<b>2</b>	<b>Model .....</b>	<b>7</b>
2.1	Model Formulation .....	7
2.2	Model Implementation .....	9
<b>3</b>	<b>Software Tools .....</b>	<b>10</b>
3.1	Design Tool.....	10
3.2	Simulation Tool .....	12
3.3	Viewer Tool .....	15
<b>4</b>	<b>The Experimental Data from Flume Tank Tests .....</b>	<b>18</b>
4.1	Winch Speed .....	18
4.2	Layout Patterns .....	18
4.3	Seine Rope Types .....	18
4.4	Clump Weight .....	18
4.5	Summary for Experimental Cases .....	18
<b>5</b>	<b>Validation of Simulation model.....</b>	<b>20</b>
5.1	Square Layout .....	20
5.1.1	Combination Rope; Light; Slow.....	20
5.1.2	Combination Rope; Light; Fast.....	22
5.1.3	Combination Rope; Heavy; Slow .....	24
5.1.4	Combination Rope; Heavy; Fast .....	26
5.1.5	Polyester Rope; Light; Slow .....	28
5.1.6	Polyester Rope; Light; Fast .....	30
5.1.7	Polyester Rope; Heavy; Slow .....	32
5.1.8	Polyester Rope; Heavy; Fast .....	34
5.2	Diamond Layout.....	36
5.2.1	Combination Rope; Light; Slow.....	36
5.2.2	Combination Rope; Light, Fast.....	38
5.2.3	Combination Rope; Heavy; Slow .....	40
5.2.4	Combination Rope; Heavy; Fast .....	42
5.2.5	Polyester Rope; Light; Slow .....	44
5.2.6	Polyester Rope; Light; Fast .....	46

5.2.7	Polyester Rope; Heavy; Slow .....	48
5.2.8	Polyester Rope; Heavy; Fast .....	50
5.3	Triangle Layout.....	52
5.3.1	Combination Rope; Light; Slow.....	52
5.3.2	Combination Rope; Light; Fast.....	54
5.3.3	Combination Rope; Heavy; Slow .....	56
5.3.4	Combination Rope; Heavy; Fast .....	58
5.3.5	Polyester Rope; Light; Slow .....	60
5.3.6	Polyester Rope; Light; Fast .....	62
5.3.7	Polyester Rope; Heavy; Slow .....	64
5.3.8	Polyester Rope; Heavy; Fast .....	66
5.4	Overall Validation of the Simulation Model.....	68
<b>6</b>	<b>Discussion &amp; Conclusions.....</b>	<b>74</b>
<b>7</b>	<b>References .....</b>	<b>75</b>

## 1 Introduction

### 1.1 Background and Objectives

The purpose of the project "Danish Seine: Computer based Development and Operation" (MAROFF-2 project no. 225193 / FHF project no. 900861), funded by Research Council of Norway (RCN) and Norwegian Seafood Research Fund (FHF), is to develop software tools to investigate Demersal Seine fishing. These tools include a model for simulating the physical behaviour of the seine ropes during the fishing process. The specific purposes of this report are to: i) describe a model for the physical behaviour of seine ropes for demersal seining; ii) describe the implementation of the model into a set of software tools that together enable simulation of seine rope kinematics for demersal fishing operations; iii) validate predictions made using the simulation toolbox against flume tank experiments.

### 1.2 The Demersal Seine Fishing Process

Demersal seining is a fishing method commonly applied worldwide to harvest species that live close to the seabed. E.g. in Norwegian fishery; cod is the most important species in the white fish fishery when measured in both tonnes landed and in value [1]. About 20% of the Norwegian cod quota is caught by demersal seining; the Norwegian style fly dragging. Thus, knowledge about the physical behaviour of this type of gear is very relevant. Demersal seining in Norwegian fishery targeting cod and other demersal species is practiced by deploying two long seine ropes connected to the wing tips of the seine net in one end and the winches of the vessel on the other end. The length of the seine ropes is restricted to 2000 m each when fishing inside the four nautical mile limit. The seine ropes, made of up to Ø60 mm combination rope (polyethylene with a steel core) weighting more than 2 kg/m, are placed on the seabed in a quadrilateral pattern in order to encircle the targeted fish [2]. Once the ropes and the net have reached the seabed the vessel starts moving forward at a speed of 1-1.5 knots. As a result of the vessel movement the seine ropes are moving towards each other and herd the fish into the centre of the encircled area; the collecting phase. At some instance the net will start to move along the seabed when pulled by the seine ropes. When the distance between the ropes has decreased to a certain level the rope drums are activated in order to close the wings fast and to force the last fraction of collected fish into the seine net; the closing phase. This fly dragging principle of demersal seining is shown in FIGURE 1.

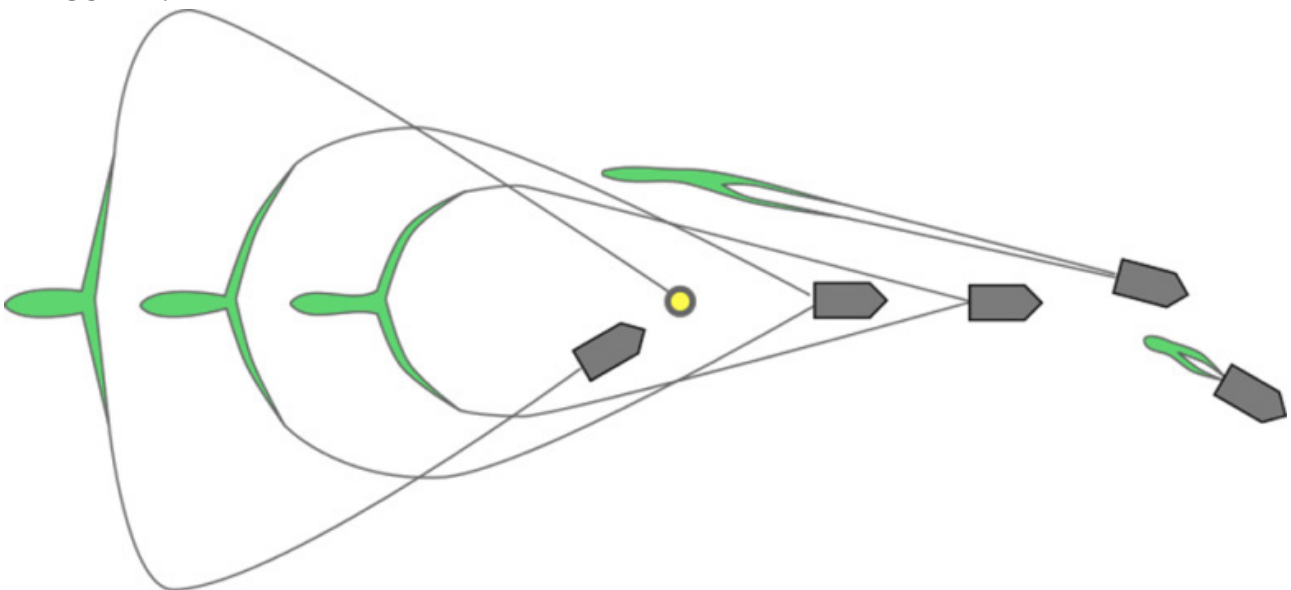


**FIGURE 1: demersal seine fishing process**

Underwater observations [3] have confirmed that fish starts entering the funnel of the net as soon as the seine net is set in motion during the collecting phase. However, the majority of those fish herded by the ropes enter the belly and codend of the seine net in the later stages of the closing phase. The actual fishing time, i.e. the collecting and closing phases, may be as short as 15 minutes. The area on the seabed encircled by the seine ropes is typically much larger than the swept area that will be covered by the seine net during the fishing process. Therefore the catching performance of a demersal seine fishing operation depends to a large extent on the efficiency by which the seine ropes are able to herd the fish into and subsequently maintain them in the path of the net until they are overtaken by it in the later stages of the fishing process. Knowledge about how the size and shape of the area encircled by the seine ropes gradually change during the fishing process is therefore important for an efficient fishery. Thus, being able to model the physical behaviour of the seine ropes is an important aspect of simulating the demersal seine fishing process.

## 2 Model

### 2.1 Model Formulation

The dynamics of the demersal seine gear is dominated by the behaviour of the seine ropes. Hence, the numeric simulation model was developed with two cables modelling the seine ropes, attached to a weight representing the seine net. There are several methods which can be used to represent cable mechanics in simulations such as presented in [4-10]. The demersal seine fishing is of dynamic nature and a time-domain formulation of the cable dynamics was required. The model implements the method found in [9], which contains a model where the cable dynamics are formulated as a collection of hinged rigid bodies.

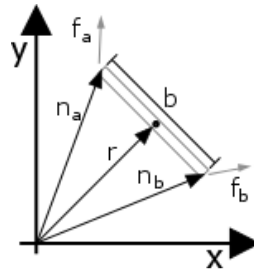


**Figure 2: constraint formulation of rigid body dynamics for a single element**

A single rigid element can be defined by the vectors to the element end points, see Eqn. 1 and FIGURE 2:

$$\mathbf{b} = \mathbf{n}_b - \mathbf{n}_a \quad (1)$$

And the translational dynamics of the element centre follows from Newton's 2<sup>nd</sup> law:

$$\ddot{\mathbf{r}} = \frac{1}{m}(\mathbf{f}_a + \mathbf{f}_b) \quad (2)$$

The rotational dynamics of the element can be expressed in terms of the rotational momentum:

$$\mathbf{h} = \int_V (\mathbf{r}_v \times \dot{\mathbf{r}}_v) \rho dV \quad (3)$$

$$\mathbf{h} = m \mathbf{b} \times \dot{\mathbf{b}} \int_{-\frac{1}{2}}^{\frac{1}{2}} \zeta^2 d\zeta \rightarrow \mathbf{h} = \frac{m}{12} \mathbf{b} \times \dot{\mathbf{b}} \quad (4)$$

$$\dot{\mathbf{h}} = \frac{m}{12} (\dot{\mathbf{b}} \times \dot{\mathbf{b}} + \mathbf{b} \times \ddot{\mathbf{b}}) = \frac{m}{6} \mathbf{b} \times \ddot{\mathbf{b}} = \mathbf{b} \times (\mathbf{f}_b - \mathbf{f}_a) \quad (5)$$

$\mathbf{b} \times \dot{\mathbf{b}}$  is rank deficient and an additional equation is needed in order to fully specify the element dynamics. The additional equation takes the form of a constraint and the resulting set of equations is on the differential algebraic form. The equations can be formulated in the time-domain by double-differentiation, which in turn can be arranged as a set of coupled ordinary differential equations.

$$\mathbf{C}(\mathbf{q}) = 0 \quad (6)$$

$$\dot{\mathbf{C}} = \mathbf{W}(\mathbf{q})\dot{\mathbf{q}} + \dot{\mathbf{W}}(\mathbf{q})\dot{\mathbf{q}} = 0 \quad (7)$$

With the derivative of the constraint equation with respect to the degrees of freedom in the constraint defined as:



$$W(q) = \frac{\partial c}{\partial q} \quad (8)$$

The length of the element can be used as a constraint with  $W(q) = \mathbf{b}^T$ .

$$\mathbf{C}_l = \mathbf{b}^T \mathbf{b} - L^2 = 0 \quad (9)$$

$$\dot{\mathbf{C}}_l = \mathbf{b}^T \dot{\mathbf{b}} - 2L\dot{L} = 0 \quad (10)$$

$$\ddot{\mathbf{C}}_l = \mathbf{b}^T \ddot{\mathbf{b}} + \dot{\mathbf{b}}^T \dot{\mathbf{b}} - 2L\ddot{L} - 2\dot{L}^2 = 0 \quad (11)$$

This gives the following for the rigid element dynamics:

$$\ddot{\mathbf{r}} = \frac{1}{m} (\mathbf{f}_a + \mathbf{f}_b) \quad (12)$$

$$\mathbf{b} \times \ddot{\mathbf{b}} = \frac{6}{m} \mathbf{b} \times (\mathbf{f}_b - \mathbf{f}_a) \quad (13)$$

$$\mathbf{b}^T \ddot{\mathbf{b}} = -\dot{\mathbf{b}}^T \dot{\mathbf{b}} + 2(L\ddot{L} + \dot{L}^2) \quad (14)$$

An advantage of the constraint formulation is that it may be used to formulate structural continuity between a set of rigid bodies. A discretized cable can be constructed by applying a constraint which imposes continuity between the endpoints as seen in FIGURE 3 and Eqn. 15.

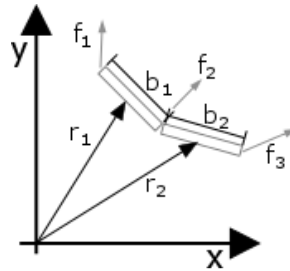


FIGURE 3: constraint for continuity of a hinged structure

$$\mathbf{C}_c = \mathbf{r}_1 + \frac{1}{2} \mathbf{b}_1 + \frac{1}{2} \mathbf{b}_2 - \mathbf{r}_2 = 0 \quad (15)$$

The constraint equation will not be satisfied with two integration steps as time progresses. The error of the constraint equation can be eliminated by introduction of a control law which guarantees global asymptotic stability.

$$\ddot{\mathbf{C}}_l = \mathbf{u}_l \quad (16)$$

$$\mathbf{u}_l = -K_{dL} \dot{\mathbf{C}}_l - K_{pL} \mathbf{C}_l \quad (17)$$

The control law that ensures fulfilment of the constraint equation will introduce properties such as stiffness and damping to the composite structure. The control law is in the form of a linear system, or filter, and the constants can be chosen to represent any material and response dynamics. The frequency response of this system will also determine the response frequencies, or lack thereof, in the structure. A proper choice of parameters allows the formulation to admit low and medium frequency responses while attenuating high frequency oscillations. This is an important property when considering time domain integration schemes where numeric stability is closely related to the step size.

## 2.2 Model Implementation

The previously described model formulation was used to implement the simulation model for the seine ropes behaviour in the FhSim simulation framework [10]. Hence the seine ropes were modelled by cables consisting of a collection of six degree of freedom elements. The cables were connected to the weight at one end, representing the seine net, and to a winch at the other. The cables were initialized by a list of waypoints which specified the cable length between points in space. The rigid body elements were distributed along a catenary curve between these points. The simulation model as implemented in FhSim is seen in FIGURE 4. The orientation of the catenary curve was smoothly rotated from vertical to horizontal near the bottom to avoid initializing cable segments beneath the bottom. The lump weight was modelled as a capsule geometry and initialized at the average end point of the cables.

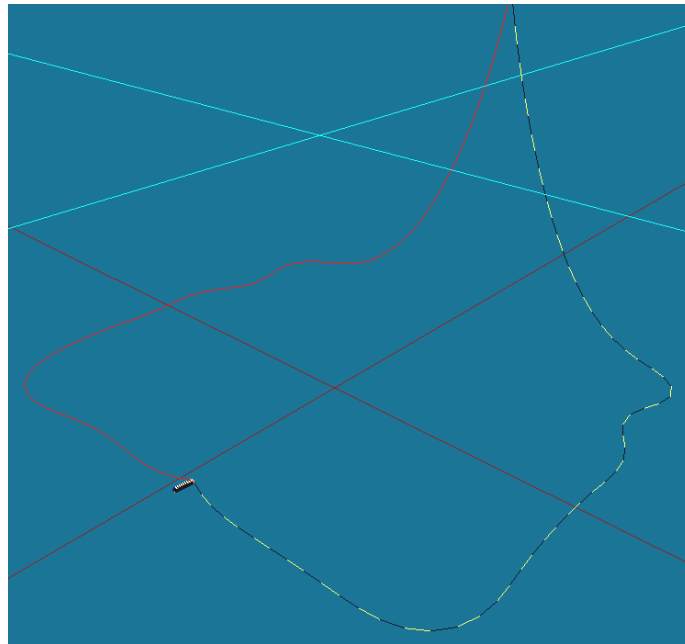


**FIGURE 4: Numerical seine cable model shown in FhSim. The cables are retracted at the top of the image while the weight is seen in the lower left corner.**

The simulation model used an existing bottom contact model from FhSim [10], which calculates a reaction force normal to the bottom from an overlap between element cylinder geometry and the flat bottom surface. The normal force results in a transversal friction force modelled by a friction coefficient with value in the range 0.0 to 1.0. Time integration was performed with a simple forward Euler scheme [11] and a time-step of  $1e-3s$ .

The rigid body implementation of the cable assumes that each element consists of a homogenous and isotropic material. This assumption is violated by the weaved structure of seine ropes, and the large difference between bending and axial stiffness observed was introduced in the model by a scaling of the material stiffness. The effective material stiffness in bending was scaled linearly from the axial stiffness.

### 3 Software Tools

Three software tools that respectively enable defining (Design Tool), simulating (Simulation Tool) and viewing the kinematic behaviour (Viewer Tool) of a demersal seine were implemented. In the current version the focus is on the seine ropes. The three software tools are applied sequentially with using first the Design Tool to define the fishing gear properties (seine rope properties) and initial layout pattern on the fishing ground. The design is visualised as it is created. The developed design is saved in a file on the computer and can later be edited or copied to another new design as needed in the tool. Following a successful design procedure the stored fishing gear design can be loaded into the simulation tool. In the simulation tool a description of the fishing ground, the fishing boat as well as a description of the fishing operation can be created. These descriptions can then be saved individually to files on the computer for easy reuse in different simulated fishing processes. Furthermore, the design of the fishing gear can be stored together with a boat description, a fishing ground description and a fishing operation description together in a single file. This combined description of a complete simulation setup we name the "fishing process". This description of a fishing process is convenient for enabling making multiple simulations with slightly varying simulation parameters based on the same baseline process. Following a successful simulation the results can afterwards be replayed using the Viewer Tool without having to run the simulation. The Viewer Tool enables detailed inspected of the kinematic behaviour of the fishing gear (seine ropes) during the simulated fishing process including automatic extraction of different process indicator values.

#### 3.1 Design Tool

The design tool enables the user to create a simplified design of a Danish seine fishing gear. The design is divided into a net part and a rigging part. The net part specifies the length and height of the belly and of the wings, see FIGURE 5. For the rigging part, see FIGURE 6, the length and diameter of the seine ropes can be specified. Also the density and E Modulus of the seine rope is specifiable. All four parameters of the seine rope can be set individually and independent for the starboard and port side. The design is given a name and is stored in a *danish seine design* '.dsd' file with the same name. The design is editable from within the design tool. As seen in FIGURE 5 the design tool will provide a listing of all *danish seine design* files in the current design folder.

To help the simulation the design tool enables the user to specify a state (layout pattern) for both seine ropes and the simplified seine net. Based on this state information the design tool visualises the seine ropes. The state information is basic information about the initial geometry of the seine. The visualisation is done in three 2D projections, seen from above and seen from the side towards east and north.

For the seine ropes the number of points and their location along the seine rope is also used in the subsequent simulation to define the users request for information about the kinematic behaviour of seine ropes during the fishing process. That is, if the design file has initial state information for ten points along the starboard seine rope and hundred along the port seine rope then simulations with this design will also give a higher resolution on the port seine rope than the starboard seine rope.

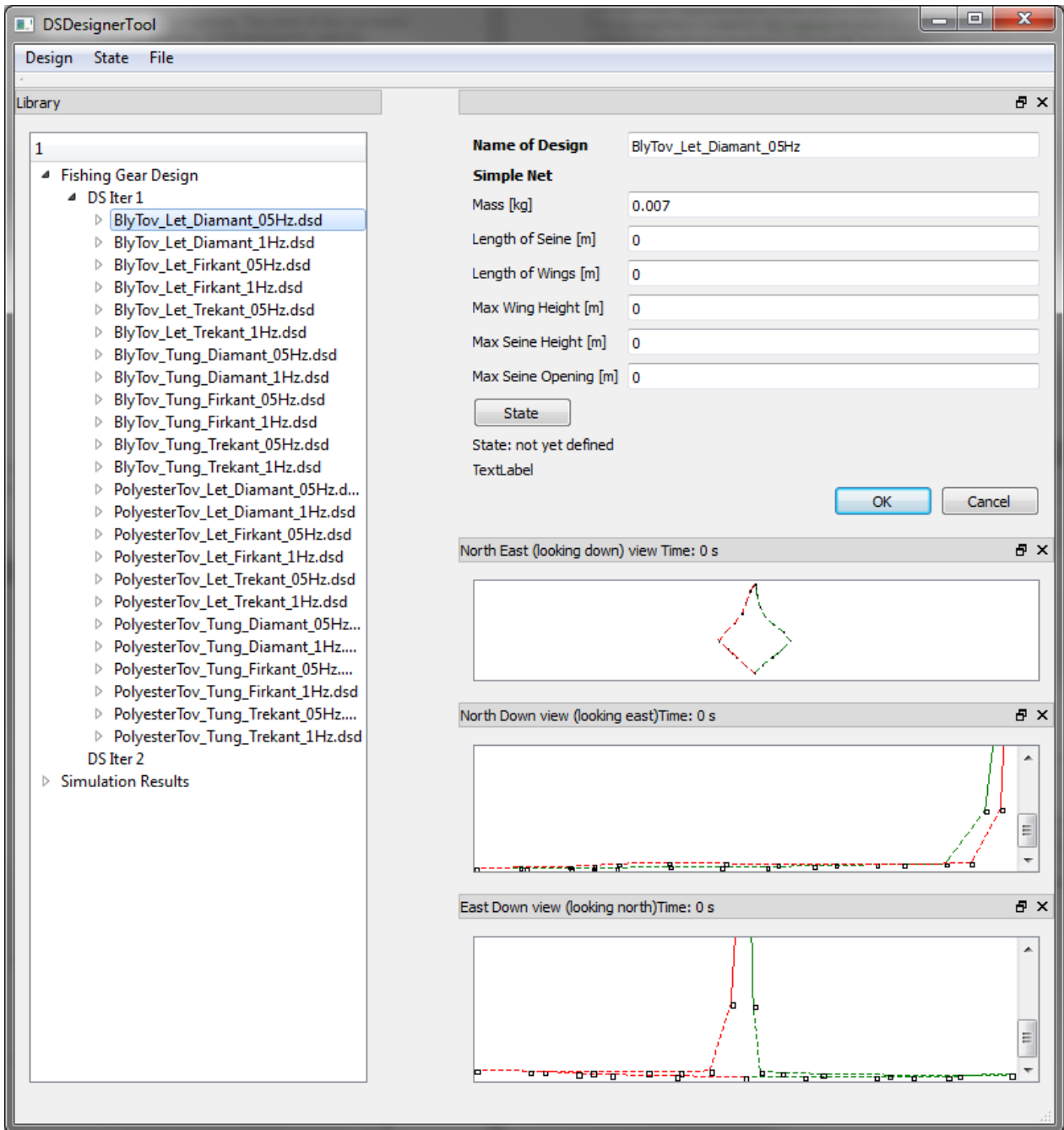


**FIGURE 5: designing a simple net**

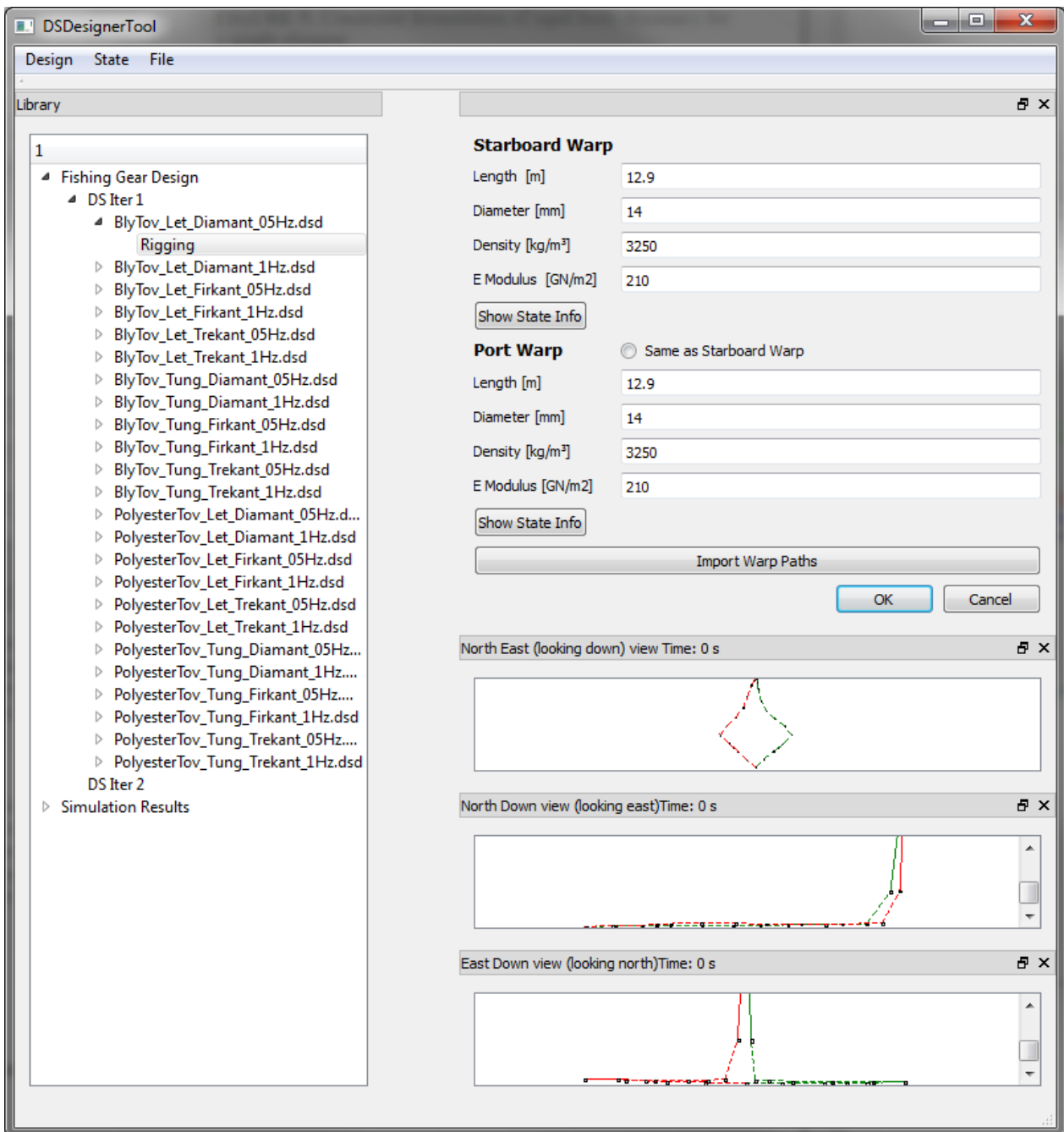


**FIGURE 6: designing the warps.**

### 3.2 Simulation Tool

The simulation tool enables the user to create a fishing process and to simulate it with a given sets of parameters.

The fishing process is defined to consist of a fishing gear design, as specified in the design tool, a fishing ground, a fishing operation procedure and a boat. The latter is only used for visualisation purposes. The fishing process, as well as the fishing ground, fishing operations and the boat can be specified, saved,

and edited in the simulation tool. This way a given fishing operation can be specified once and reused for a number of simulations with e.g. a different fishing gear design. The fishing process once saved to file can be reused for an unlimited number of simulations should the user wish to test the various simulation parameters like e.g. the calculation step of the time step integration.

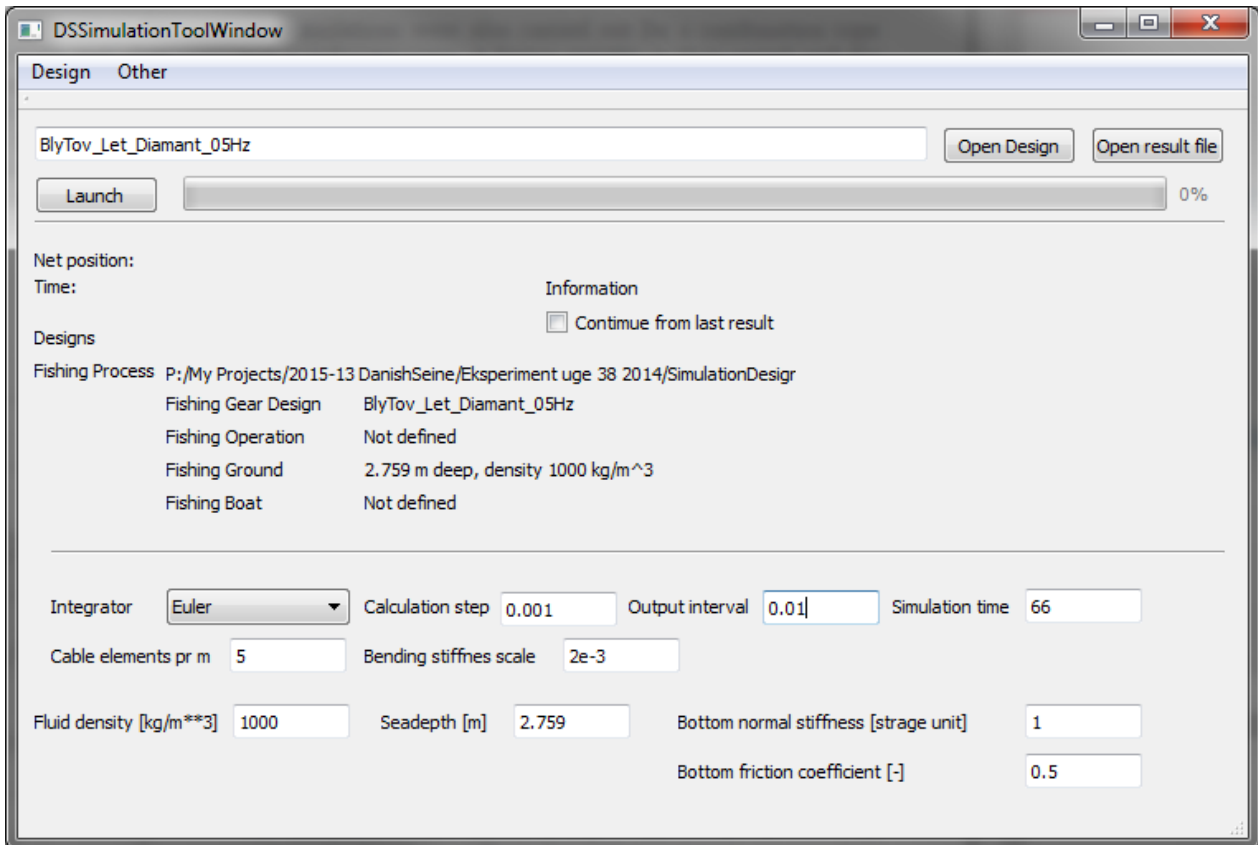


**FIGURE 7: simulation set up with fishing gear, fishing ground and simulation parameters.**

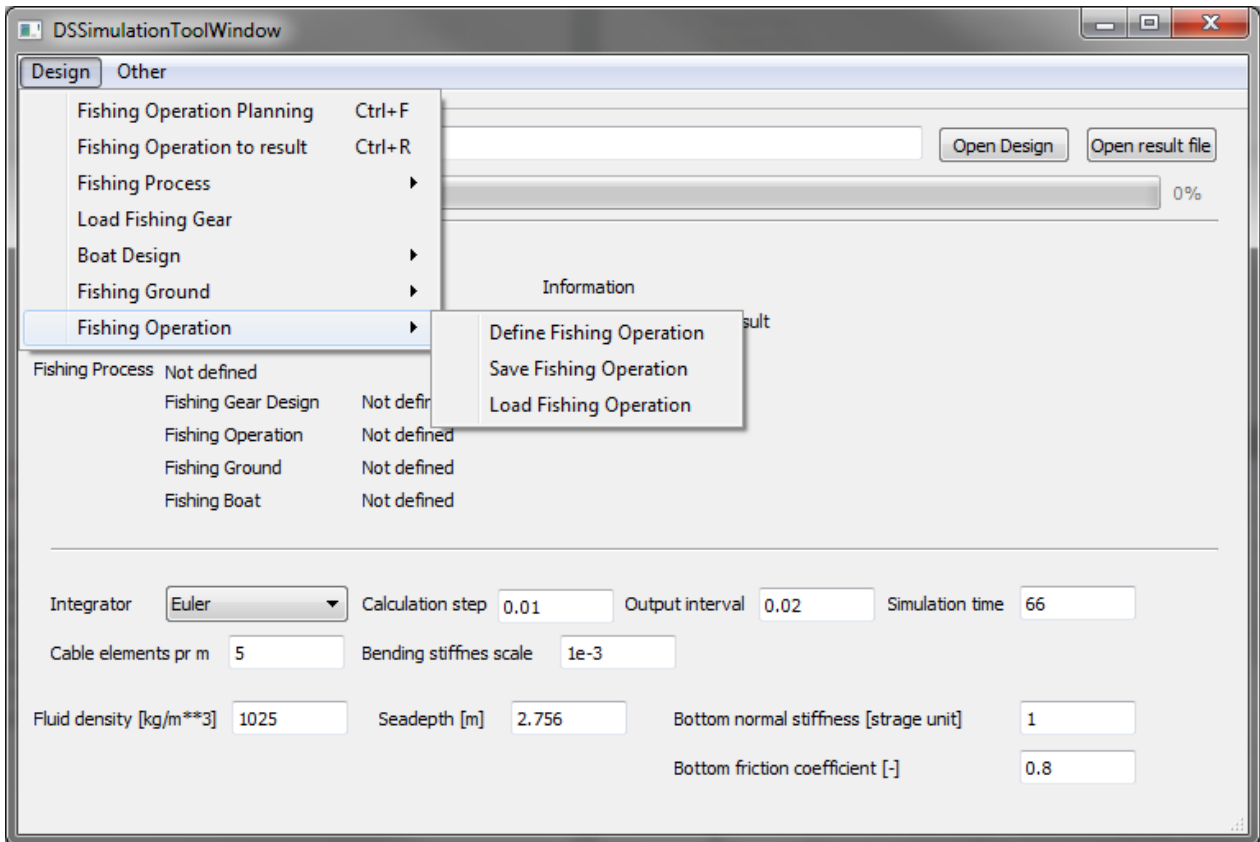


**FIGURE 8: the menu used to define save and load the various parameters**

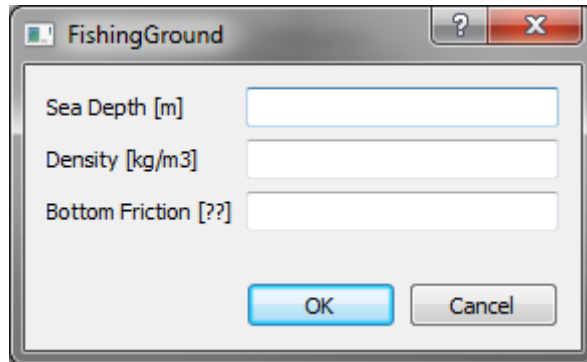
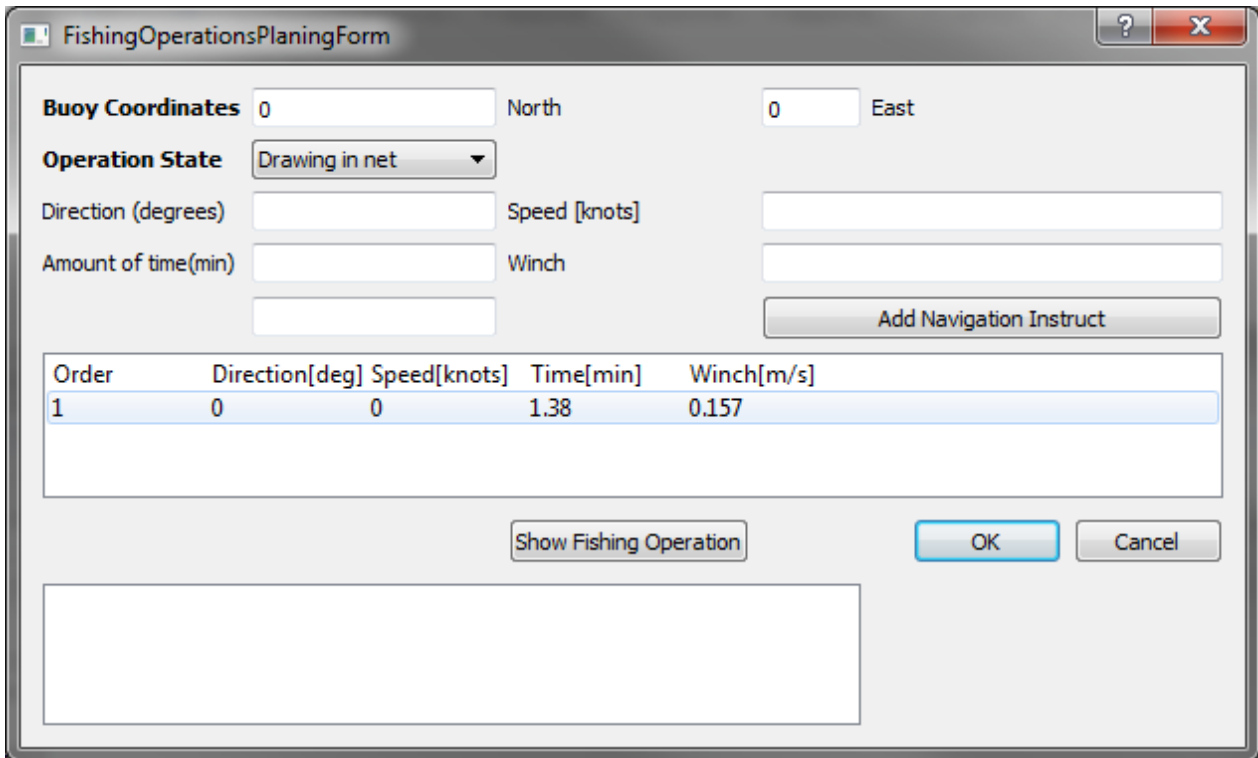


**FIGURE 9: defining the fishing ground.**

The fishing ground defines the depth of the waters, the density of the water, typically  $1025 \text{ kg/m}^3$  for saline water. Also the bottom friction is specifiable.



**Buoy Coordinates** 0 North 0 East

**Operation State** Drawing in net

Direction (degrees) Speed [knots]

Amount of time(min) Winch

Add Navigation Instruct

Order	Direction[deg]	Speed[knots]	Time[min]	Winch[m/s]
1	0	0	1.38	0.157

Show Fishing Operation OK Cancel

**FIGURE 10: defining the fishing operation**

Setting the fishing operations includes setting a number of navigation instructions. Each navigation instruction is defined as a direction for the fishing boat, speed in knots of the boat, a winch speed and an amount of time that this navigation instruction should be applied. By using a variation of these navigation instructions the towing and haul back can be specified in a very flexible manner.

### 3.3 Viewer Tool

The viewer tool is constructed to enable the simulation result to be inspected and visualised in detail even after the simulation has been completed. Each time step in the simulation result can be single stepped with both visualisation and read out of observables, e.g. the positions along the seine ropes. The simulation result can be viewed in 'play' mode, various ways of speeding up the viewing are available for the user.



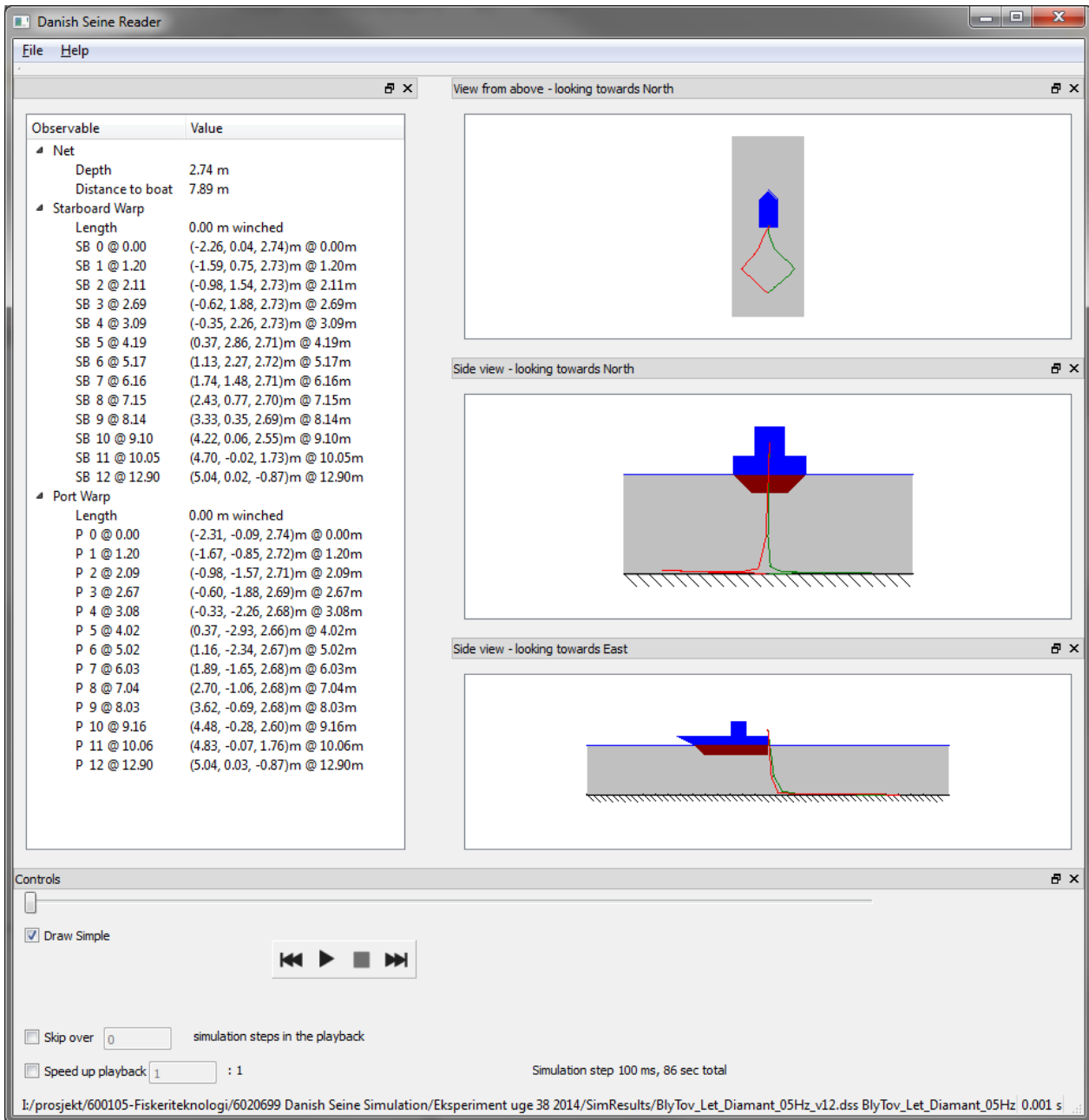


**FIGURE 11: simulation result loaded into the viewer software.**

Below FIGURE 12 shows snapshots taken from the viewer at the start of a simulation, at 11 and 21 seconds and at the end of the simulation run. The simulation shown in FIGURE 11 and FIGURE 12 corresponds to the simulation results to be presented in section 5.2.1.

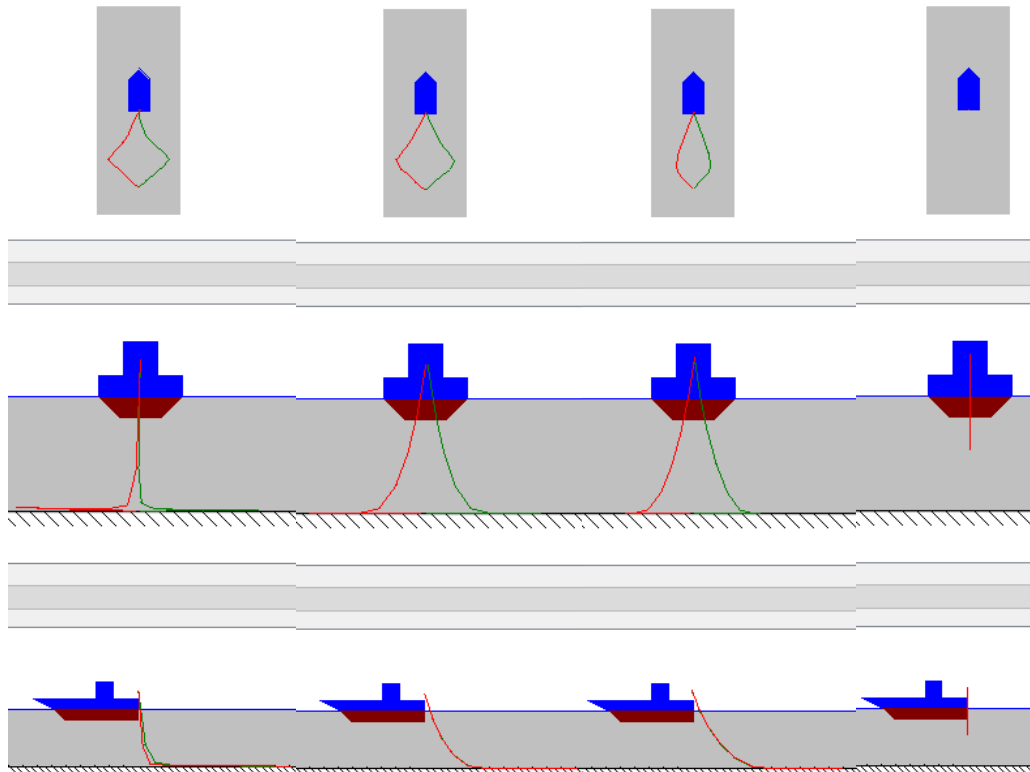


**FIGURE 12: visualisation of a simulation**

## 4 The Experimental Data from Flume Tank Tests

The flume tank experiments [13] were conducted for seine ropes with different physical properties and for different initial layout patterns on the flume tank floor. Further the seine ropes were hauled back from the tank floor at different speeds. A motion tracking system based on stereo vision with six underwater cameras was applied to record the gradual change in the geometry of the area encircled by the ropes. Information about the kinematic behaviour of the seine ropes and its dependency on its physical properties, initial layout pattern and hauling speed were acquired through this procedure. The flume tank experiments and the results obtained are thorough described in [13].

### 4.1 Winch Speed

During the experiments we conducted the same haul back cases with two different winch speeds at respectively 0.157 m/s and 0.314 m/s.

### 4.2 Layout Patterns

The seine rope was laid out on the flume tank floor in a specific pattern before starting the haul back process.

Since the seine rope behaviour might be different for different initial layout patterns we acquired motion tracking data for three different initial layout patterns: diamond, square and triangle.

### 4.3 Seine Rope Types

To be able to investigate the potential effect of seine rope density on the shape encircled by the seine ropes, two ropes differing considerable regarding density were applied:

- Light weight polyester rope with diameter 14 mm and a weight of 0.18 Kg per meter rope.
- Heavy combination rope with a lead core and a polyester cover. The diameter was 14 mm and a weight of 0.50 Kg per meter rope.

Both ropes had very small bending stiffness. On the contrary the elongation stiffness was large, resulting in negligible elongation of the ropes during the flume tank experiments. The ropes were 30 m long.

### 4.4 Clump Weight

To emulate potential influence of seine net dragging resistance on seine rope behaviour during haul back two different situations were applied to both ropes during the flume tank experiment:

- Low resistance case. In this case was the middle point of the seine rope equipped with a mounting hinge weighting 7 g.
- High resistance case. In this case was the middle point of the seine rope consisted of two clumps each weighting 800 g attached to the 7 g hinge.

### 4.5 Summary for Experimental Cases

Applying three different initial layout patterns, two different winch speeds, two different seine rope types and two different winch speeds makes 24 different experimental haul back cases (TABLE 1). Motion tracking data for all these 24 cases were acquired during the flume tank experiments following the procedure described in [13].

**TABLE 1: the experiments**

<b>Layout</b>	<b>Rope</b>	<b>Net Weight</b>	<b>Winch Speed</b>
Square	Combination Rope	7g	0.157 m/s
Square	Combination Rope	1607 g	0.157 m/s
Square	Combination Rope	7 g	0.314 m/s
Square	Combination Rope	1607 g	0.314 m/s
Square	Polyester Rope	7g	0.157 m/s
Square	Polyester Rope	1607 g	0.157 m/s
Square	Polyester Rope	7 g	0.314 m/s
Square	Polyester Rope	1607 g	0.314 m/s
Diamond	Combination Rope	7g	0.157 m/s
Diamond	Combination Rope	1607 g	0.157 m/s
Diamond	Combination Rope	7 g	0.314 m/s
Diamond	Combination Rope	1607 g	0.314 m/s
Diamond	Polyester Rope	7g	0.157 m/s
Diamond	Polyester Rope	1607 g	0.157 m/s
Diamond	Polyester Rope	7 g	0.314 m/s
Diamond	Polyester Rope	1607 g	0.314 m/s
Triangle	Combination Rope	7g	0.157 m/s
Triangle	Combination Rope	1607 g	0.157 m/s
Triangle	Combination Rope	7 g	0.314 m/s
Triangle	Combination Rope	1607 g	0.314 m/s
Triangle	Polyester Rope	7g	0.157 m/s
Triangle	Polyester Rope	1607 g	0.157 m/s
Triangle	Polyester Rope	7 g	0.314 m/s
Triangle	Polyester Rope	1607 g	0.314 m/s

## 5 Validation of Simulation model

The ability of the simulation model to predict seine rope behaviour during haul back procedures was investigated by simulating each of the 24 cases conducted in the flume tank (TABLE 1). Three different comparisons were made between the experimentally obtained result (flume tank) and the corresponding simulated result (simulation model) as described below.

First, a visual comparison of the geometry of the seine ropes as seen from above and from the side at six different time steps during the haul back process.

Second, the projected area encircled on the bottom against the current amount of seine rope. This is to limit the effect of a non-perfect haul back procedure during the experimental haul back. A few cases of slipping seine rope on the winch were occurring during haul back for few of the flume tank trials. This result in for those cases in a none monotonous haul back speed for the experiment and can therefore lead to lack of agreement with the simulated results (obtained with a constant winch speed) when comparing seine rope geometry versus process time. To attempt to compensate somehow for this problem, seine rope geometry versus length of seine rope not yet winched in is also compared between experiment and simulation. Thus we try to limit the effect of the imperfect experiments by this comparison. The  $R^2$  value is presented as a measure for how well the simulated data fits the experimental data.

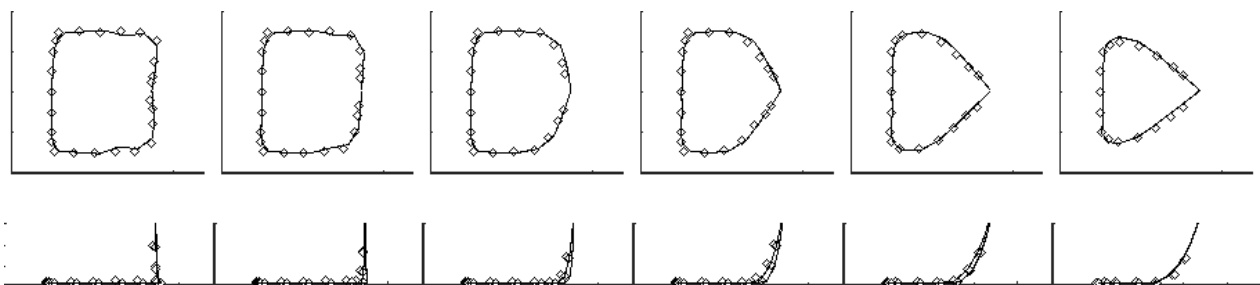
Finally, three metrics are shown as a function of time. These metrics are the projected area, the available seine rope length and the distance from the winch to the net. The  $R^2$  value is also presented.

### 5.1 Square Layout

#### 5.1.1 Combination Rope; Light; Slow

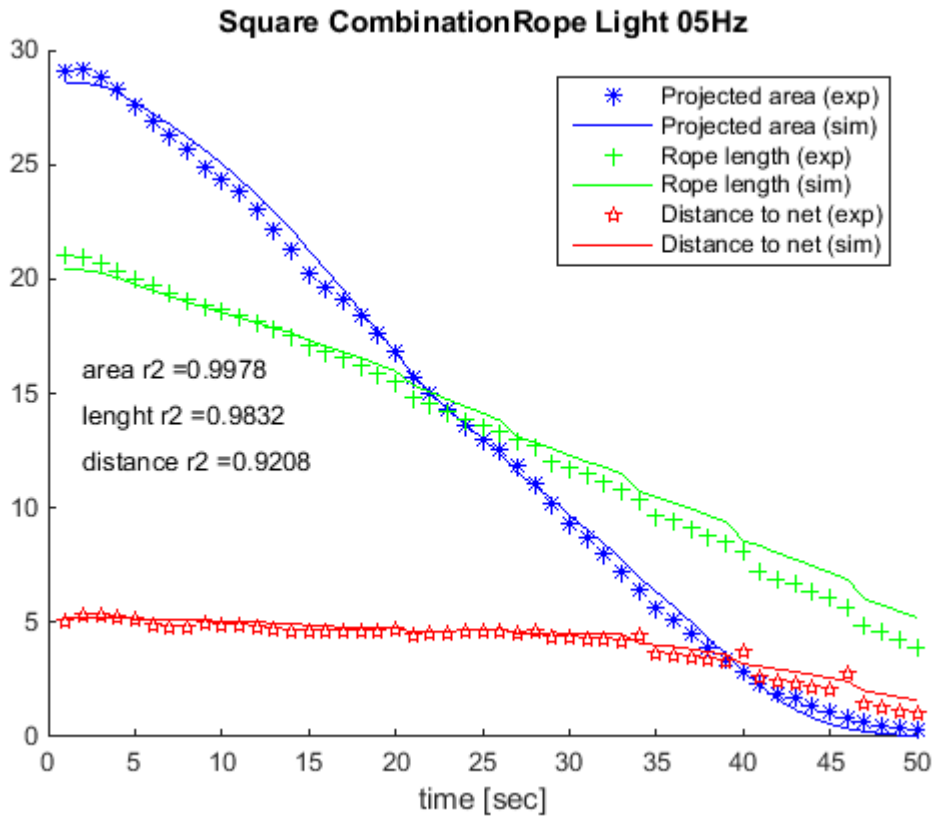
This section compares flume tank results to results from simulation for the combination rope laid out in a square, using the light weight and the slow winch speed.

FIGURE 13 shows the seine rope geometry seen from above and from the side. The time step between the pictures is four seconds. The solid lines represent the simulated result. Diamond marks represent the flume tank result. The agreement between flume tank experiment and simulation is evident.



**FIGURE 13: the geometry of the seine ropes seen from above and from the side. The six pictures are taken with four seconds interval. The diamond marks represent the flume tank results and the solid line the simulation.**

FIGURE 14 plots respectively the projected area, the rope length and the distance to the net from the winch against the time.



**FIGURE 14:** shows the projected area [m<sup>2</sup>] encircled by the seine ropes, the seine rope length [m] and the distance [m] to the net from the winch plotted against time. The marks represent the flume tank results and the solid lines the simulation.

The agreement between flume tank experiment and simulation for the projected area, rope length and distance from winch to net is evident.

FIGURE 15 shows the rope length versus the projected area. The simulation results are presented by a solid line while the experimental data is shown by the star marks.

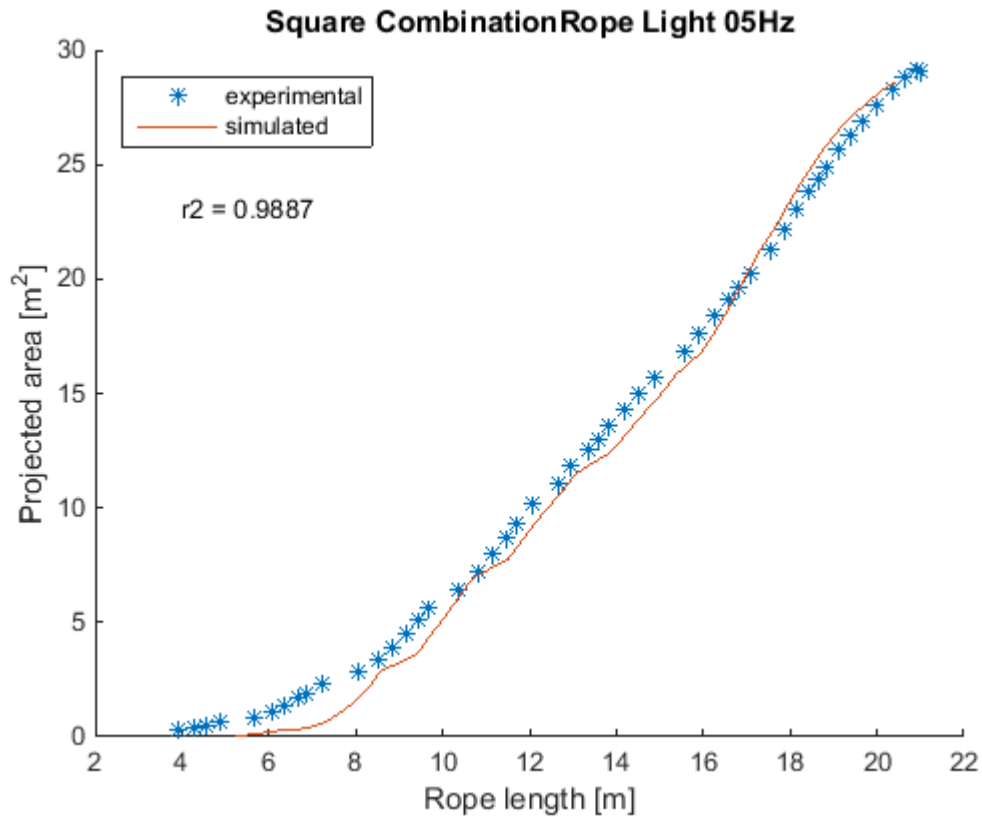


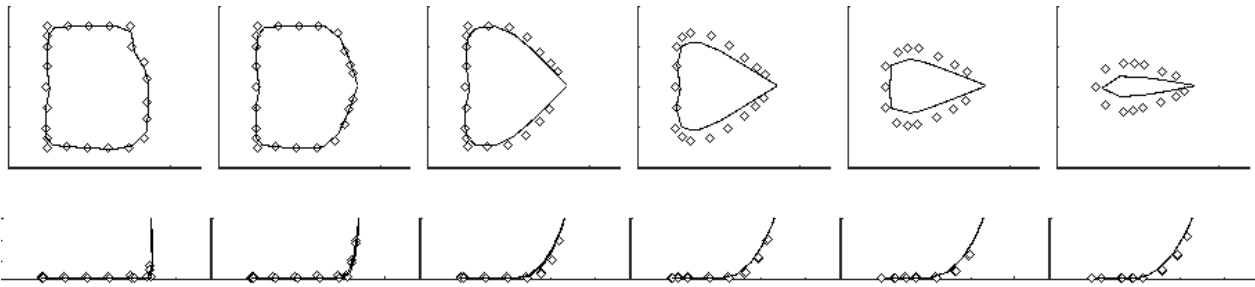
**FIGURE 15: projected area encircled by the seine ropes are plotted against the seine rope length. The star marks represent the flume tank results and the solid line the simulation.**

Good agreement between flume tank results and simulation is evident for this case.

### 5.1.2 Combination Rope; Light; Fast

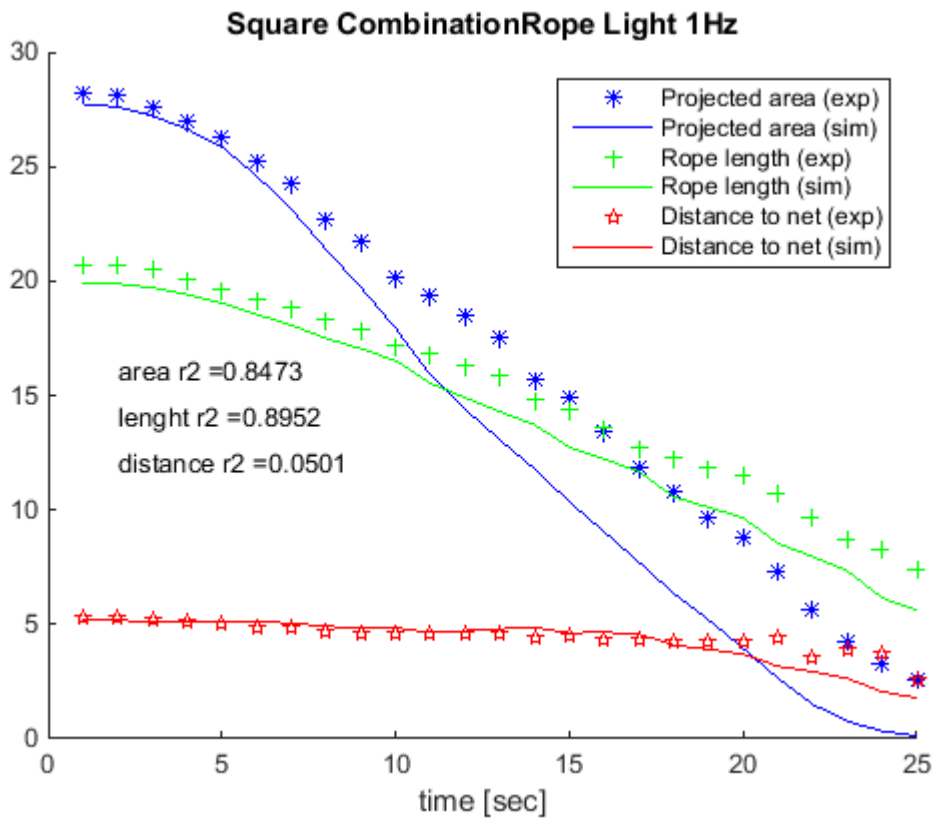
This section compares flume tank results to results from simulation for the combination rope laid out in a square, using the light weight and the fast winch speed.

FIGURE 16 shows the seine rope geometry seen from above and from the side. The time step between the pictures is four seconds. The solid lines represent the simulated result. Diamond marks represent the flume tank result. The agreement between flume tank experiment and simulation is fine initially, but worsens in the last half of the haul back procedure. The simulation appears to run faster than the flume tank experiment.



**FIGURE 16:** the geometry of the seine ropes seen from above and from the side. The six pictures are taken with four seconds interval. The diamond marks represent the flume tank results and the solid line the simulation.

FIGURE 17 plots respectively the projected area, the rope length and the distance to the net from the winch against the time.



**FIGURE 17:** shows the projected area [m<sup>2</sup>] encircled by the seine ropes, the seine rope length [m] and the distance [m] to the net from the winch plotted against time. The marks represent the flume tank results and the solid lines the simulation.

Agreement is not so good for the projected area encircled by the seine ropes.

FIGURE 18 shows the rope length versus the projected area. The simulation results are presented by a solid line while the experimental data is shown by the star marks.



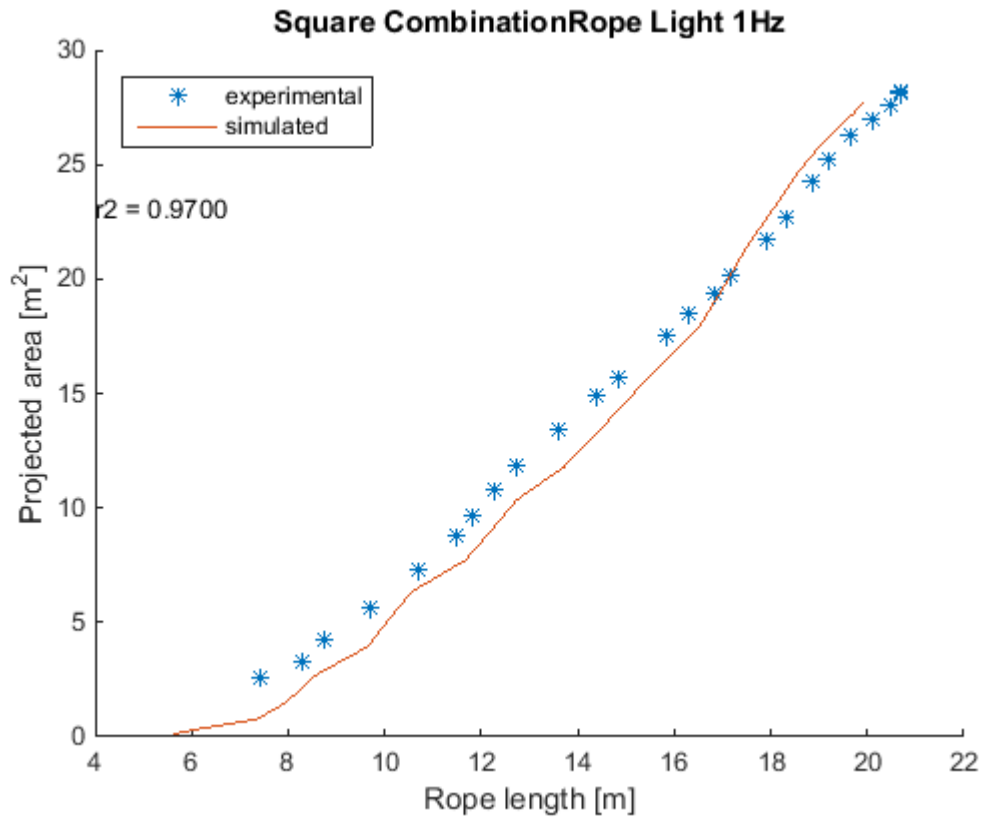


**FIGURE 18:** projected area encircled by the seine ropes are plotted against the seine rope length. The star marks represent the flume tank results and the solid line the simulation.

Good agreement between flume tank results and simulation is evident when the imperfect synchronisation was eliminated.

### 5.1.3 Combination Rope; Heavy; Slow

This section compares flume tank results to results from simulation for the combination rope laid out in a square, using the heavy weight and the slow winch speed.

FIGURE 19 shows the seine rope geometry seen from above and from the side. The time step between the pictures is four seconds. The solid lines represent the simulated result. Diamond marks represent the flume tank result. The agreement between flume tank experiment and simulation is evident.

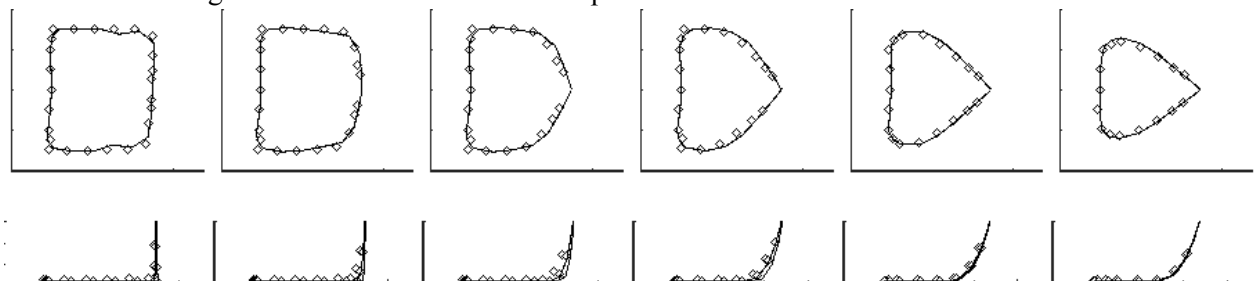


**FIGURE 19:** the geometry of the seine ropes seen from above and from the side. The six pictures are taken with four seconds interval. The diamond marks represent the flume tank results and the solid line the simulation.

FIGURE 20 plots respectively the projected area, the rope length and the distance to the net from the winch against the time.

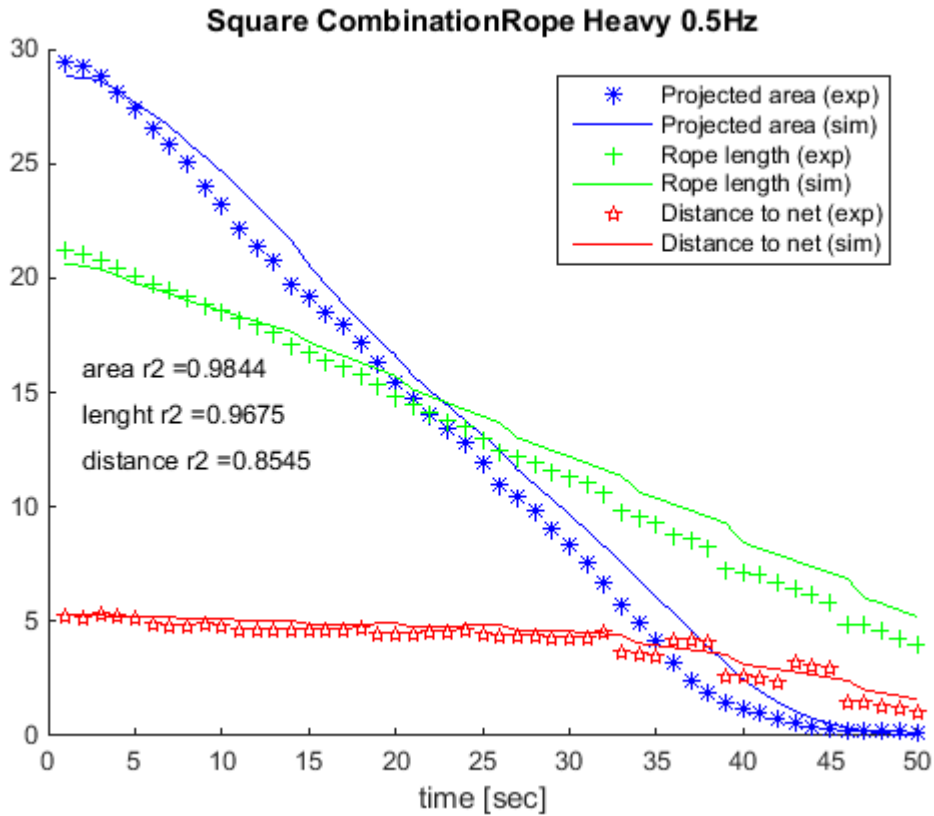
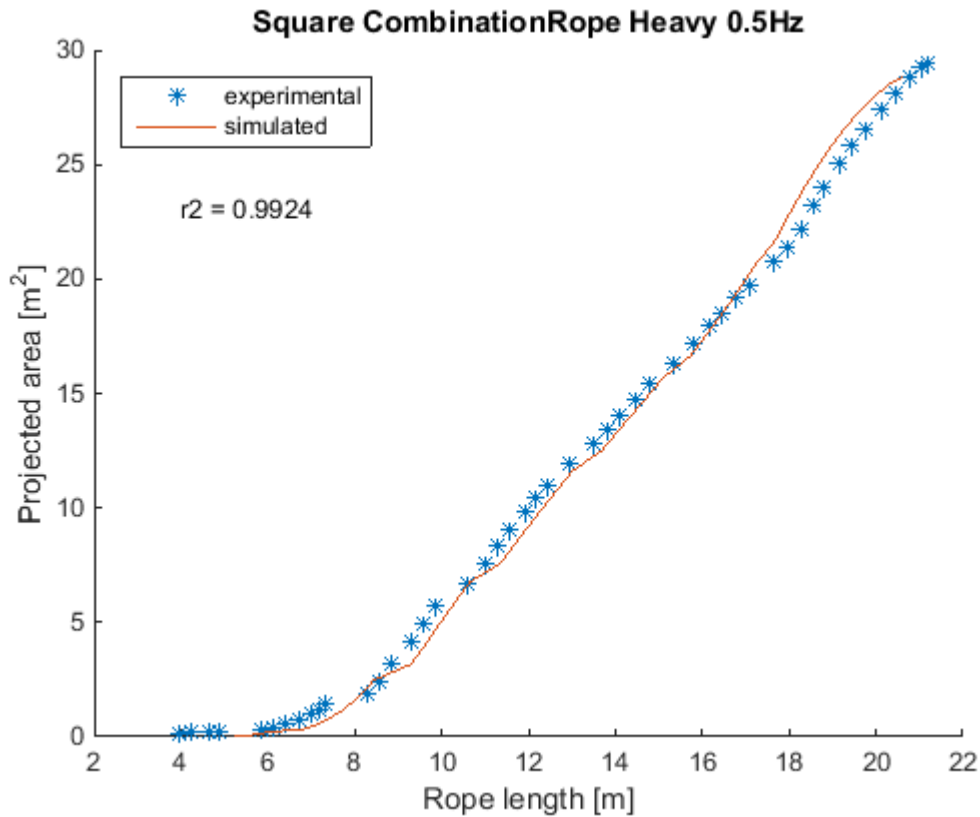


FIGURE 20: shows the projected area [m<sup>2</sup>] encircled by the seine ropes, the seine rope length [m] and the distance [m] to the net from the winch plotted against time. The marks represent the flume tank results and the solid lines the simulation.

The agreement between flume tank experiment and simulation for the projected area, rope length and distance from winch to net is evident.

FIGURE 21 shows the rope length versus the projected area. The simulation results are presented by a solid line while the experimental data is shown by the star marks.



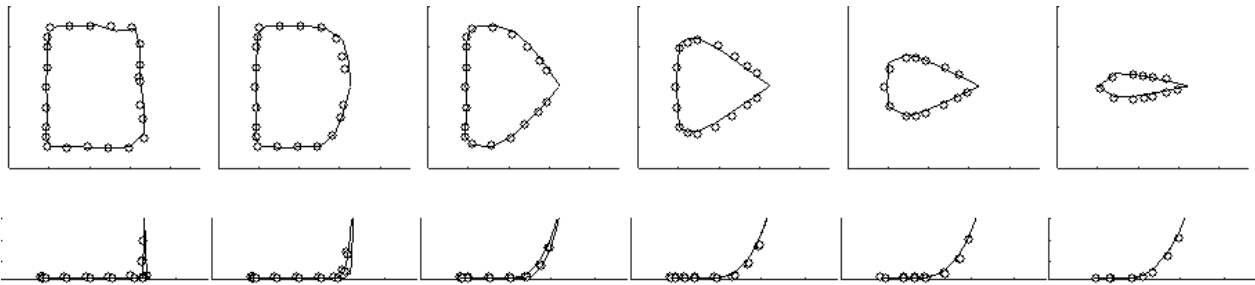
**FIGURE 21: projected area encircled by the seine ropes are plotted against the seine rope length. The star marks represent the flume tank results and the solid line the simulation.**

By using the rope length as the indicator for how far along the haul back procedure is we eliminate the effect of the experiment being imperfect (taking a small break in the hauling back). The  $R^2$  value is here showing good agreement between experiment and simulation.

**5.1.4 Combination Rope; Heavy; Fast**

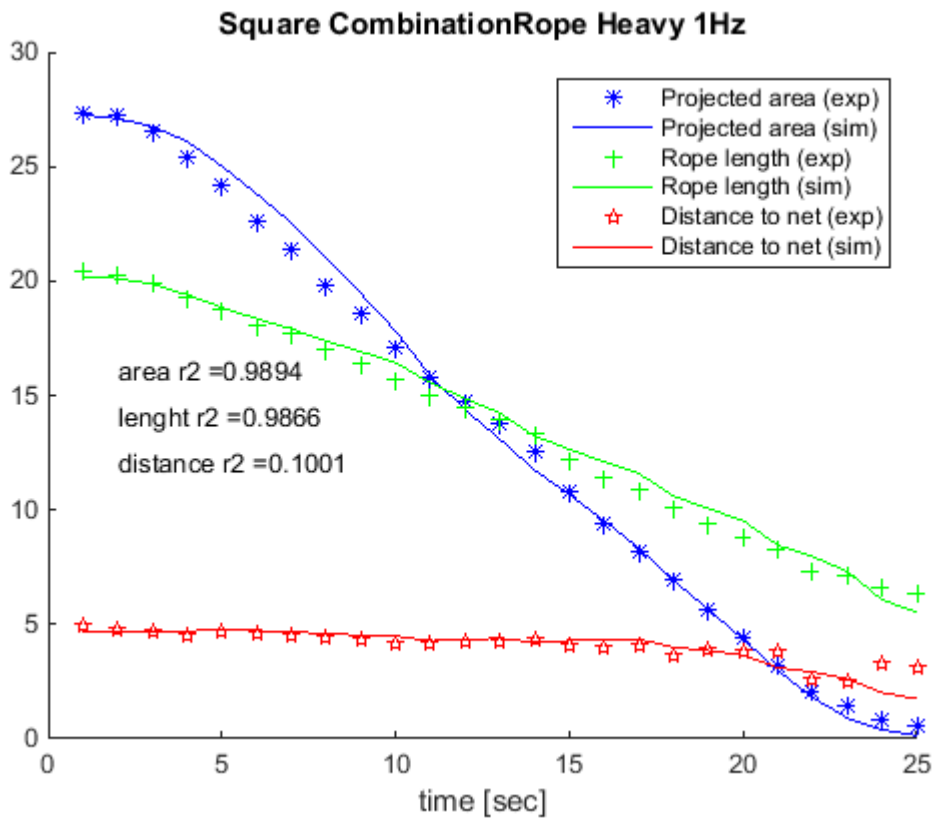
This section compares flume tank results to results from simulation for the combination rope laid out in a square, using the heavy weight and the fast winch speed.

FIGURE 22 shows the seine rope geometry seen from above and from the side. The time step between the pictures is four seconds. The solid lines represent the simulated result. Diamond marks represent the flume tank result. The agreement between flume tank experiment and simulation is evident.



**FIGURE 22: the geometry of the seine ropes seen from above and from the side. The six pictures are taken with four seconds interval. The diamond marks represent the flume tank results and the solid line the simulation.**

FIGURE 23 plots respectively the projected area, the rope length and the distance to the net from the winch against the time.



**FIGURE 23: shows the projected area [m<sup>2</sup>] encircled by the seine ropes, the seine rope length [m] and the distance [m] to the net from the winch plotted against time. The marks represent the flume tank results and the solid lines the simulation.**

The agreement between flume tank experiment and simulation for the projected area, rope length and distance from winch to net is evident.

FIGURE 24 shows the rope length versus the projected area. The simulation results are presented by a solid line while the experimental data is shown by the star marks.

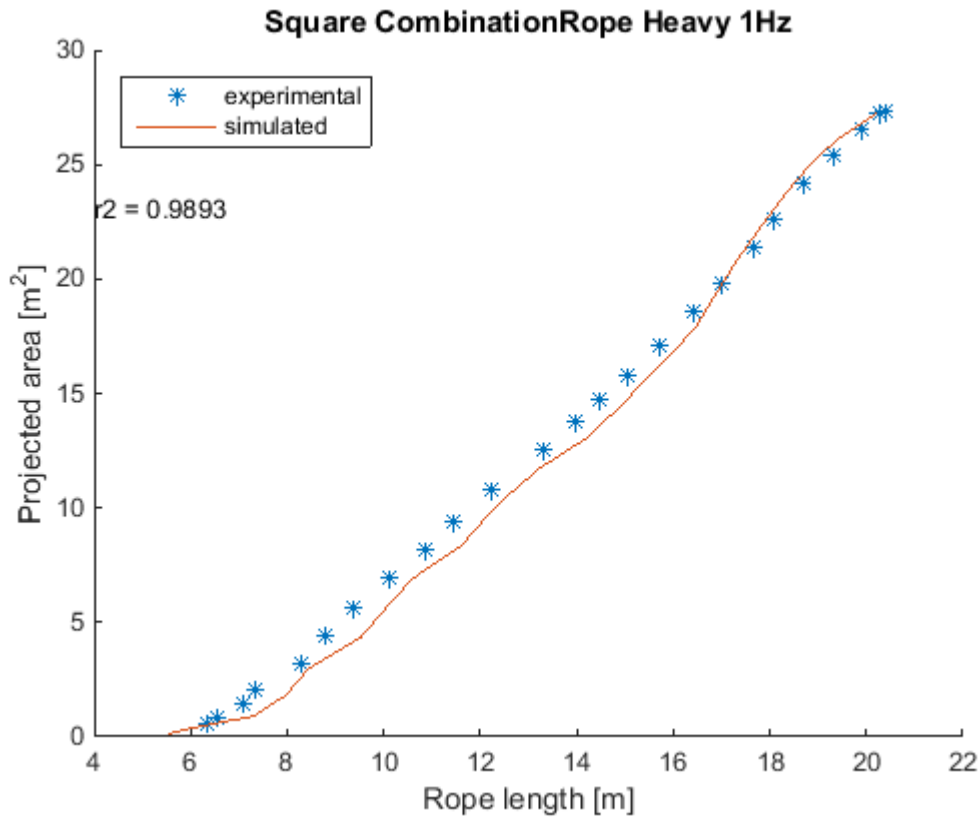


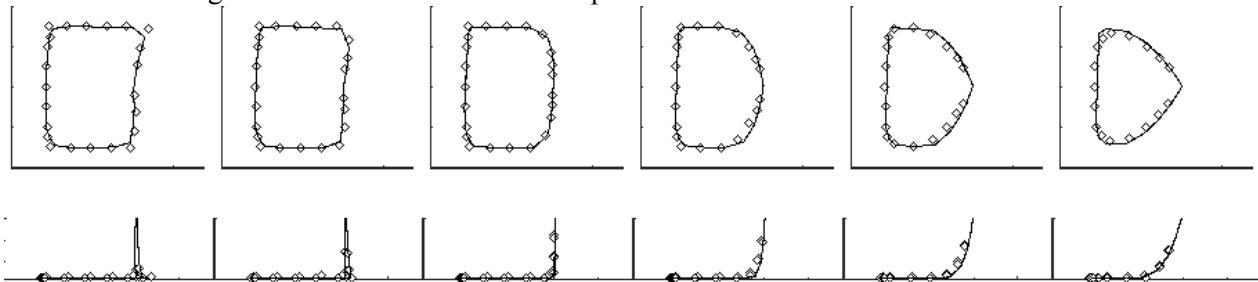
**FIGURE 24:** projected area encircled by the seine ropes are plotted against the seine rope length. The star mark represents the flume tank results and the solid line the simulation.

By using the rope length as the indicator for how far along the haul back procedure is we eliminate the effect of the experiment being imperfect (taking a small break in the hauling back). The  $R^2$  value is here showing good agreement between experiment and simulation.

### 5.1.5 Polyester Rope; Light; Slow

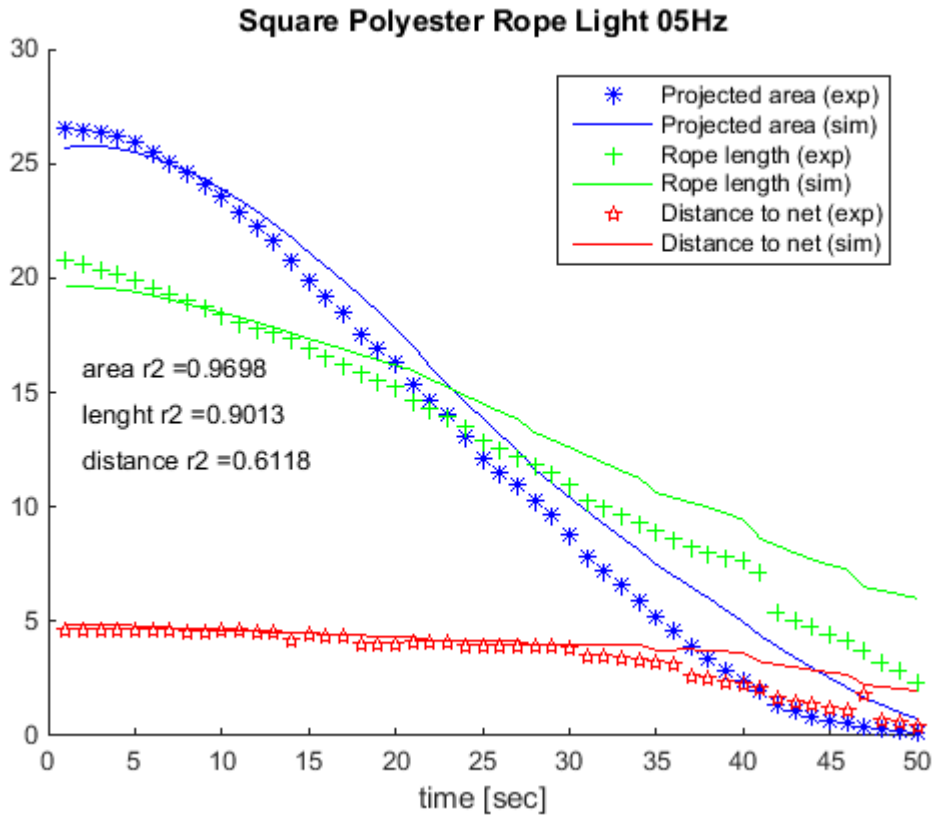
This section compares flume tank results to results from simulation for the polyester rope laid out in a square, using the light weight and the slow winch speed.

FIGURE 25 shows the seine rope geometry seen from above and from the side. The time step between the pictures is four seconds. The solid lines represent the simulated result. Diamond marks represent the flume tank result. The agreement between flume tank experiment and simulation is evident.



**FIGURE 25:** the geometry of the seine ropes seen from above and from the side. The six pictures are taken with four seconds interval. The diamond marks represent the flume tank results and the solid line the simulation.

FIGURE 26 plots respectively the projected area, the rope length and the distance to the net from the winch against the time.



**FIGURE 26:** shows the projected area [m<sup>2</sup>] encircled by the seine ropes, the seine rope length [m] and the distance [m] to the net from the winch plotted against time. The marks represent the flume tank results and the solid lines the simulation.

The agreement between flume tank experiment and simulation for the projected area, rope length and distance from winch to net is evident in the first third of the haul back procedure.

FIGURE 27 shows the rope length versus the projected area. The simulation results are presented by a solid line while the experimental data is shown by the star marks.

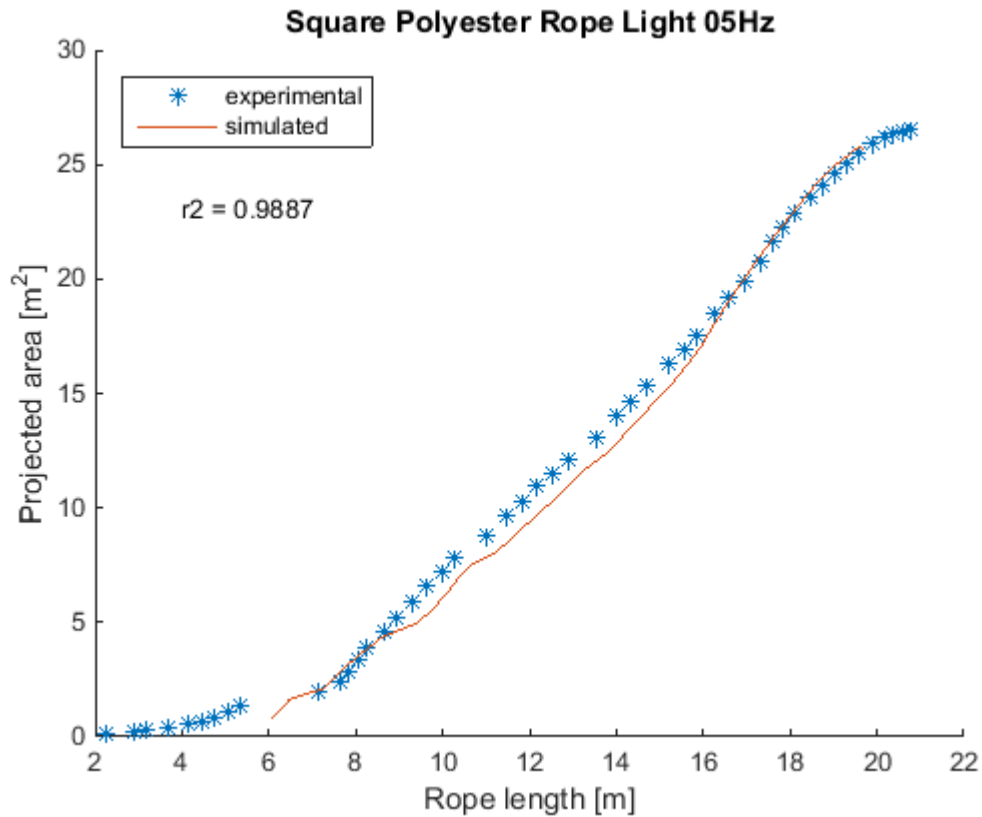


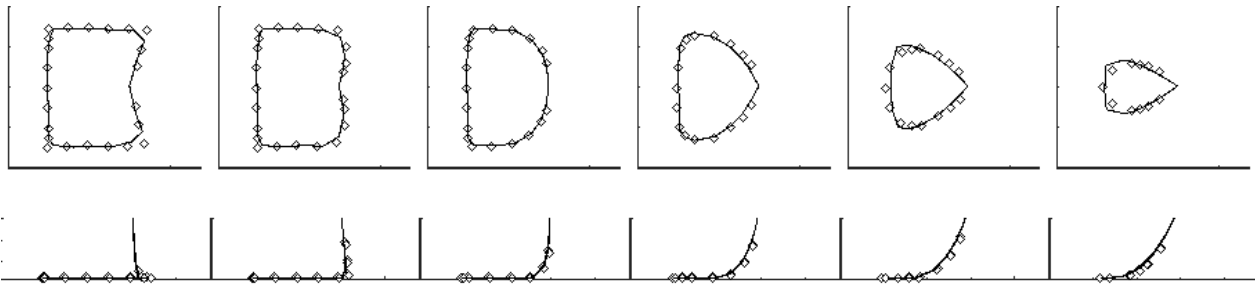
**FIGURE 27: projected area encircled by the seine ropes are plotted against the seine rope length. The star mark represents the flume tank results and the solid line the simulation.**

By using the rope length as the indicator for how far along the haul back procedure is we eliminate the effect of the experiment being imperfect (taking a small break in the hauling back). The  $R^2$  value is here showing good agreement between experiment and simulation.

### 5.1.6 Polyester Rope; Light; Fast

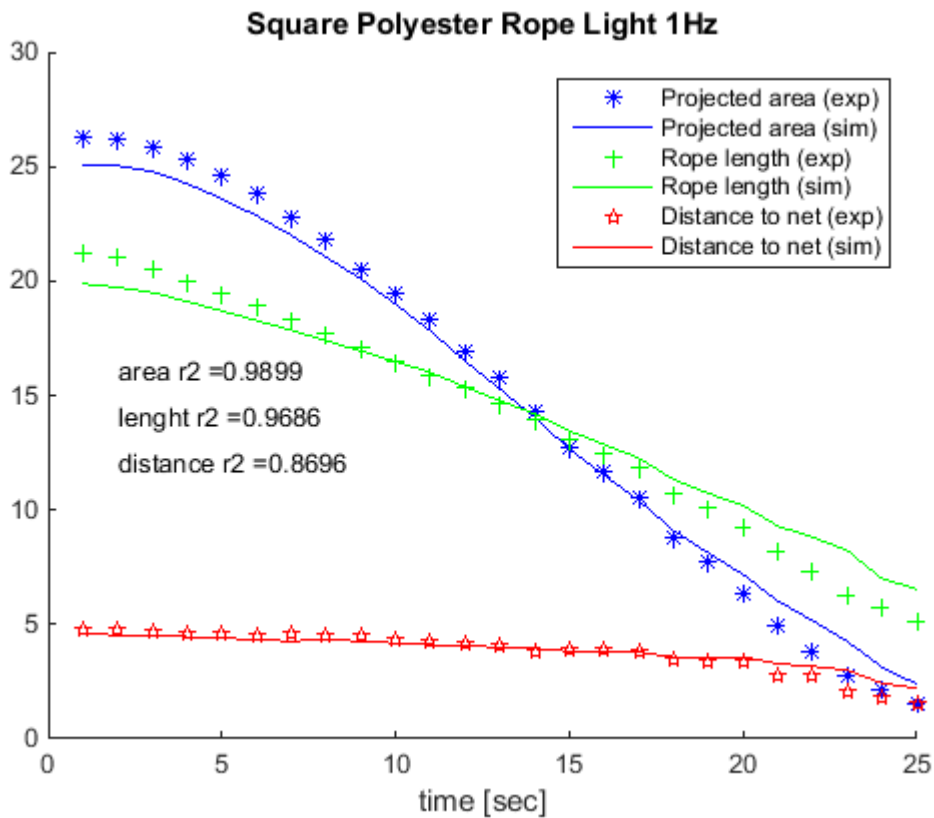
This section compares flume tank results to results from simulation for the polyester rope laid out in a square, using the light weight and the fast winch speed.

FIGURE 28 shows the seine rope geometry seen from above and from the side. The time step between the pictures is four seconds. The solid lines represent the simulated result. Diamond marks represent the flume tank result. A reasonable agreement between flume tank experiment and simulation is seen.



**FIGURE 28:** the geometry of the seine ropes seen from above and from the side. The six pictures are taken with four seconds interval. The diamond marks represent the flume tank results and the solid line the simulation.

FIGURE 29 plots respectively the projected area, the rope length and the distance to the net from the winch against the time.



**FIGURE 29:** shows the projected area [m<sup>2</sup>] encircled by the seine ropes, the seine rope length [m] and the distance [m] to the net from the winch plotted against time. The marks represent the flume tank results and the solid lines the simulation.

The agreement between flume tank experiment and simulation for the projected area, rope length and distance from winch to net is evident.

FIGURE 30 shows the rope length versus the projected area. The simulation results are presented by a solid line while the experimental data is shown by the star marks.



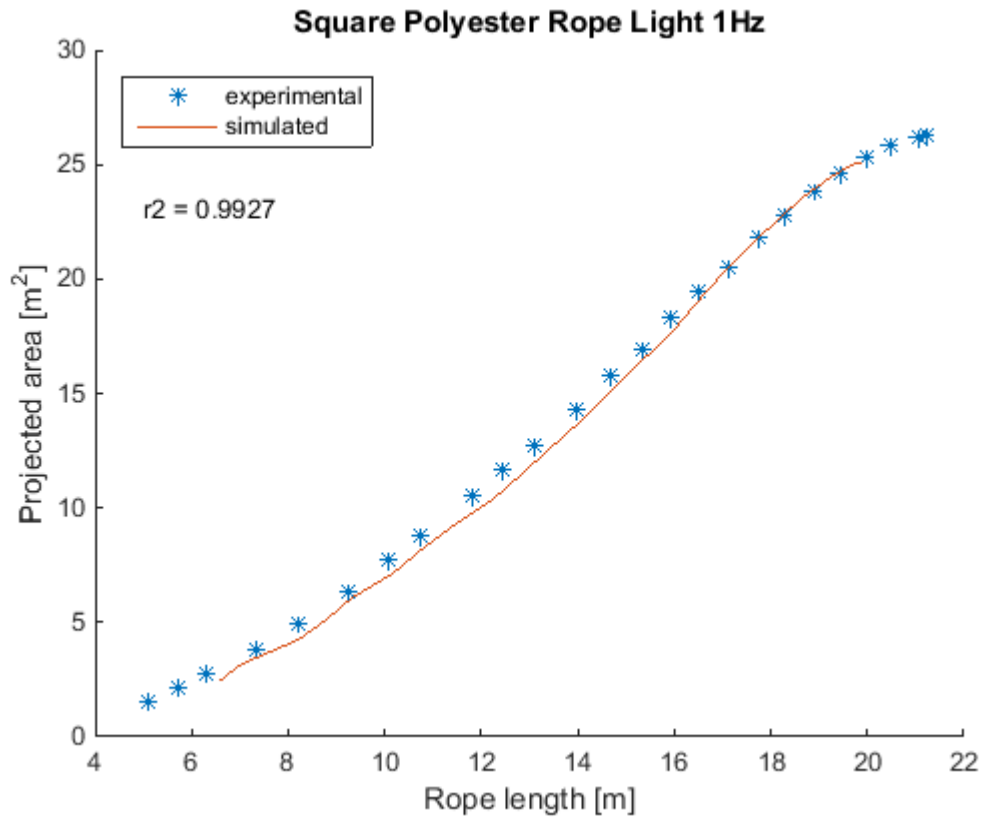


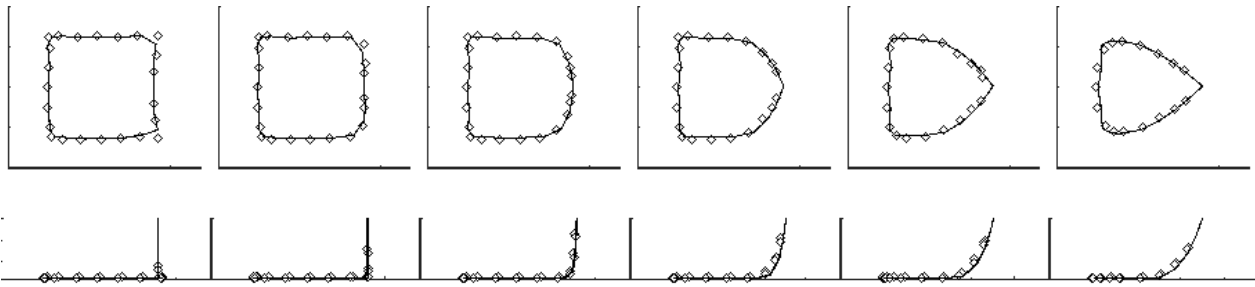
**FIGURE 30: projected area encircled by the seine ropes are plotted against the seine rope length. The star marks represent the flume tank results and the solid line the simulation.**

By using the rope length as the indicator for how far along the haul back procedure is we eliminate the effect of the experiment being imperfect (taking a small break in the hauling back). The  $R^2$  value is here showing good agreement between experiment and simulation.

### 5.1.7 Polyester Rope; Heavy; Slow

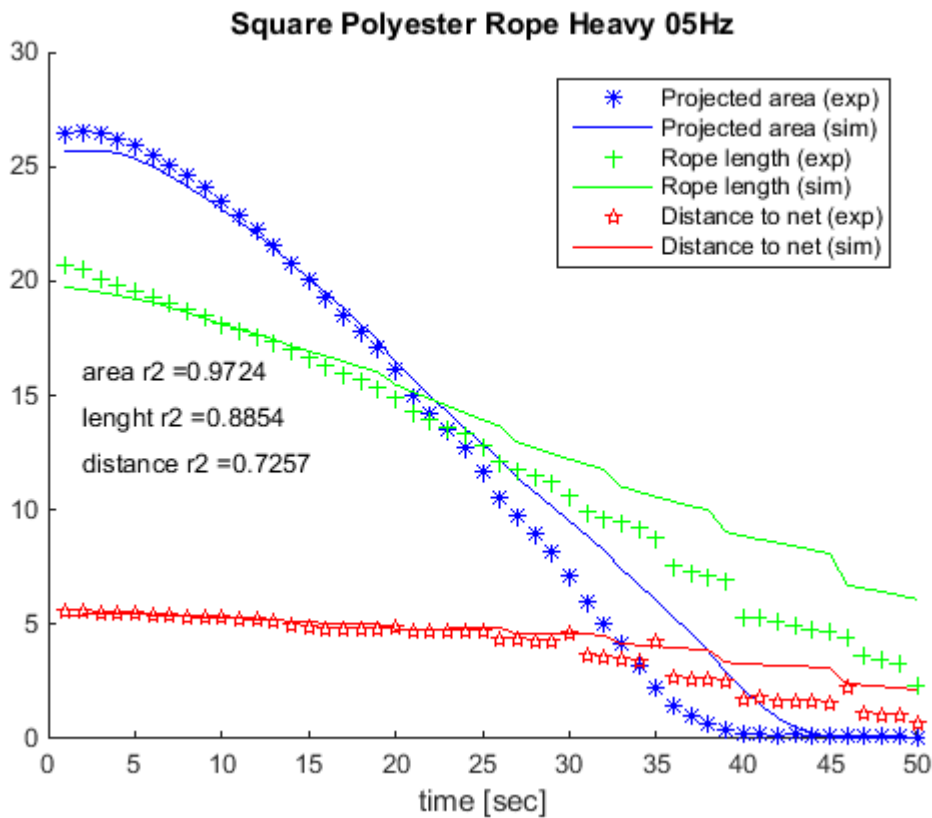
This section compares flume tank results to results from simulation for the polyester rope laid out in a square, using the light weight and the slow winch speed.

FIGURE 31 shows the seine rope geometry seen from above and from the side. The time step between the pictures is four seconds. The solid lines represent the simulated result. Diamond marks represent the flume tank result. The agreement between flume tank experiment and simulation is evident.



**FIGURE 31:** the geometry of the seine ropes seen from above and from the side. The six pictures are taken with four seconds interval. The diamond marks represent the flume tank results and the solid line the simulation.

FIGURE 32 plots respectively the projected area, the rope length and the distance to the net from the winch against the time.



**FIGURE 32:** shows the projected area [m<sup>2</sup>] encircled by the seine ropes, the seine rope length [m] and the distance [m] to the net from the winch plotted against time. The marks represent the flume tank results and the solid lines the simulation.

The agreement between flume tank experiment and simulation for the projected area, rope length and distance from winch to net is evident.

FIGURE 33 shows the rope length versus the projected area. The simulation results are presented by a solid line while the experimental data is shown by star marks.

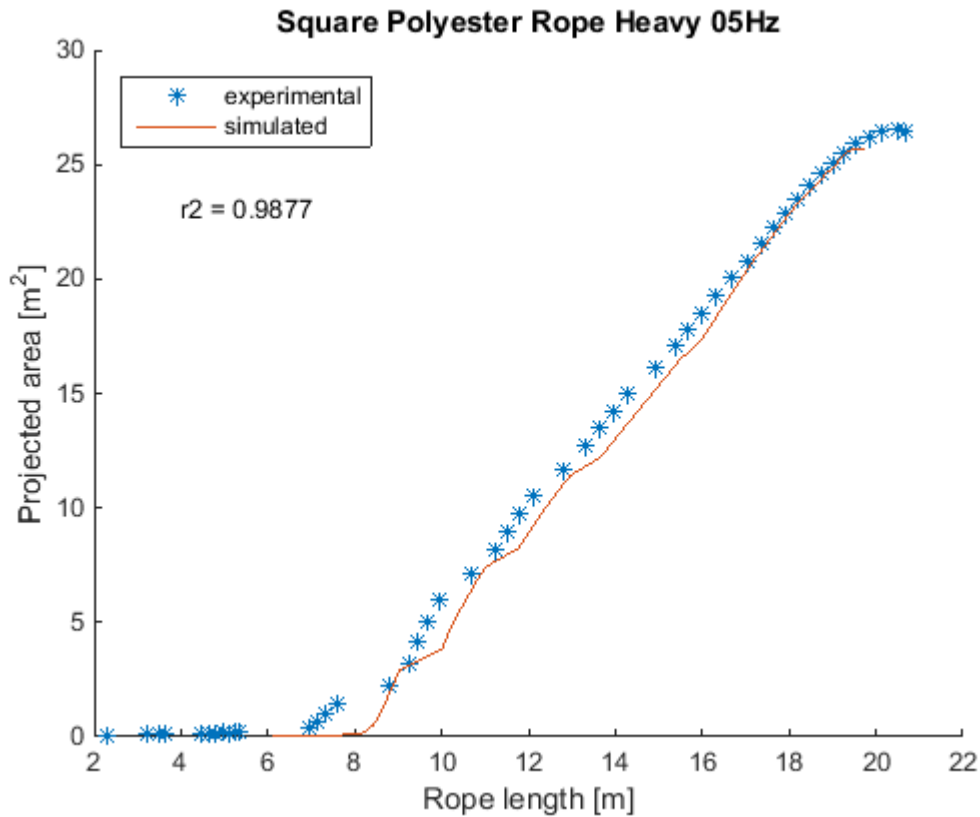


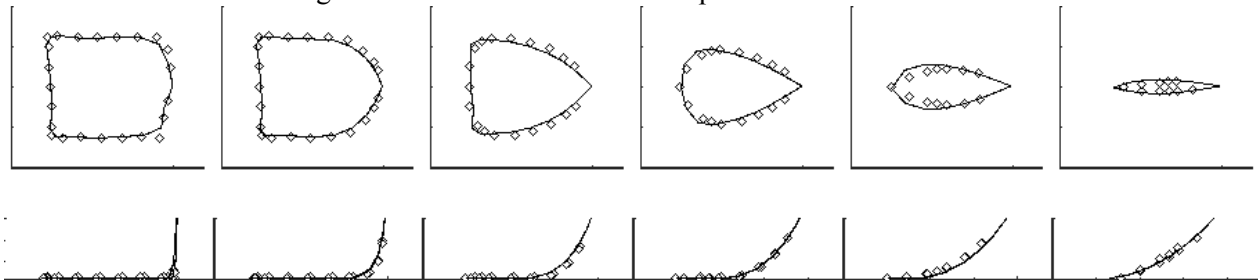
**FIGURE 33: projected area encircled by the seine ropes are plotted against the seine rope length. The star marks represent the flume tank results and the solid line the simulation.**

By using the rope length as the indicator for how far along the haul back procedure is we eliminate the effect of the experiment being imperfect (taking a small break in the hauling back). The  $R^2$  value is here showing good agreement between experiment and simulation.

**5.1.8 Polyester Rope; Heavy; Fast**

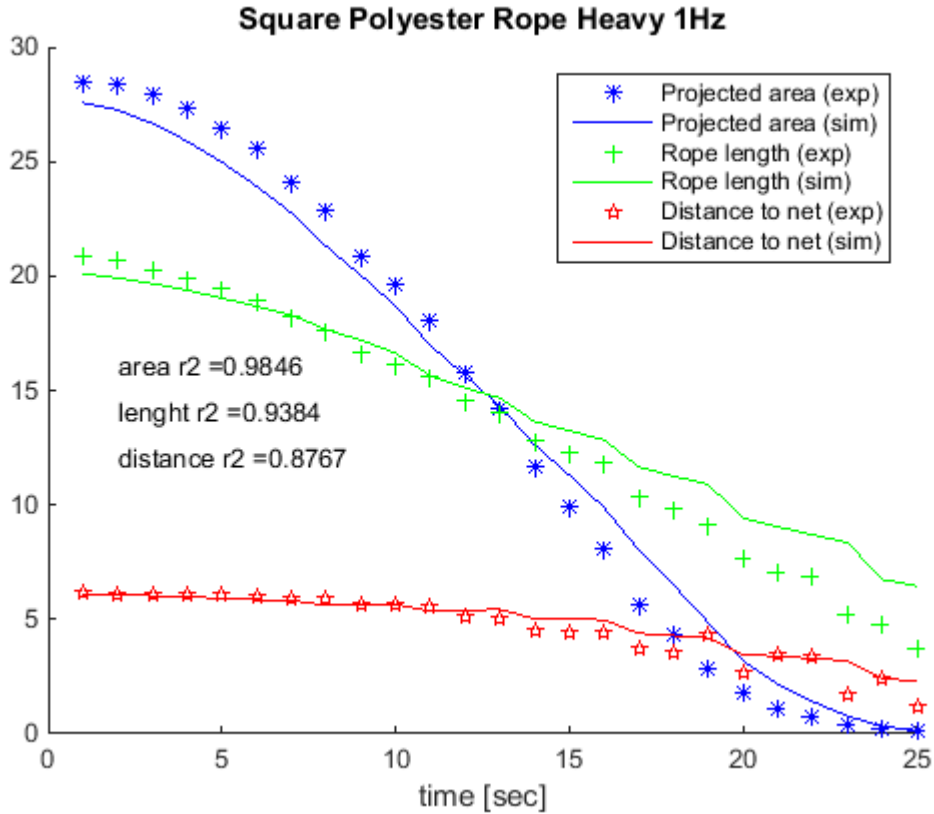
This section compares flume tank results to results from simulation for the polyester rope laid out in a square, using the heavy weight and the fast winch speed.

FIGURE 34 shows the seine rope geometry seen from above and from the side. The time step between the pictures is four seconds. The solid lines represent the simulated result. Diamond marks represent the flume tank result. A reasonable agreement between flume tank experiment and simulation is seen.



**FIGURE 34: the geometry of the seine ropes seen from above and from the side. The six pictures are taken with four seconds interval. The diamond marks represent the flume tank results and the solid line the simulation.**

FIGURE 35 plots respectively the projected area, the rope length and the distance to the net from the winch against the time.



**FIGURE 35:** shows the projected area [m<sup>2</sup>] encircled by the seine ropes, the seine rope length [m] and the distance [m] to the net from the winch plotted against time. The marks represent the flume tank results and the solid lines the simulation.

The simulated projected area is slightly below initially and midway through flips to be slightly above the measured. The agreement between flume tank experiment and simulation for the projected area, rope length and distance from winch to net is evident.

FIGURE 36 shows the rope length versus the projected area. The simulation results are presented by a solid line while the experimental data is shown by star marks.

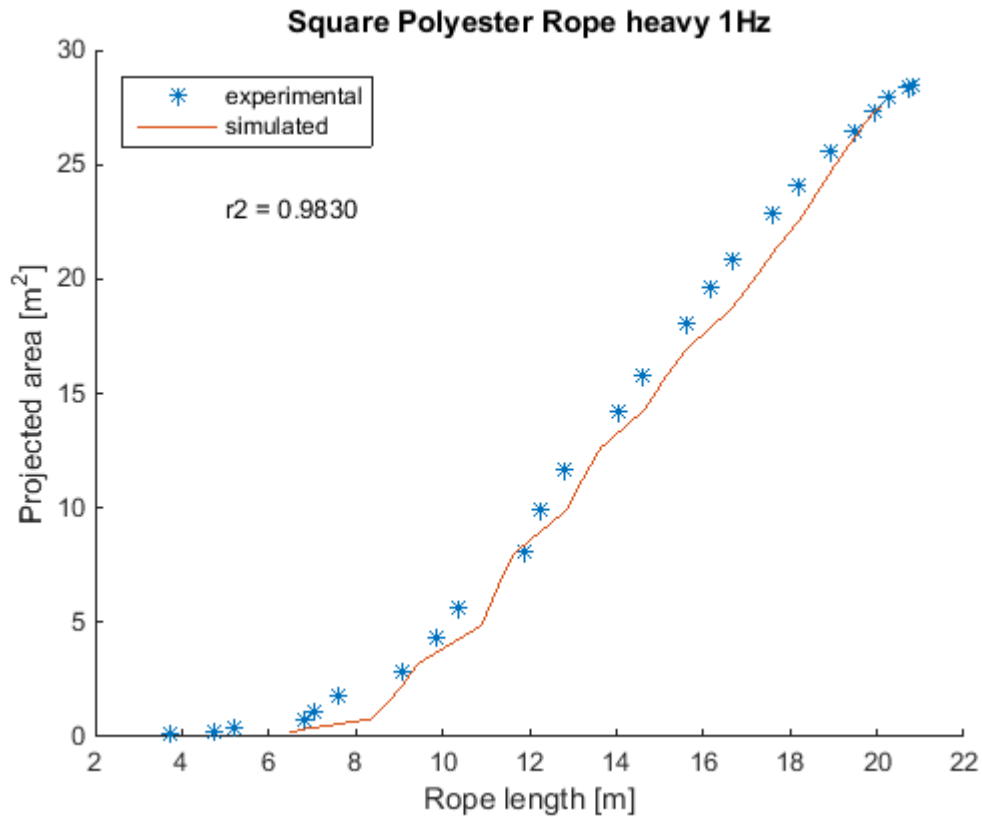


**FIGURE 36: projected area encircled by the seine ropes are plotted against the seine rope length. The star marks represent the flume tank results and the solid line the simulation.**

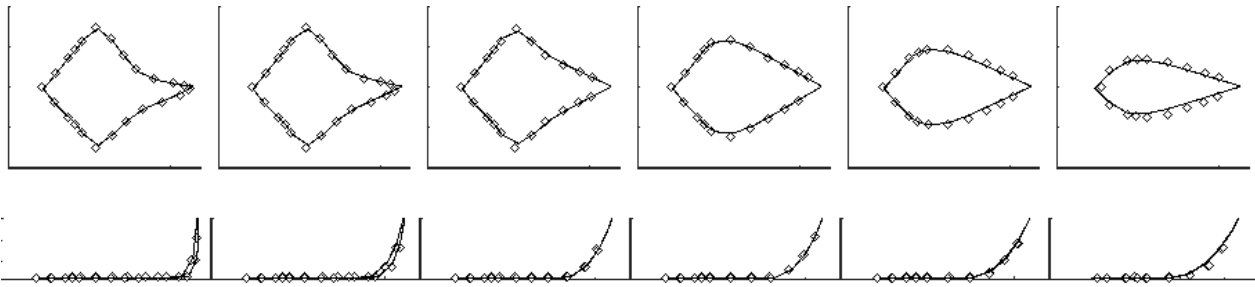
By using the rope length as the indicator for how far along the haul back procedure is we eliminate the effect of the experiment being imperfect (taking a small break in the hauling back). The  $R^2$  value is here showing good agreement between experiment and simulation.

## 5.2 Diamond Layout

### 5.2.1 Combination Rope; Light; Slow

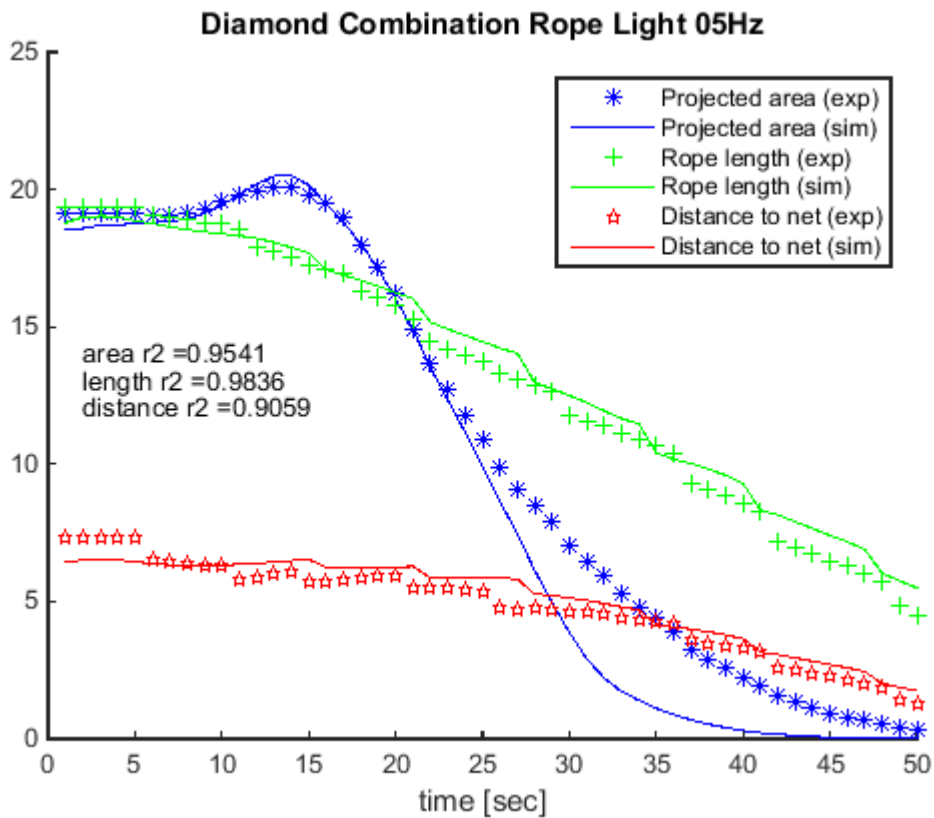
This section compares flume tank results to results from simulation for the combination rope laid out in a diamond shape, using the light weight and the slow winch speed.

FIGURE 37 shows the seine rope geometry seen from above and from the side. The time step between the pictures is four seconds. The solid lines represent the simulated result. Diamond marks represent the flume tank result. The agreement between flume tank experiment and simulation is evident.



**FIGURE 37:** the geometry of the seine ropes seen from above and from the side. The six pictures are taken with four seconds interval. The diamond marks represent the flume tank results and the solid line the simulation.

FIGURE 38 plots respectively the projected area, the rope length and the distance to the net from the winch against the time.



**FIGURE 38:** shows the projected area [m<sup>2</sup>] encircled by the seine ropes, the seine rope length [m] and the distance [m] to the net from the winch plotted against time. The marks represent the flume tank results and the solid lines the simulation.

The agreement between flume tank experiment and simulation for the projected area, rope length and distance from winch to net is evident in the initial phase. Towards the end the simulated projected area is significant smaller than the experimental.

FIGURE 39 shows the rope length versus the projected area. The simulation results are presented by a solid line while the experimental data is shown by star marks.

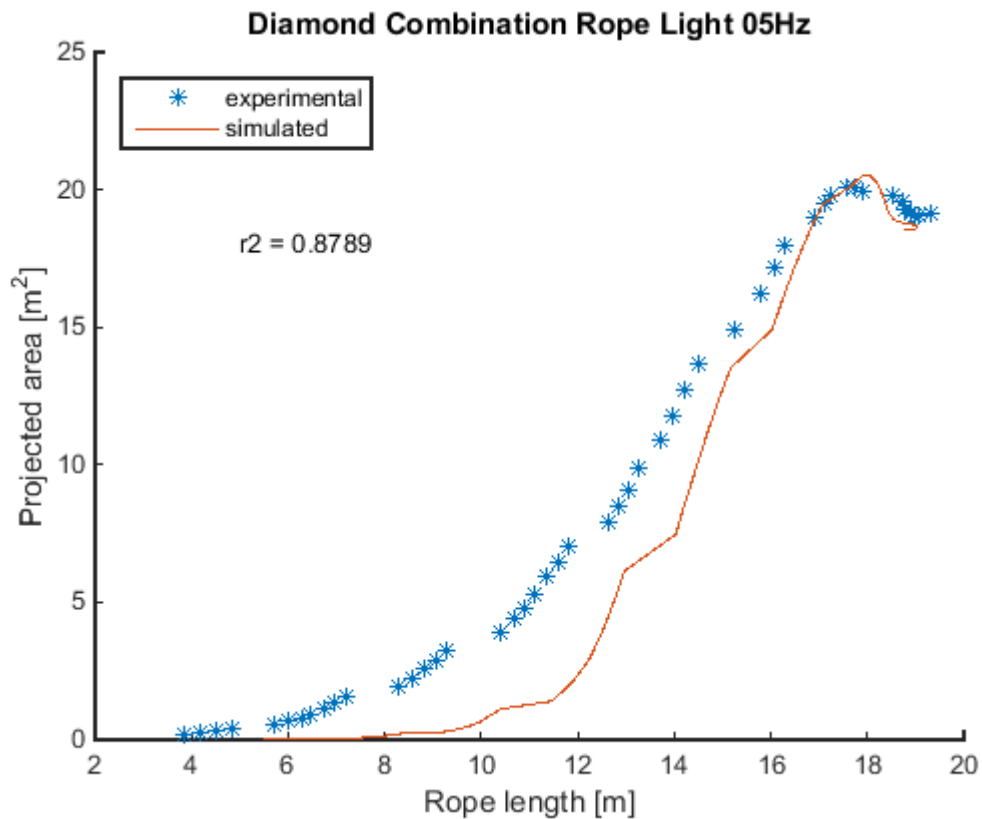


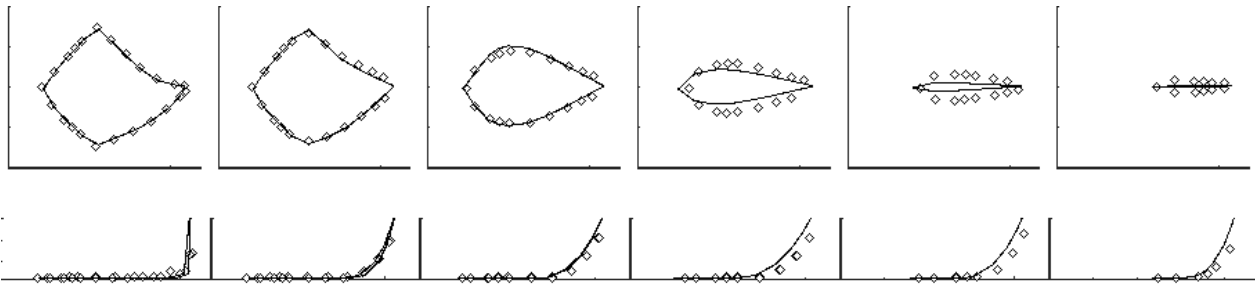
**FIGURE 39: projected area encircled by the seine ropes are plotted against the seine rope length. The star marks represent the flume tank results and the solid line the simulation.**

By using the rope length as the indicator for how far along the haul back procedure is we try to eliminate the effect of the experiment being imperfect (taking a small break in the hauling back). The  $R^2$  value here is below 0.9 and is therefore not showing good agreement between experiment and simulation.

### 5.2.2 Combination Rope; Light, Fast

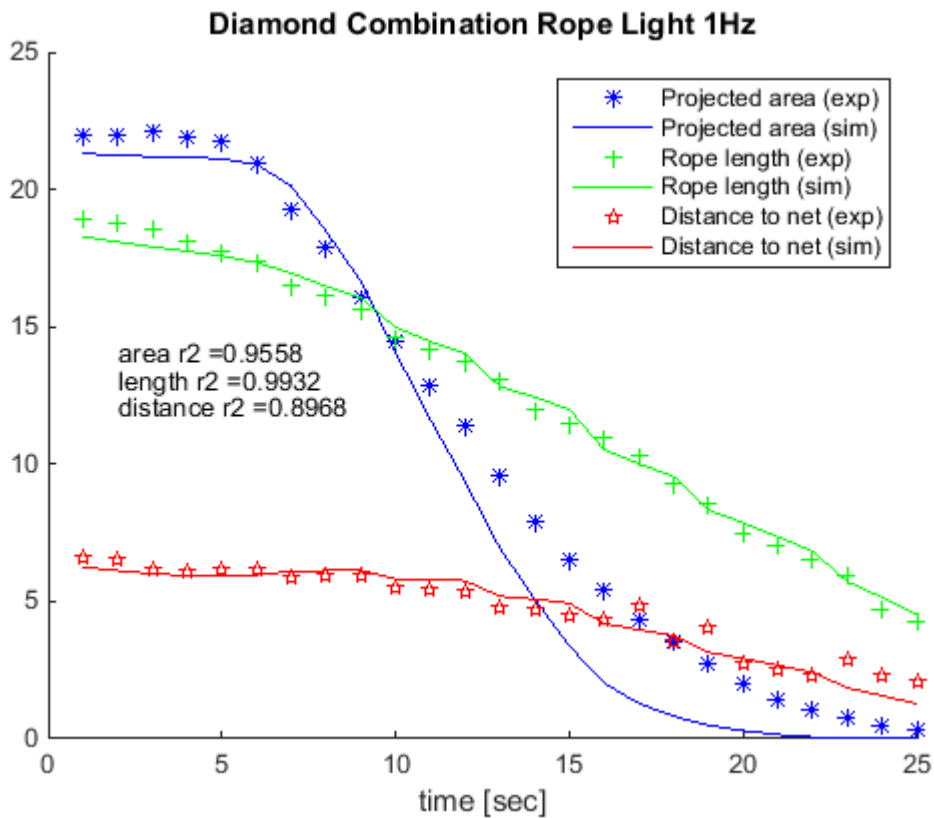
This section compares flume tank results to results from simulation for the combination rope laid out in a diamond shape, using the light weight and the fast winch speed.

FIGURE 40 shows the seine rope geometry seen from above and from the side. The time step between the pictures is four seconds. The solid lines represent the simulated result. Diamond marks represent the flume tank result. The agreement between flume tank experiment and simulation is evident during the first half of the haul back procedure. Later on the simulation appears to run ahead of the experiment.



**FIGURE 40:** the geometry of the seine ropes seen from above and from the side. The six pictures are taken with four seconds interval. The diamond marks represent the flume tank results and the solid line the simulation.

FIGURE 41 plots respectively the projected area, the rope length and the distance to the net from the winch against the time.



**FIGURE 41:** shows the projected area [m<sup>2</sup>] encircled by the seine ropes, the seine rope length [m] and the distance [m] to the net from the winch plotted against time. The marks represent the flume tank results and the solid lines the simulation.

The agreement between flume tank experiment and simulation for the rope length and distance from winch to net is evident. The simulated projected area is smaller than the experimental result after the initial 10 seconds.

FIGURE 42 shows the rope length versus the projected area. The simulation results are presented by a solid line while the experimental data is shown by star marks.



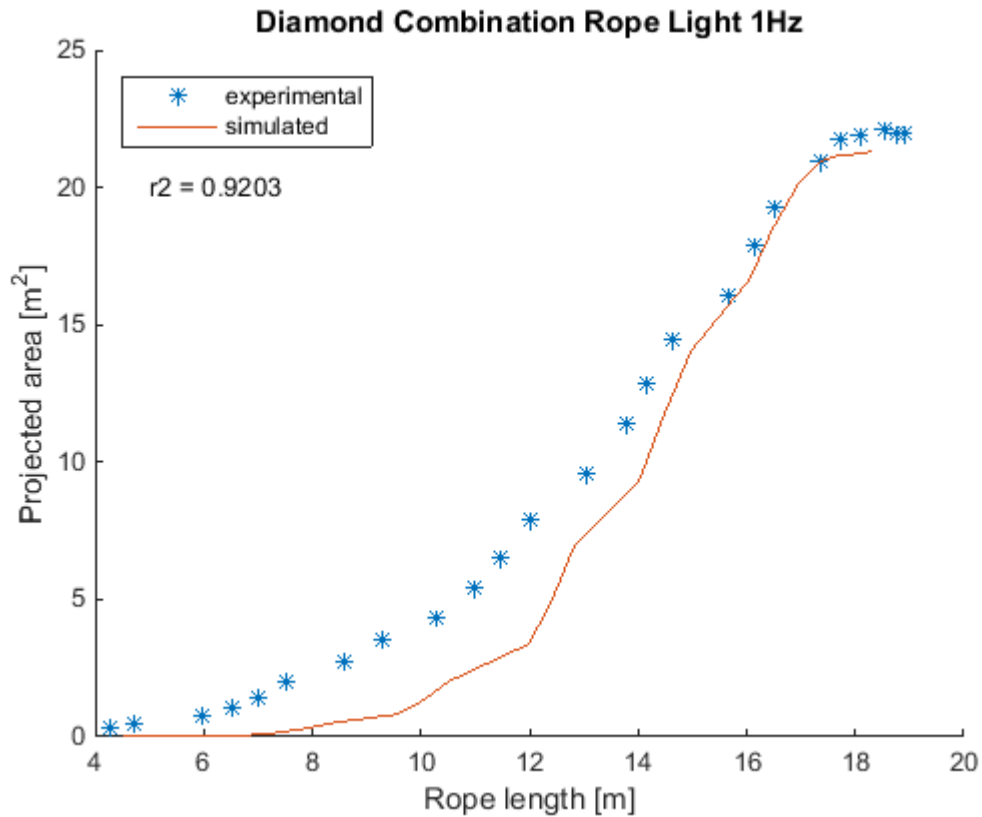


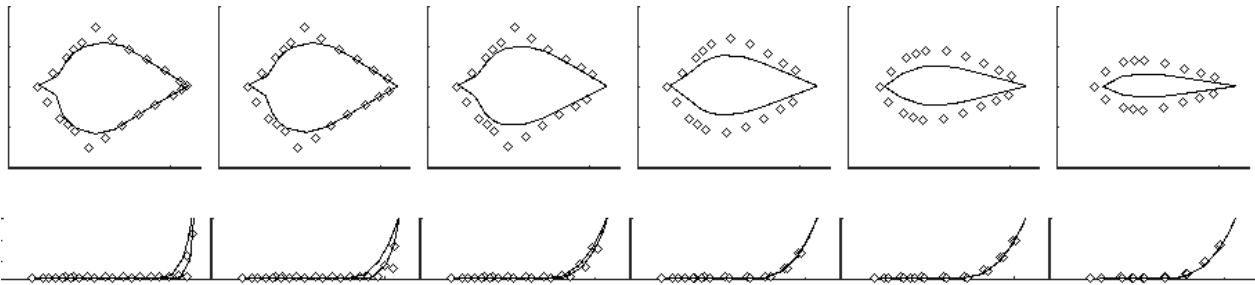
**FIGURE 42: projected area encircled by the seine ropes are plotted against the seine rope length. The star marks represent the flume tank results and the solid line the simulation.**

By using the rope length as the indicator for how far along the haul back procedure is we eliminate the effect of the experiment being imperfect (taking a small break in the hauling back). The  $R^2$  value is here showing reasonable agreement between experiment and simulation.

### 5.2.3 Combination Rope; Heavy; Slow

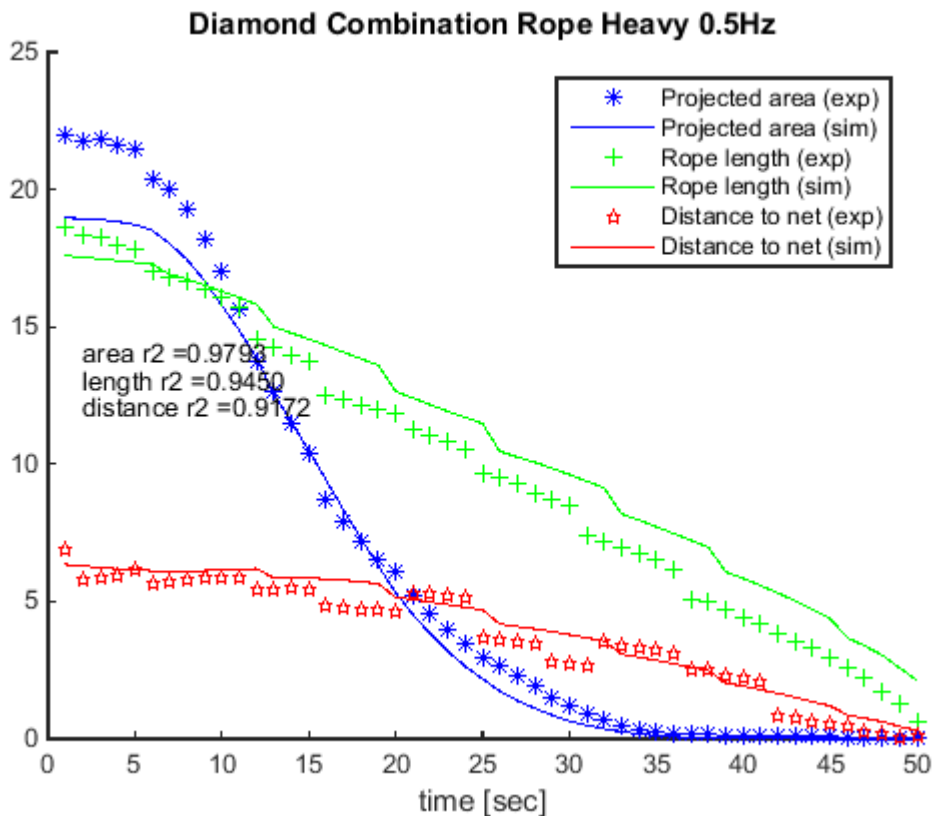
This section compares flume tank results to results from simulation for the combination rope laid out in a diamond shape, using the heavy weight and the slow winch speed.

FIGURE 43 shows the seine rope geometry seen from above and from the side. The time step between the pictures is four seconds. The solid lines represent the simulated result. Diamond marks represent the flume tank result. A good agreement between flume tank experiment and simulation is not present. The simulation appears to be running ahead of the experiment.



**FIGURE 43:** the geometry of the seine ropes seen from above and from the side. The six pictures are taken with four seconds interval. The diamond marks represent the flume tank results and the solid line the simulation.

FIGURE 44 plots respectively the projected area, the rope length and the distance to the net from the winch against the time.



**FIGURE 44:** shows the projected area [m<sup>2</sup>] encircled by the seine ropes, the seine rope length [m] and the distance [m] to the net from the winch plotted against time. The marks represent the flume tank results and the solid lines the simulation.

The agreement between flume tank experiment and simulation for the projected area, rope length and distance from winch to net is not evident. The projected area simulated being smaller than expected and the simulated rope length being larger. The simulation and experiment appear to be out of synchronisation.

FIGURE 45 shows the rope length versus the projected area. The simulation results are presented by a solid line while the experimental data is shown by star marks.

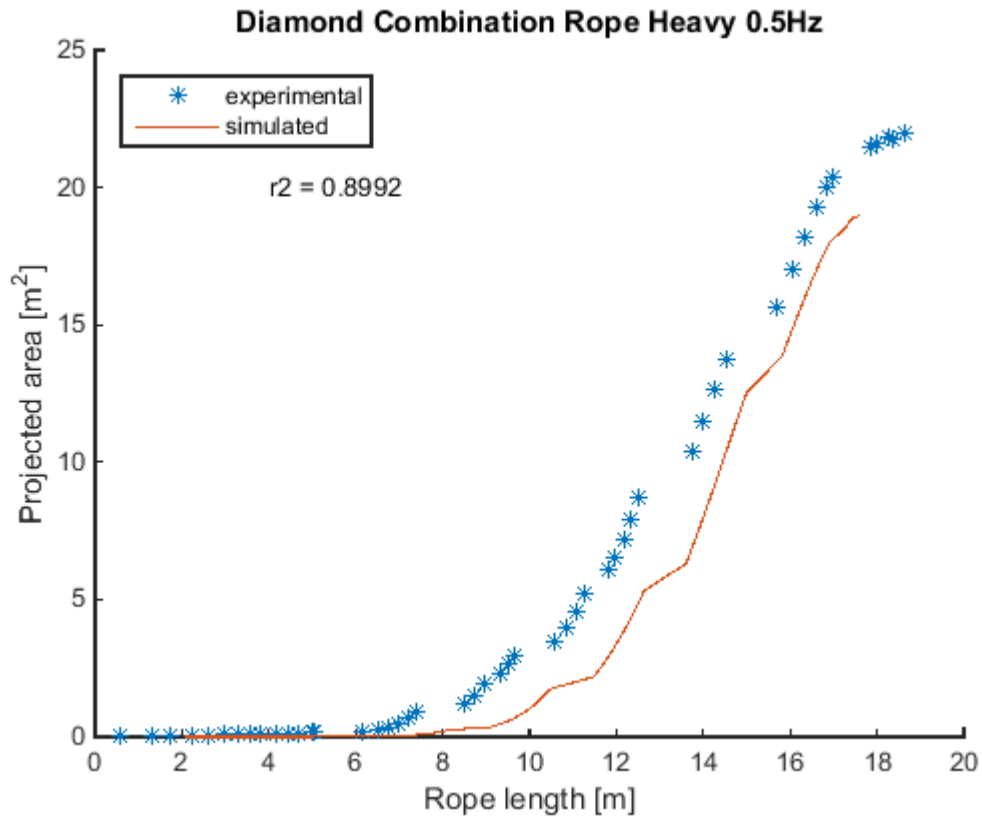


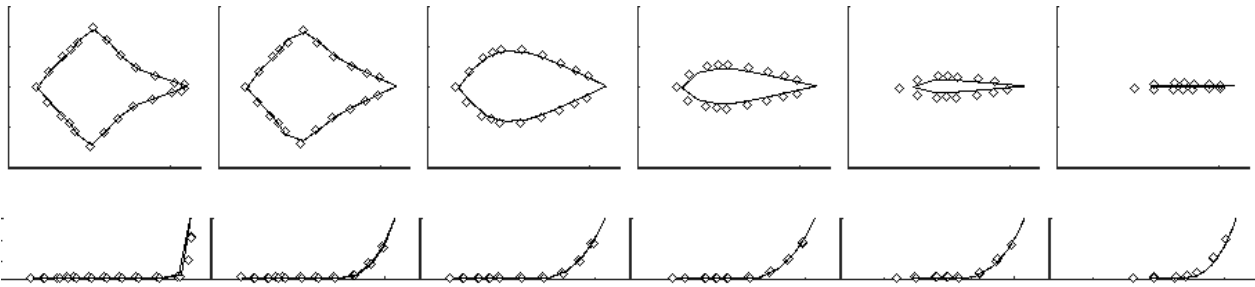
**FIGURE 45: projected area encircled by the seine ropes are plotted against the seine rope length. The star marks represent the flume tank results and the solid line the simulation.**

By using the rope length as the indicator for how far along the haul back procedure is we try to eliminate the effect of the experiment being imperfect (taking a small break in the hauling back). The  $R^2$  value is not showing good agreement between experiment and simulation since the value is below 0.9.

#### 5.2.4 Combination Rope; Heavy; Fast

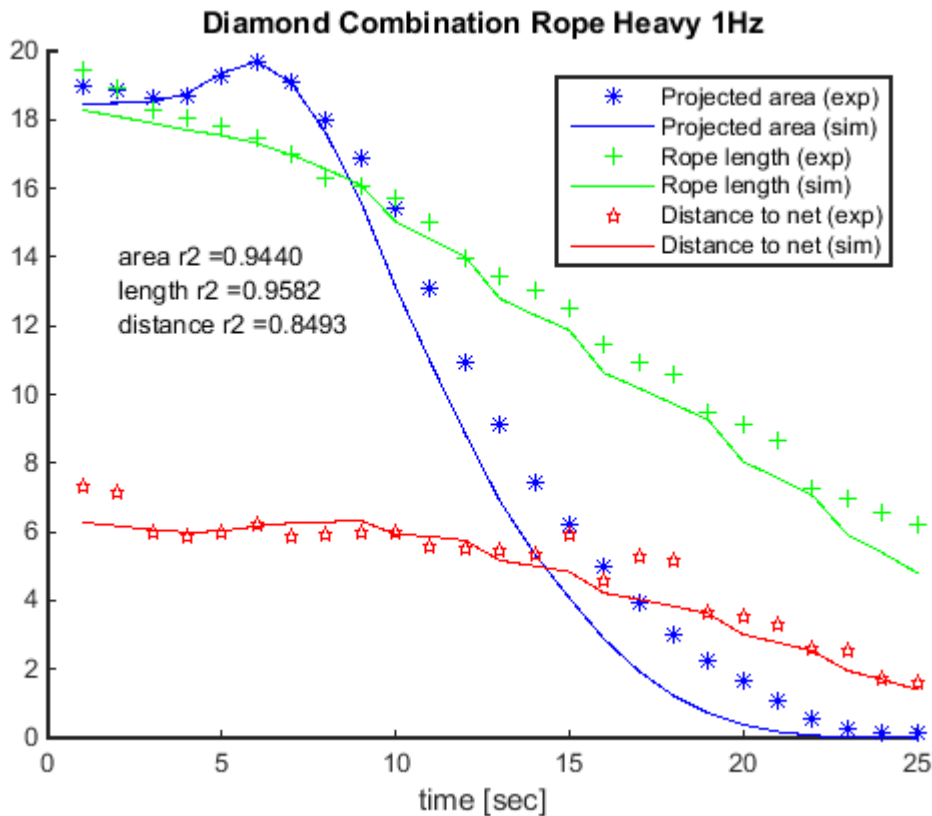
This section compares flume tank results to results from simulation for the combination rope laid out in a diamond shape, using the heavy weight and the fast winch speed.

FIGURE 46 shows the seine rope geometry seen from above and from the side. The time step between the pictures is four seconds. The solid lines represent the simulated result. Diamond marks represent the flume tank result. The agreement between flume tank experiment and simulation is evident.



**FIGURE 46:** the geometry of the seine ropes seen from above and from the side. The six pictures are taken with four seconds interval. The diamond marks represent the flume tank results and the solid line the simulation.

FIGURE 47 plots respectively the projected area, the rope length and the distance to the net from the winch against the time.



**FIGURE 47:** shows the projected area [m<sup>2</sup>] encircled by the seine ropes, the seine rope length [m] and the distance [m] to the net from the winch plotted against time. The marks represent the flume tank results and the solid lines the simulation.

The agreement between flume tank experiment and simulation for the projected area, rope length and distance from winch to net is evident.

FIGURE 48 shows the rope length versus the projected area. The simulation results are presented by a solid line while the experimental data is shown by star marks.

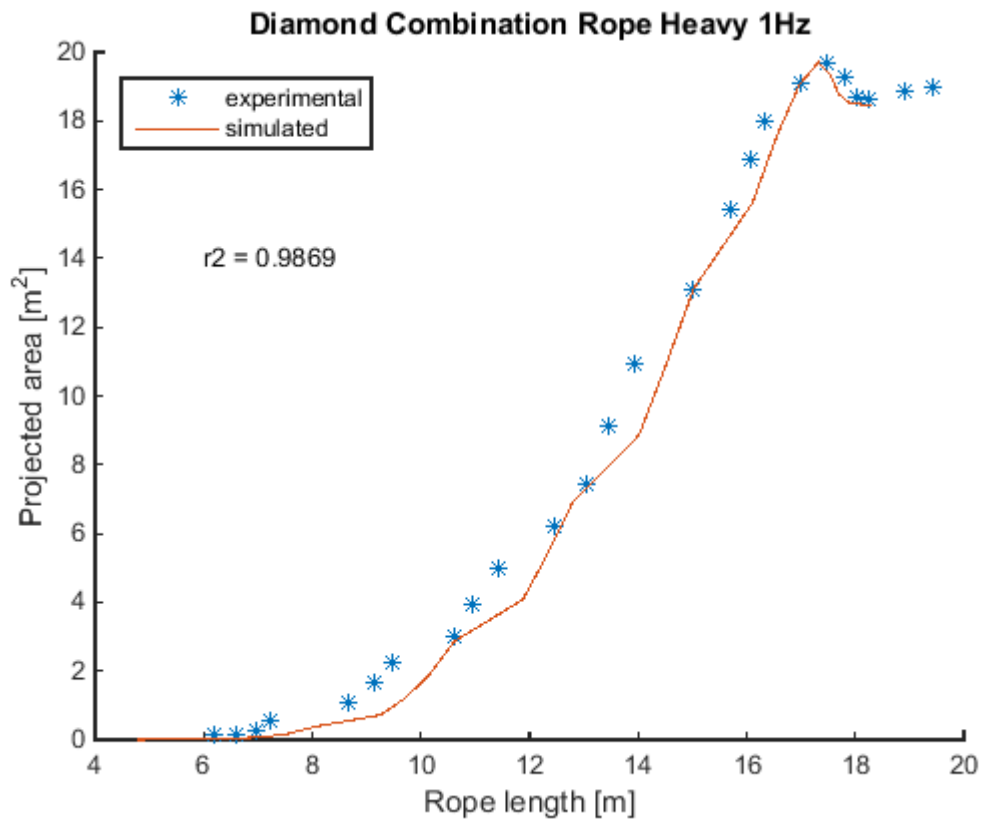


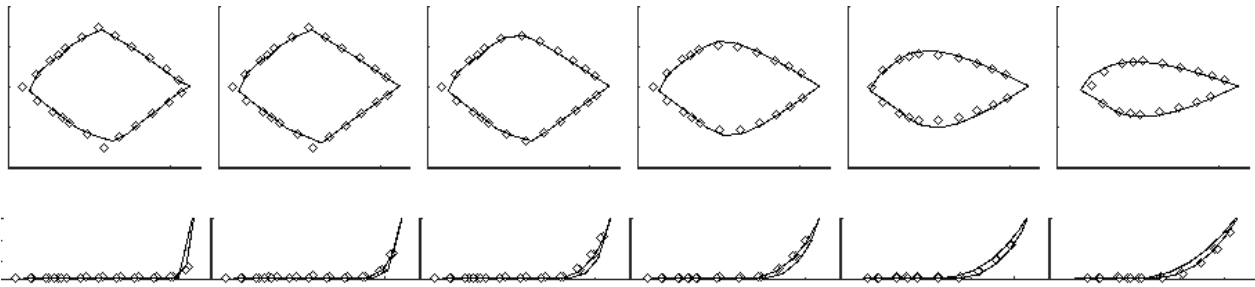
**FIGURE 48: projected area encircled by the seine ropes are plotted against the seine rope length. The star marks represent the flume tank results and the solid line the simulation.**

By using the rope length as the indicator for how far along the haul back procedure is we eliminate the effect of the experiment being imperfect (taking a small break in the hauling back). The  $R^2$  value is here showing good agreement between experiment and simulation.

### 5.2.5 Polyester Rope; Light; Slow

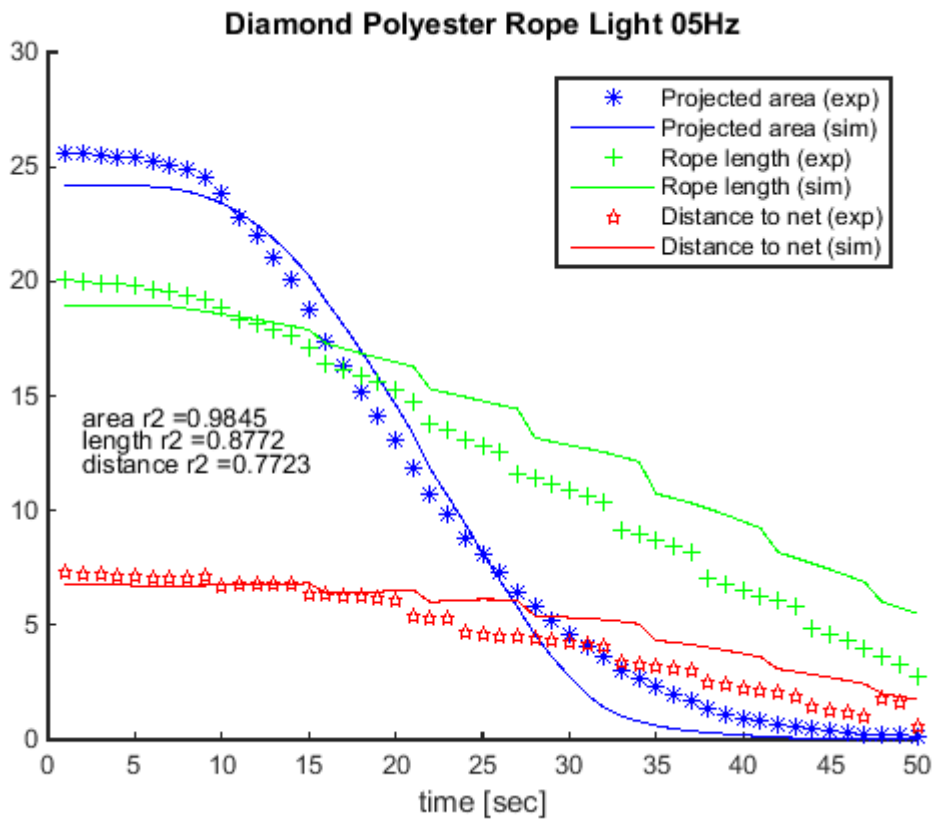
This section compares flume tank results to results from simulation for the combination rope laid out in a diamond shape, using the light weight and the slow winch speed.

FIGURE 37 shows the seine rope geometry seen from above and from the side. The time step between the pictures is four seconds. The solid lines represent the simulated result. Diamond marks represent the flume tank result. The agreement between flume tank experiment and simulation is evident.



**FIGURE 49:** the geometry of the seine ropes seen from above and from the side. The six pictures are taken with four seconds interval. The diamond marks represent the flume tank results and the solid line the simulation.

FIGURE 50 plots respectively the projected area, the rope length and the distance to the net from the winch against the time.



**FIGURE 50:** shows the projected area [m<sup>2</sup>] encircled by the seine ropes, the seine rope length [m] and the distance [m] to the net from the winch plotted against time. The marks represent the flume tank results and the solid lines the simulation.

The agreement between flume tank experiment and simulation for the projected area, rope length and distance from winch to net is not evident.

FIGURE 51 shows the rope length versus the projected area. The simulation results are presented by a solid line while the experimental data is shown by star marks.



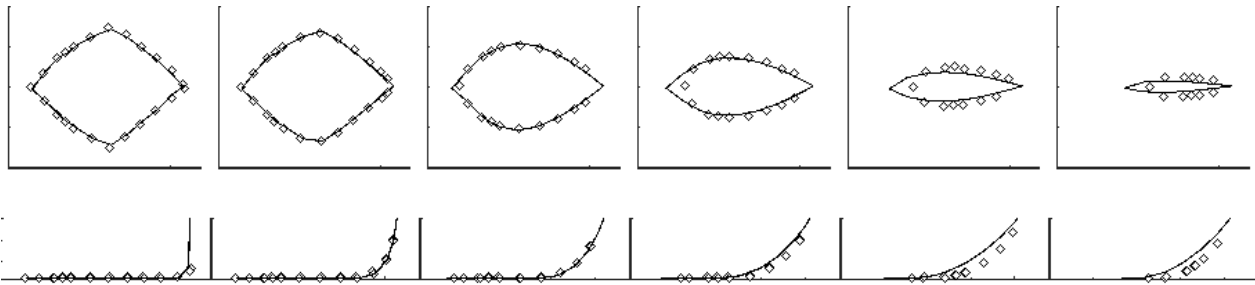


**FIGURE 52:** the geometry of the seine ropes seen from above and from the side. The six pictures are taken with four seconds interval. The diamond marks represent the flume tank results and the solid line the simulation.

FIGURE 53 plots respectively the projected area, the rope length and the distance to the net from the winch against the time.

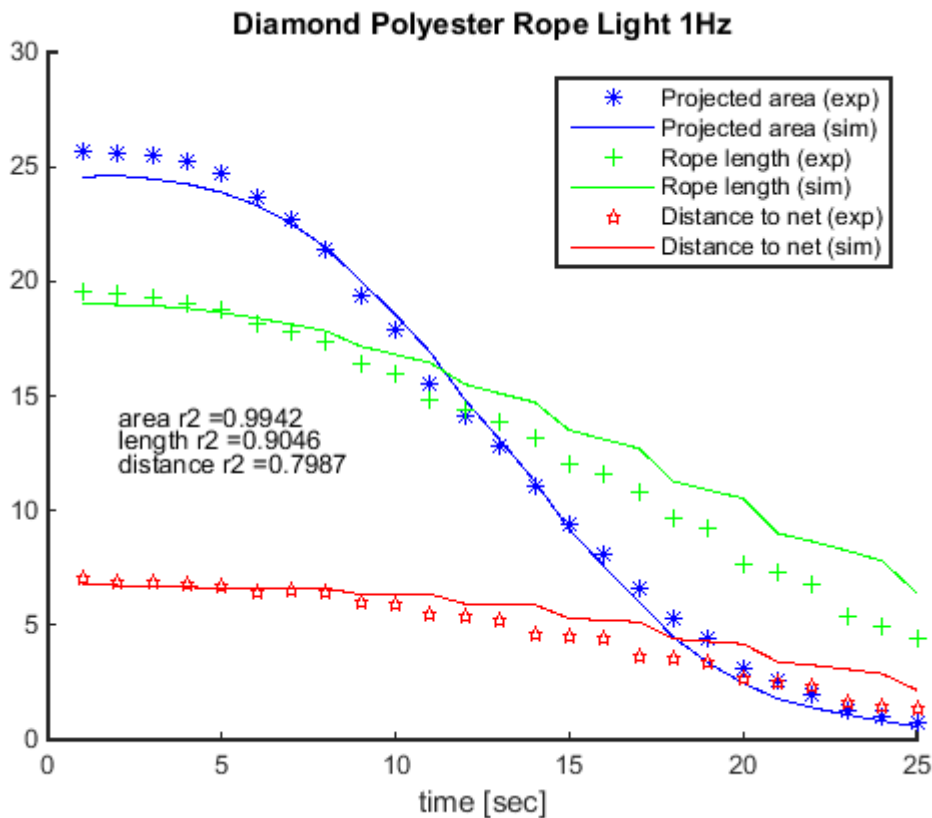


**FIGURE 53:** shows the projected area [m<sup>2</sup>] encircled by the seine ropes, the seine rope length [m] and the distance [m] to the net from the winch plotted against time. The marks represent the flume tank results and the solid lines the simulation.

The agreement between flume tank experiment and simulation for the projected area is evident, while the rope length and distance from winch to net is not.

FIGURE 54 shows the rope length versus the projected area. The simulation results are presented by a solid line while the experimental data is shown by star marks.



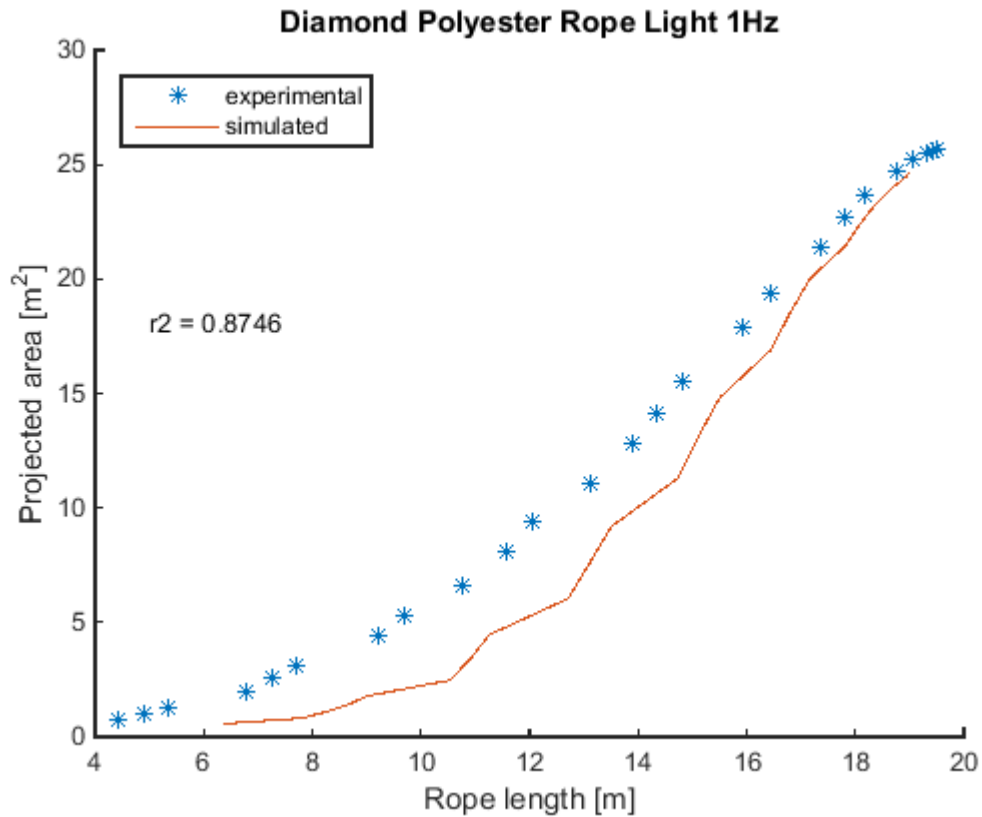


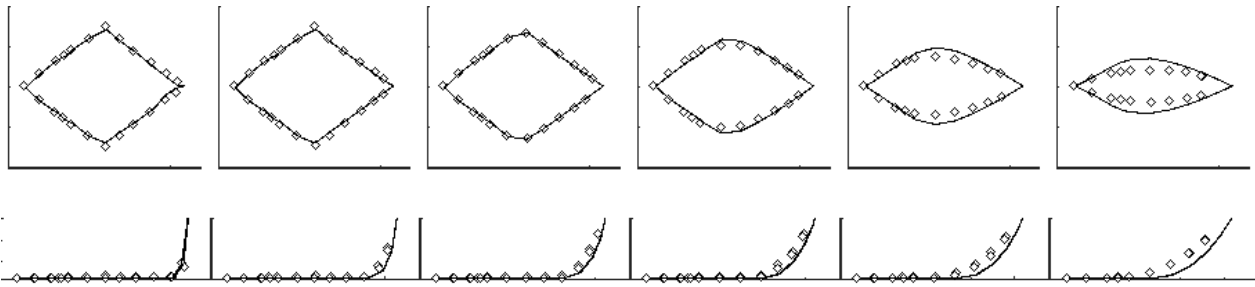
**FIGURE 54: projected area encircled by the seine ropes are plotted against the seine rope length. The star marks represent the flume tank results and the solid line the simulation.**

By using the rope length as the indicator for how far along the haul back procedure is we eliminate the effect of the experiment being imperfect (taking a small break in the hauling back). The  $R^2$  value is not showing good agreement between experiment and simulation.

**5.2.7 Polyester Rope; Heavy; Slow**

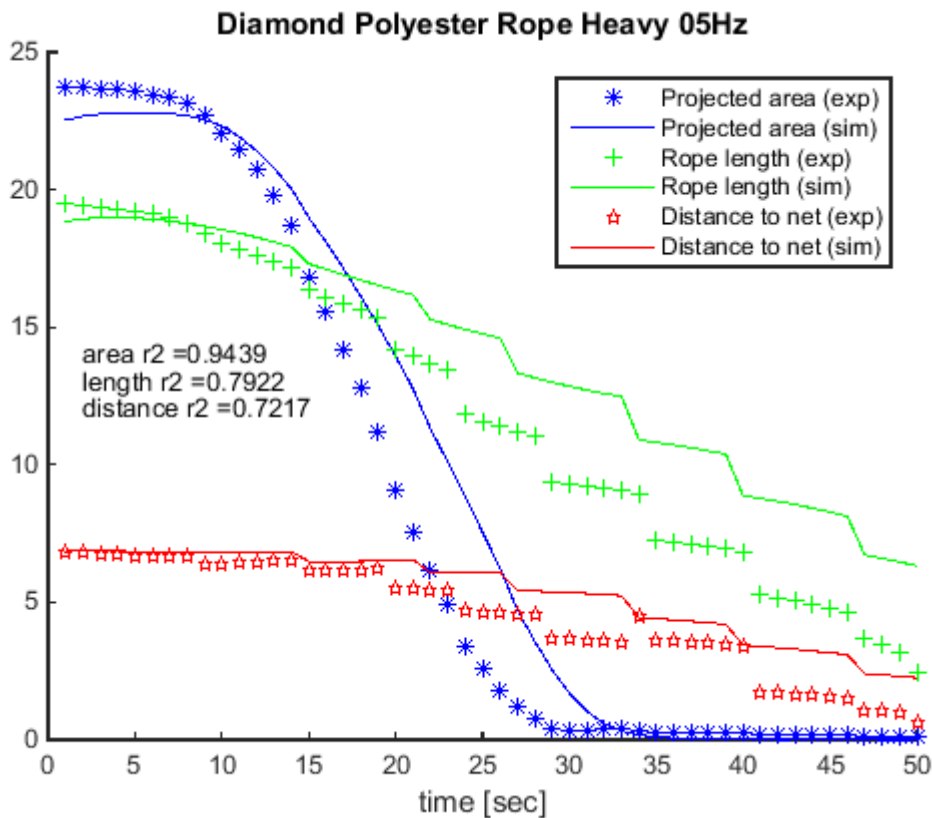
This section compares flume tank results to results from simulation for the combination rope laid out in a diamond shape, using the heavy weight and the slow winch speed.

FIGURE 55 shows the seine rope geometry seen from above and from the side. The time step between the pictures is four seconds. The solid lines represent the simulated result. Diamond marks represent the flume tank result. The agreement between flume tank experiment and simulation is evident initially, later the experimental results appears to run ahead of the simulation.



**FIGURE 55:** the geometry of the seine ropes seen from above and from the side. The six pictures are taken with four seconds interval. The diamond marks represent the flume tank results and the solid line the simulation.

FIGURE 56 plots respectively the projected area, the rope length and the distance to the net from the winch against the time.



**FIGURE 56:** shows the projected area [m<sup>2</sup>] encircled by the seine ropes, the seine rope length [m] and the distance [m] to the net from the winch plotted against time. The marks represent the flume tank results and the solid lines the simulation.

The agreement between flume tank experiment and simulation for the projected area, rope length and distance from winch to net is not evident.

FIGURE 57 shows the rope length versus the projected area. The simulation results are presented by a solid line while the experimental data is shown by star marks.

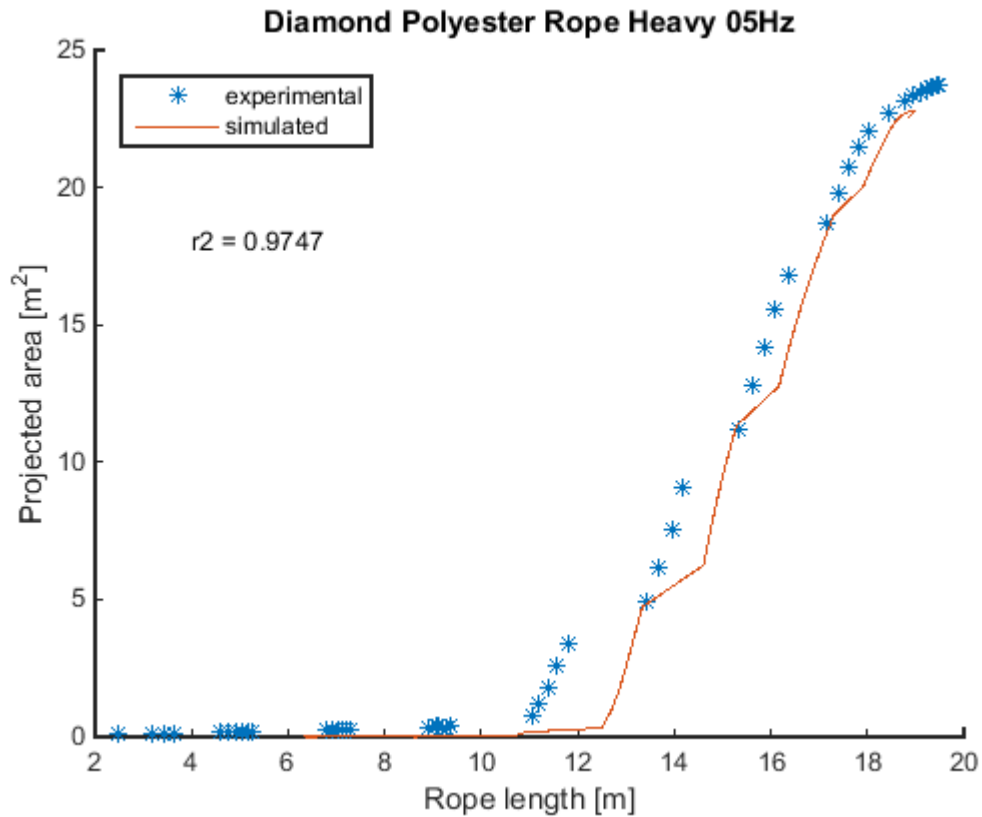


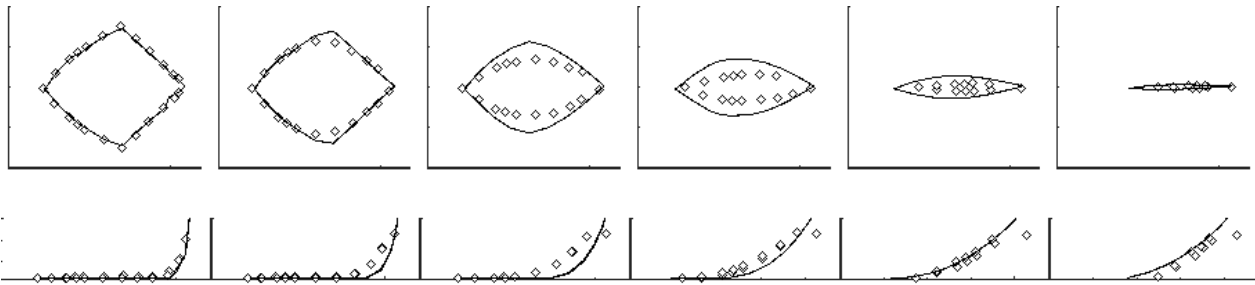
**FIGURE 57: projected area encircled by the seine ropes are plotted against the seine rope length. The star marks represent the flume tank results and the solid line the simulation.**

By using the rope length as the indicator for how far along the haul back procedure is we eliminate the effect of the experiment being imperfect (taking a small break in the hauling back). The  $R^2$  value is showing good agreement between experiment and simulation.

### 5.2.8 Polyester Rope; Heavy; Fast

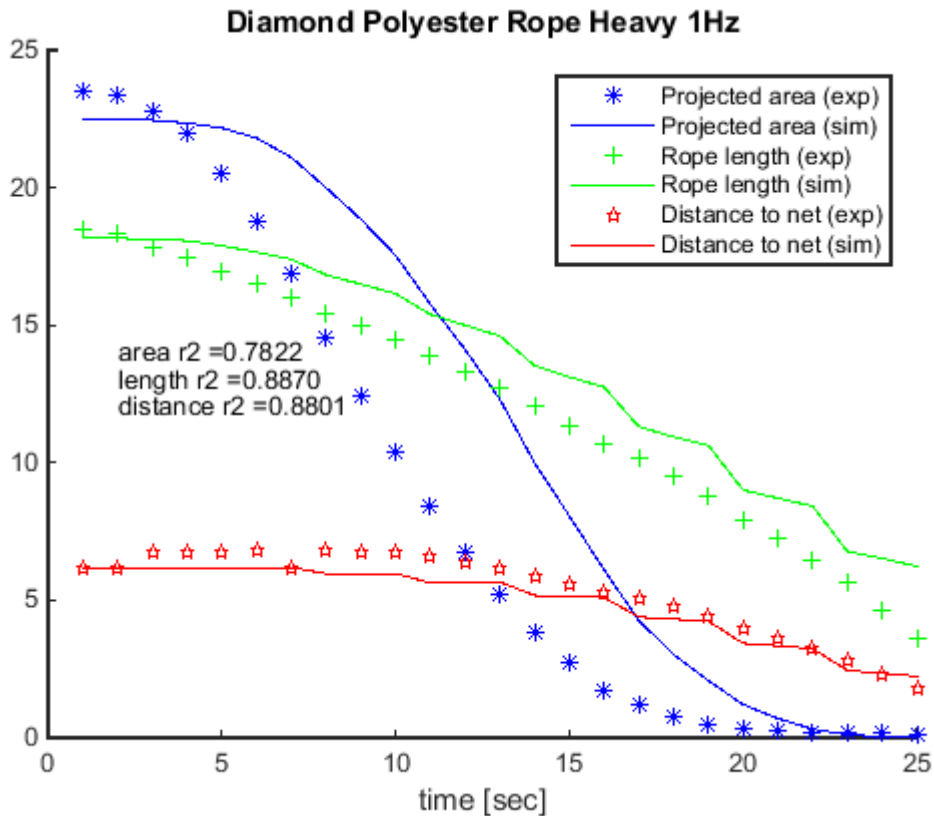
This section compares flume tank results to results from simulation for the combination rope laid out in a diamond shape, using the heavy weight and the fast winch speed.

FIGURE 58 shows the seine rope geometry seen from above and from the side. The time step between the pictures is four seconds. The solid lines represent the simulated result. Diamond marks represent the flume tank result. The agreement between flume tank experiment and simulation is not evident the experimental results appears to run ahead of the simulation.



**FIGURE 58:** the geometry of the seine ropes seen from above and from the side. The six pictures are taken with four seconds interval. The diamond marks represent the flume tank results and the solid line the simulation.

FIGURE 59 plots respectively the projected area, the rope length and the distance to the net from the winch against the time.



**FIGURE 59:** shows the projected area [m<sup>2</sup>] encircled by the seine ropes, the seine rope length [m] and the distance [m] to the net from the winch plotted against time. The marks represent the flume tank results and the solid lines the simulation.

The agreement between flume tank experiment and simulation for the projected area, rope length and distance from winch to net is not evident. The experiment appears significantly out of synchronisation with the simulation.

FIGURE 60 shows the rope length versus the projected area. The simulation results are presented by a solid line while the experimental data is shown by star marks.

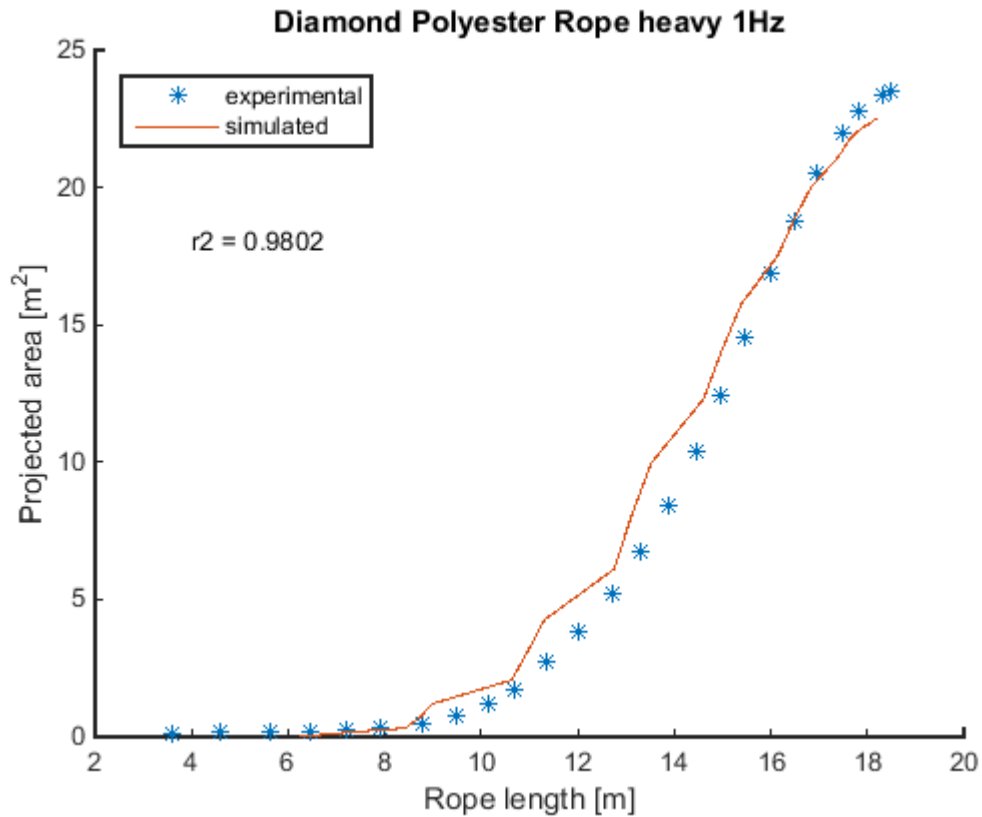


**FIGURE 60: projected area encircled by the seine ropes are plotted against the seine rope length. The star marks represent the flume tank results and the solid line the simulation.**

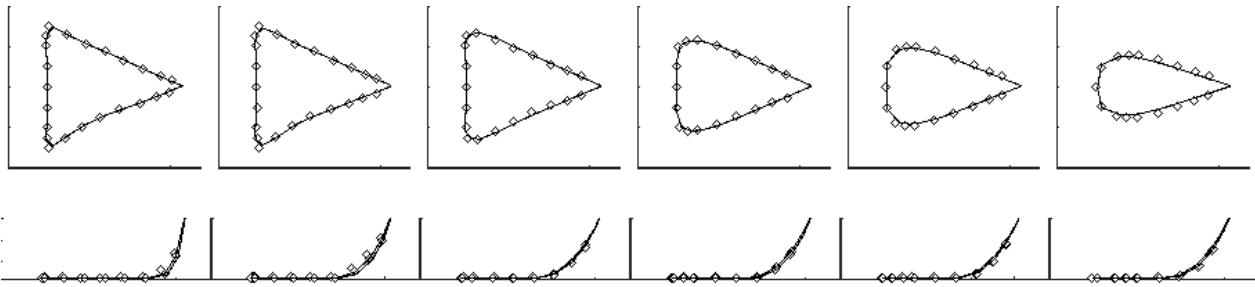
By using the rope length as the indicator for how far along the haul back procedure is we eliminate the effect of the experiment being imperfect (taking a small break in the hauling back). The  $R^2$  value is showing good agreement between experiment and simulation.

### 5.3 Triangle Layout

#### 5.3.1 Combination Rope; Light; Slow

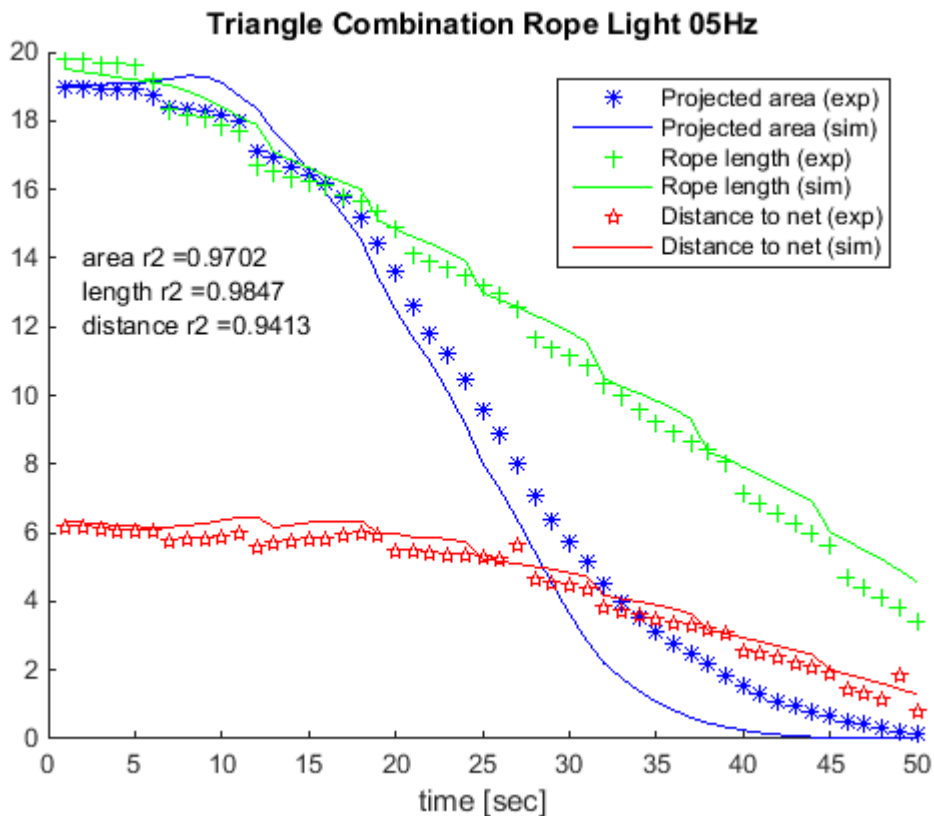
This section compares flume tank results to results from simulation for the combination rope laid out in a triangle, using the light weight and the slow winch speed.

FIGURE 61 shows the seine rope geometry seen from above and from the side. The time step between the pictures is four seconds. The solid lines represent the simulated result. Diamond marks represent the flume tank result. The agreement between flume tank experiment and simulation is evident.



**FIGURE 61:** the geometry of the seine ropes seen from above and from the side. The six pictures are taken with four seconds interval. The diamond marks represent the flume tank results and the solid line the simulation.

FIGURE 62 plots respectively the projected area, the rope length and the distance to the net from the winch against the time.



**FIGURE 62:** Shown here is projected area encircled by the seine ropes, the seine rope length and the distance to the net plotted against time.

The agreement between flume tank experiment and simulation for the projected area, rope length and distance from winch to net is evident.

FIGURE 63 shows the rope length versus the projected area. The simulation results are presented by a solid line while the experimental data is shown by star marks.

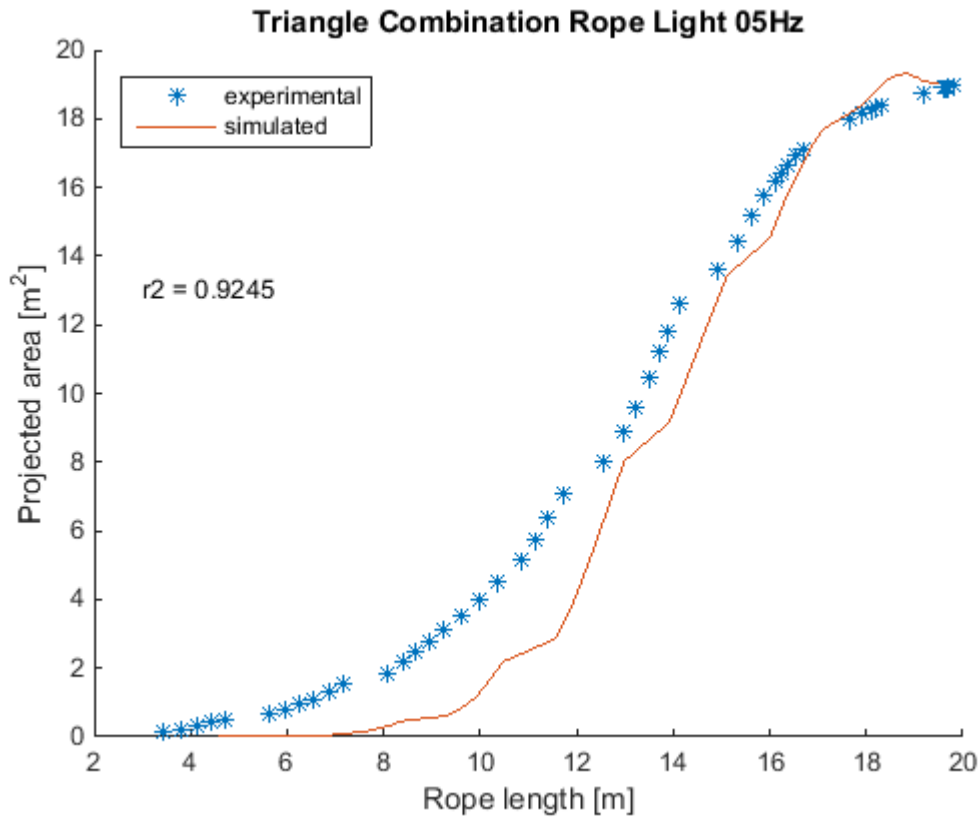


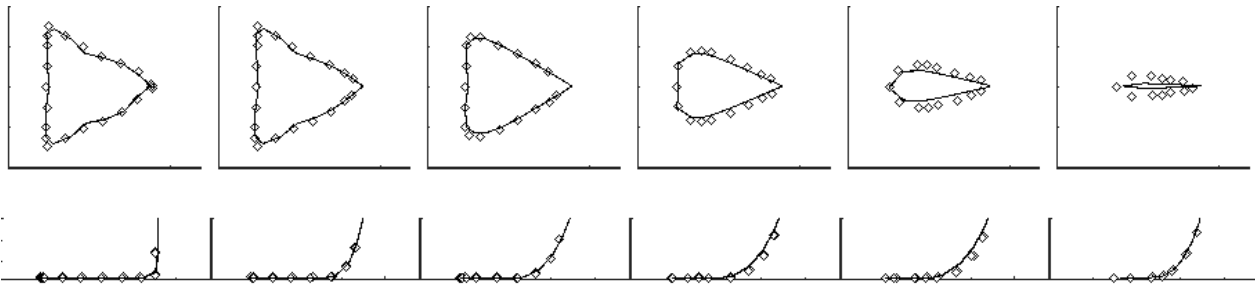
**FIGURE 63: projected area encircled by the seine ropes are plotted against the seine rope length. The star marks represent the flume tank results and the solid line the simulation.**

By using the rope length as the indicator for how far along the haul back procedure is we eliminate the effect of the experiment being imperfect (taking a small break in the hauling back). The  $R^2$  value is showing good agreement between experiment and simulation.

### 5.3.2 Combination Rope; Light; Fast

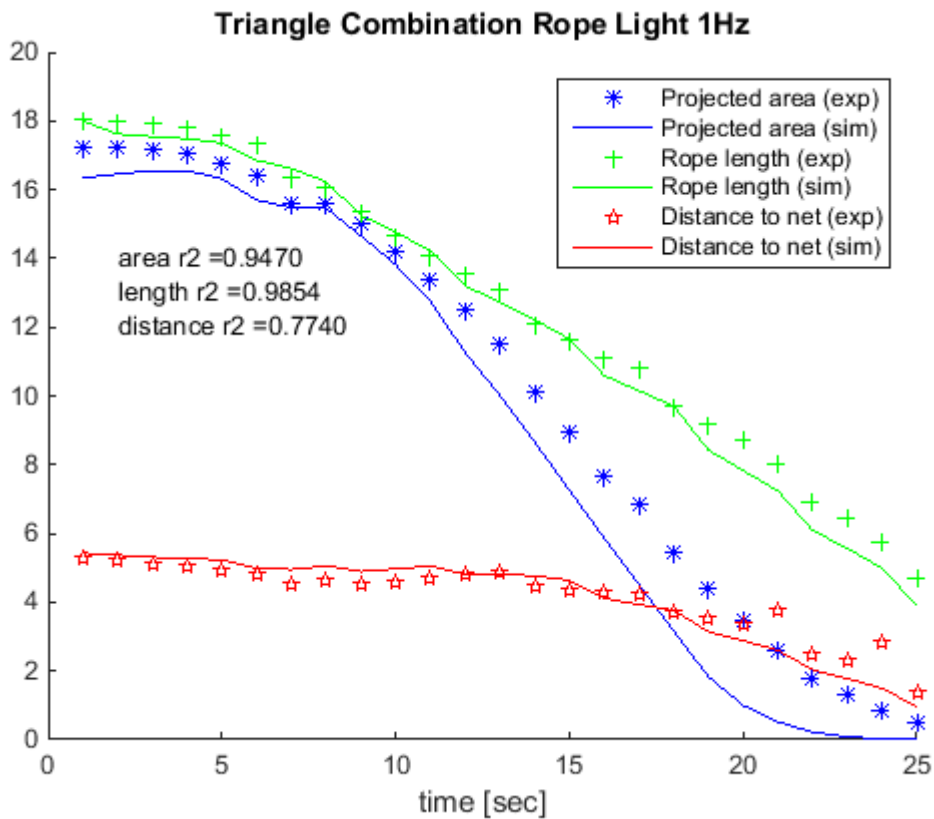
This section compares flume tank results to results from simulation for the combination rope laid out in a triangle, using the light weight and the fast winch speed.

FIGURE 64 shows the seine rope geometry seen from above and from the side. The time step between the pictures is four seconds. The solid lines represent the simulated result. Diamond marks represent the flume tank result. The agreement between flume tank experiment and simulation is evident.



**FIGURE 64:** the geometry of the seine ropes seen from above and from the side. The six pictures are taken with four seconds interval. The diamond marks represent the flume tank results and the solid line the simulation.

FIGURE 65 plots respectively the projected area, the rope length and the distance to the net from the winch against the time.



**FIGURE 65:** shows the projected area [m<sup>2</sup>] encircled by the seine ropes, the seine rope length [m] and the distance [m] to the net from the winch plotted against time. The marks represent the flume tank results and the solid lines the simulation.

The agreement between flume tank experiment and simulation for the projected area, rope length and distance from winch to net is evident.

FIGURE 66 shows the rope length versus the projected area. The simulation results are presented by a solid line while the experimental data is shown by star marks.



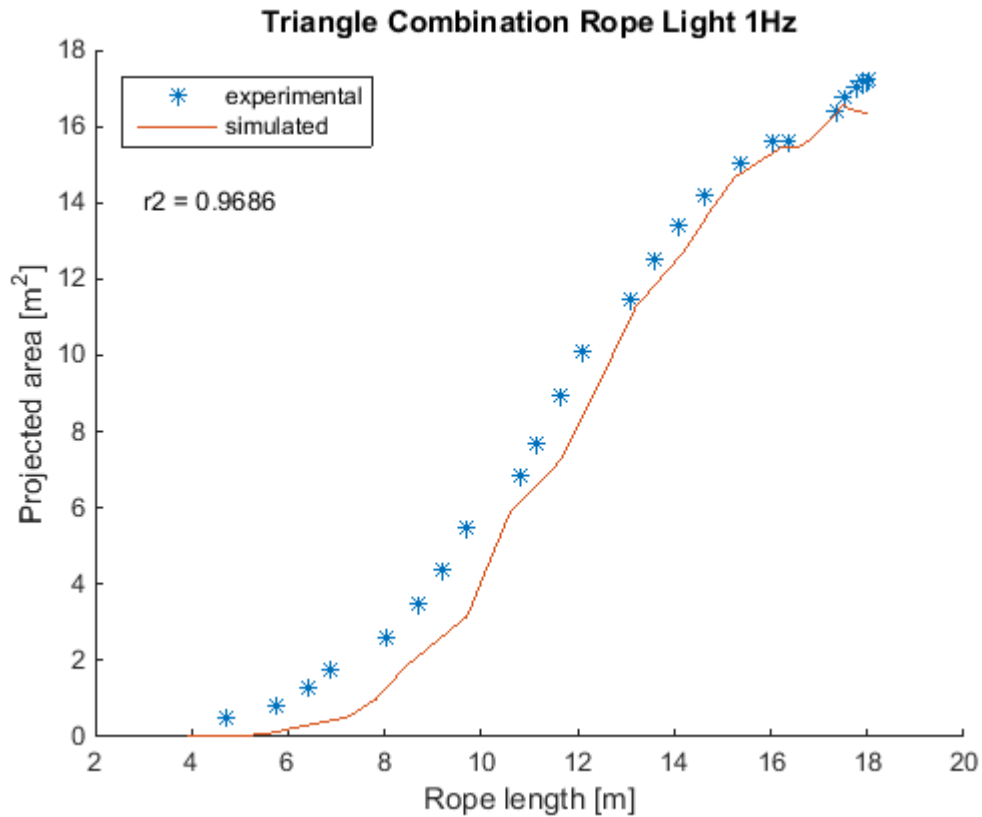


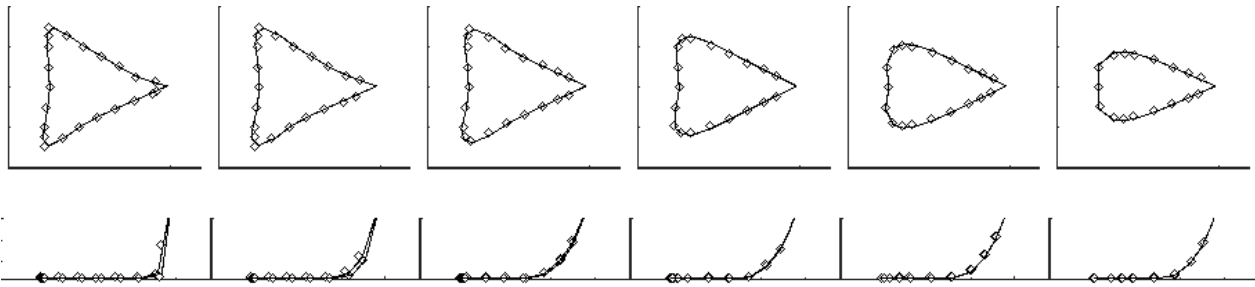
**FIGURE 66: projected area encircled by the seine ropes are plotted against the seine rope length. The star marks represent the flume tank results and the solid line the simulation.**

By using the rope length as the indicator for how far along the haul back procedure is we eliminate the effect of the experiment being imperfect (taking a small break in the hauling back). The  $R^2$  value is showing good agreement between experiment and simulation.

**5.3.3 Combination Rope; Heavy; Slow**

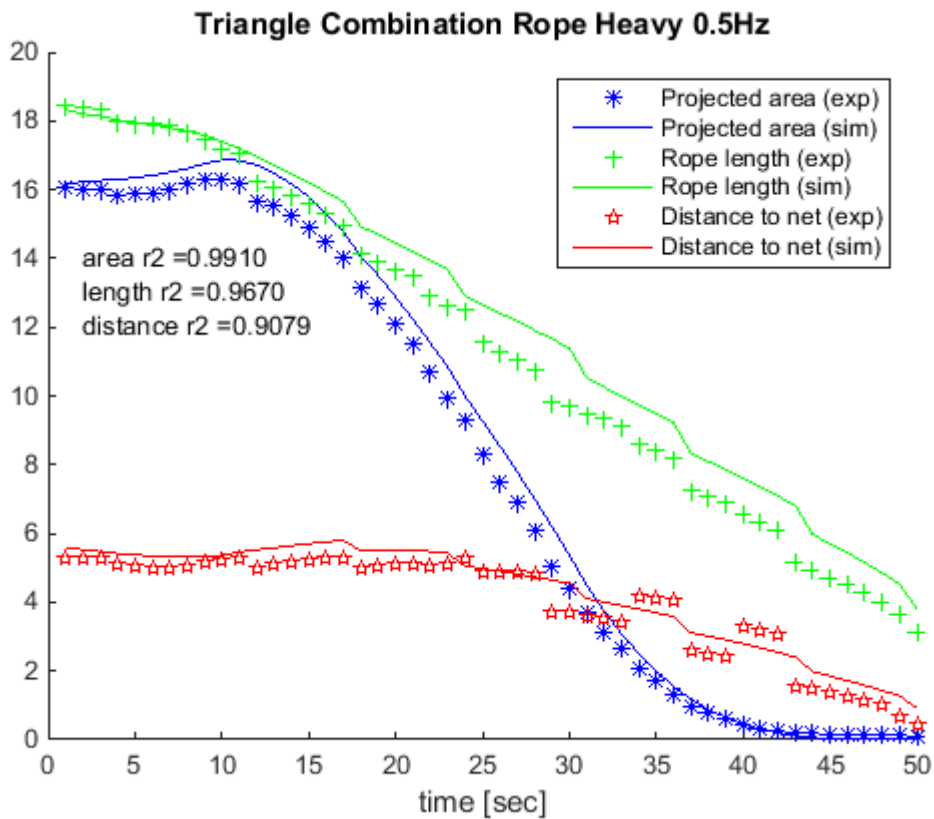
This section compares flume tank results to results from simulation for the combination rope laid out in a triangle, using the heavy weight and the slow winch speed.

FIGURE 67 shows the seine rope geometry seen from above and from the side. The time step between the pictures is four seconds. The solid lines represent the simulated result. Diamond marks represent the flume tank result. The agreement between flume tank experiment and simulation is evident



**FIGURE 67:** the geometry of the seine ropes seen from above and from the side. The six pictures are taken with four seconds interval. The diamond marks represent the flume tank results and the solid line the simulation.

FIGURE 68 plots respectively the projected area, the rope length and the distance to the net from the winch against the time.



**FIGURE 68:** shows the projected area [m<sup>2</sup>] encircled by the seine ropes, the seine rope length [m] and the distance [m] to the net from the winch plotted against time. The marks represent the flume tank results and the solid lines the simulation.

The agreement between flume tank experiment and simulation for the projected area, rope length and distance from winch to net is evident.

FIGURE 69 shows the rope length versus the projected area. The simulation results are presented by a solid line while the experimental data is shown by star marks.

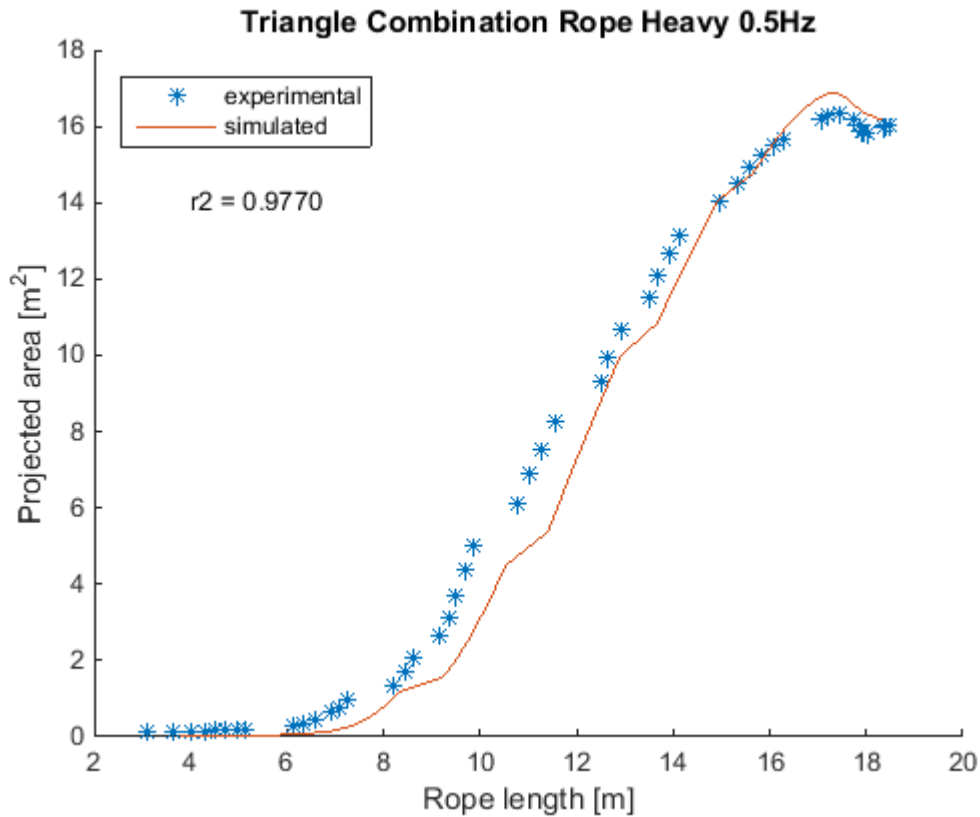


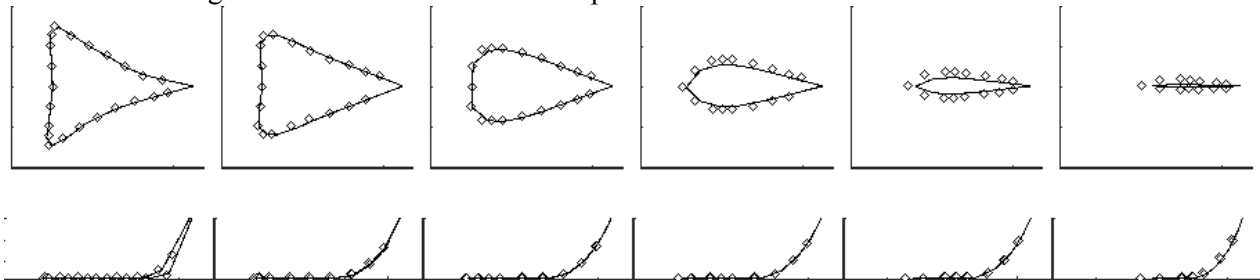
**FIGURE 69:** projected area encircled by the seine ropes are plotted against the seine rope length. The star marks represent the flume tank results and the solid line the simulation.

By using the rope length as the indicator for how far along the haul back procedure is we eliminate the effect of the experiment being imperfect (taking a small break in the hauling back). The  $R^2$  value is showing good agreement between experiment and simulation.

**5.3.4 Combination Rope; Heavy; Fast**

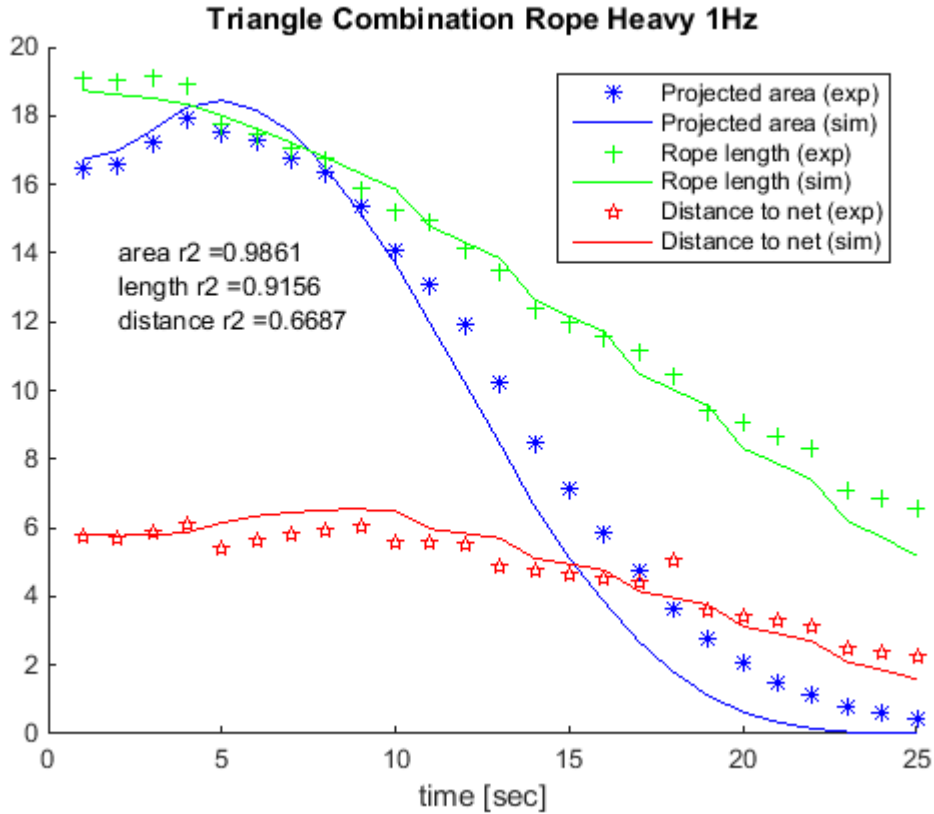
This section compares flume tank results to results from simulation for the combination rope laid out in a triangle, using the heavy weight and the fast winch speed.

FIGURE 70 shows the seine rope geometry seen from above and from the side. The time step between the pictures is four seconds. The solid lines represent the simulated result. Diamond marks represent the flume tank result. The agreement between flume tank experiment and simulation is evident.



**FIGURE 70:** the geometry of the seine ropes seen from above and from the side. The six pictures are taken with four seconds interval. The diamond marks represent the flume tank results and the solid line the simulation.

FIGURE 71 plots respectively the projected area, the rope length and the distance to the net from the winch against the time.



**FIGURE 71:** shows the projected area [m<sup>2</sup>] encircled by the seine ropes, the seine rope length [m] and the distance [m] to the net from the winch plotted against time. The marks represent the flume tank results and the solid lines the simulation.

The agreement between flume tank experiment and simulation for the projected area, rope length and distance from winch to net is evident.

FIGURE 72 shows the rope length versus the projected area. The simulation results are presented by a solid line while the experimental data is shown by star marks.

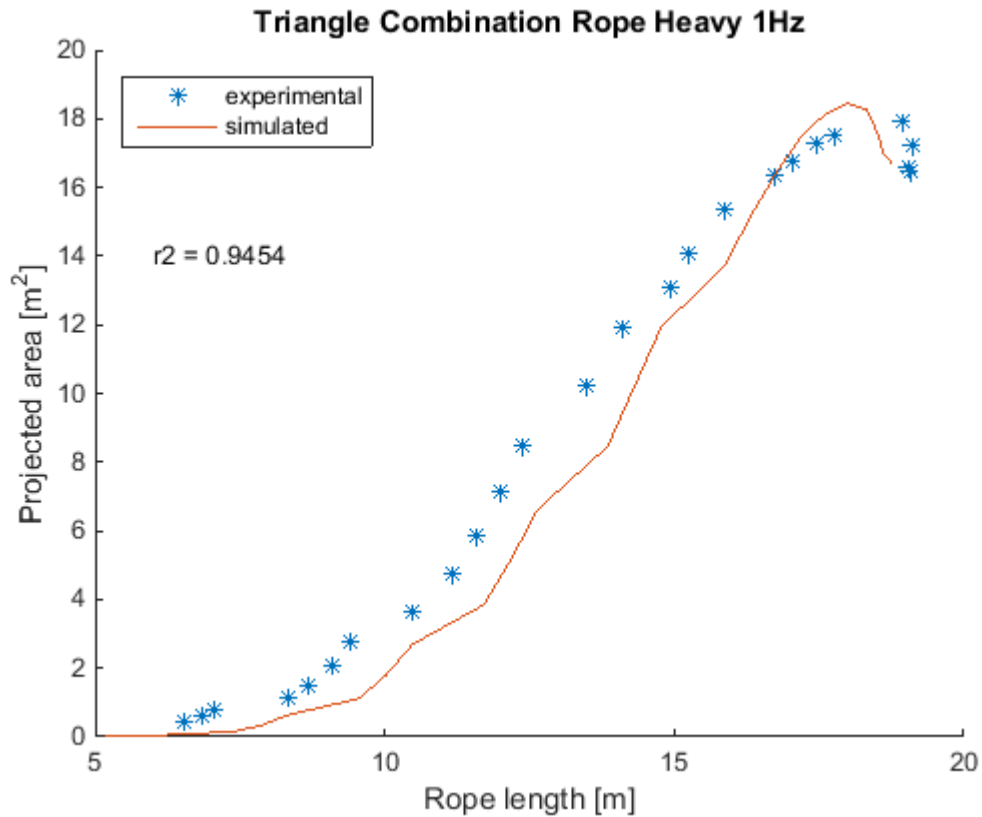


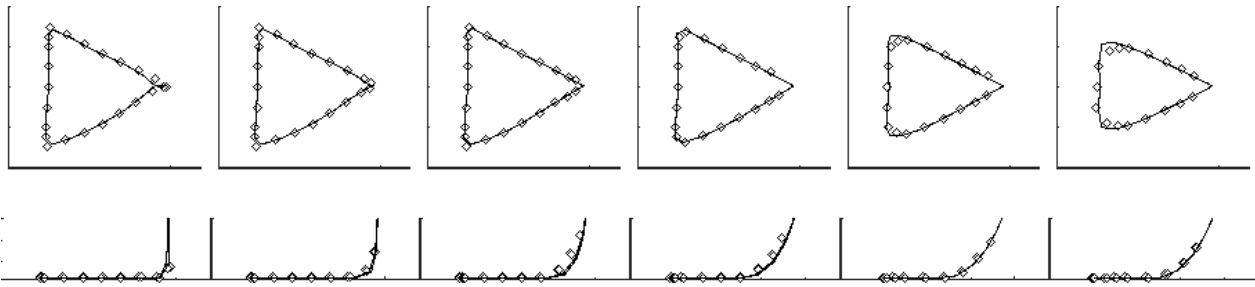
**FIGURE 72: projected area encircled by the seine ropes are plotted against the seine rope length. The star marks represent the flume tank results and the solid line the simulation.**

By using the rope length as the indicator for how far along the haul back procedure is we eliminate the effect of the experiment being imperfect (taking a small break in the hauling back). The  $R^2$  value is showing good agreement between experiment and simulation.

**5.3.5 Polyester Rope; Light; Slow**

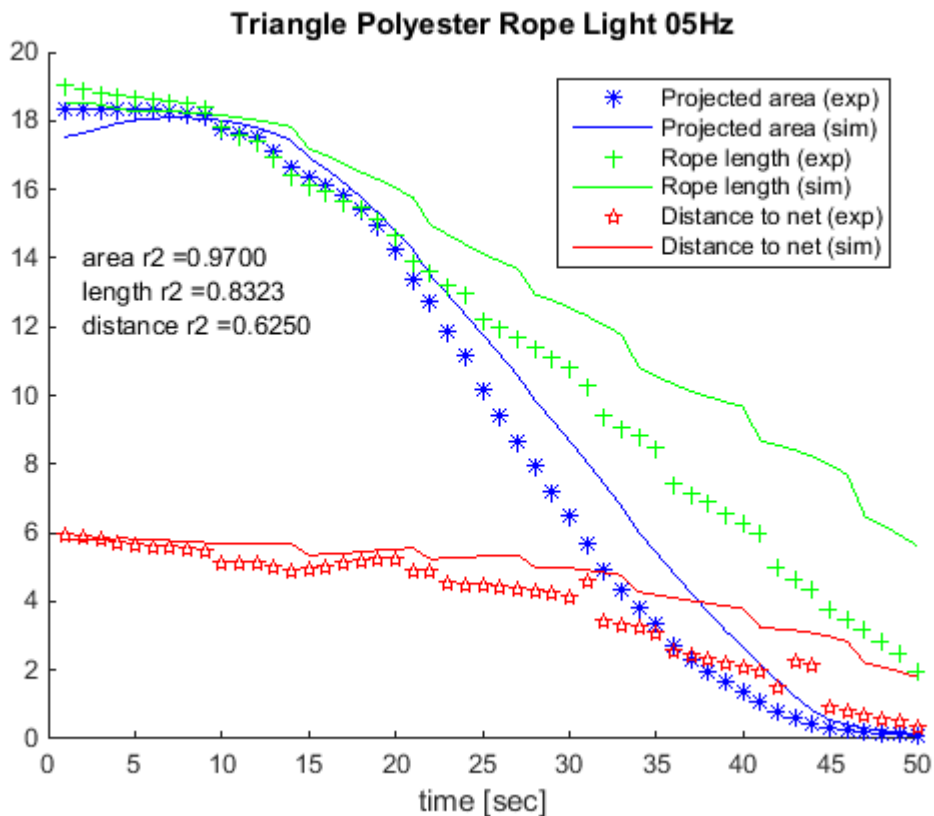
This section compares flume tank results to results from simulation for the polyester rope laid out in a triangle, using the light weight and the slow winch speed.

FIGURE 73 shows the seine rope geometry seen from above and from the side. The time step between the pictures is four seconds. The solid lines represent the simulated result. Diamond marks represent the flume tank result. The agreement between flume tank experiment and simulation is evident.



**FIGURE 73:** the geometry of the seine ropes seen from above and from the side. The six pictures are taken with four seconds interval. The diamond marks represent the flume tank results and the solid line the simulation.

FIGURE 74 plots respectively the projected area, the rope length and the distance to the net from the winch against the time.



**FIGURE 74:** shows the projected area [m<sup>2</sup>] encircled by the seine ropes, the seine rope length [m] and the distance [m] to the net from the winch plotted against time. The marks represent the flume tank results and the solid lines the simulation.

The agreement between flume tank experiment and simulation for the projected area and distance from winch to net is evident. The rope length is not in good agreement between experiment and simulation.

FIGURE 75 shows the rope length versus the projected area. The simulation results are presented by a solid line while the experimental data is shown by star marks.

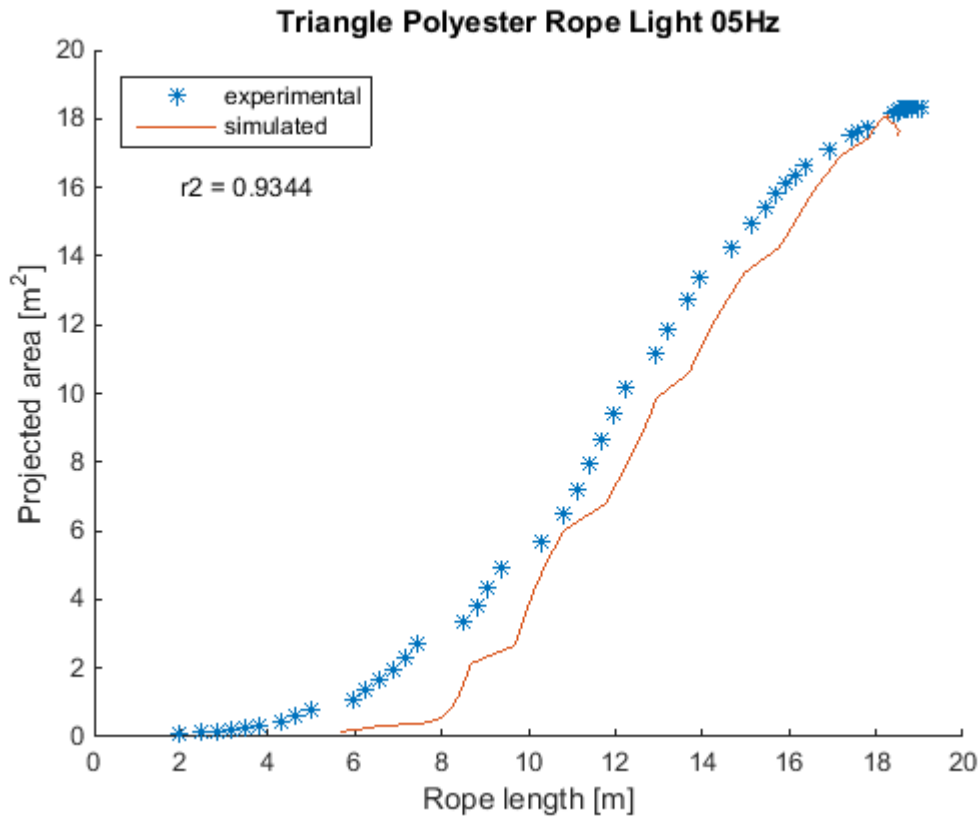


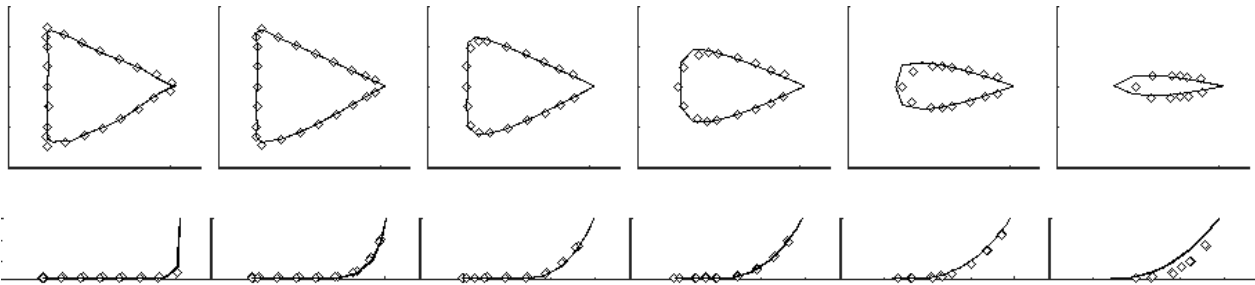
**FIGURE 75: projected area encircled by the seine ropes are plotted against the seine rope length. The star marks represent the flume tank results and the solid line the simulation.**

By using the rope length as the indicator for how far along the haul back procedure is we eliminate the effect of the experiment being imperfect (taking a small break in the hauling back). The  $R^2$  value is showing good agreement between experiment and simulation.

### 5.3.6 Polyester Rope; Light; Fast

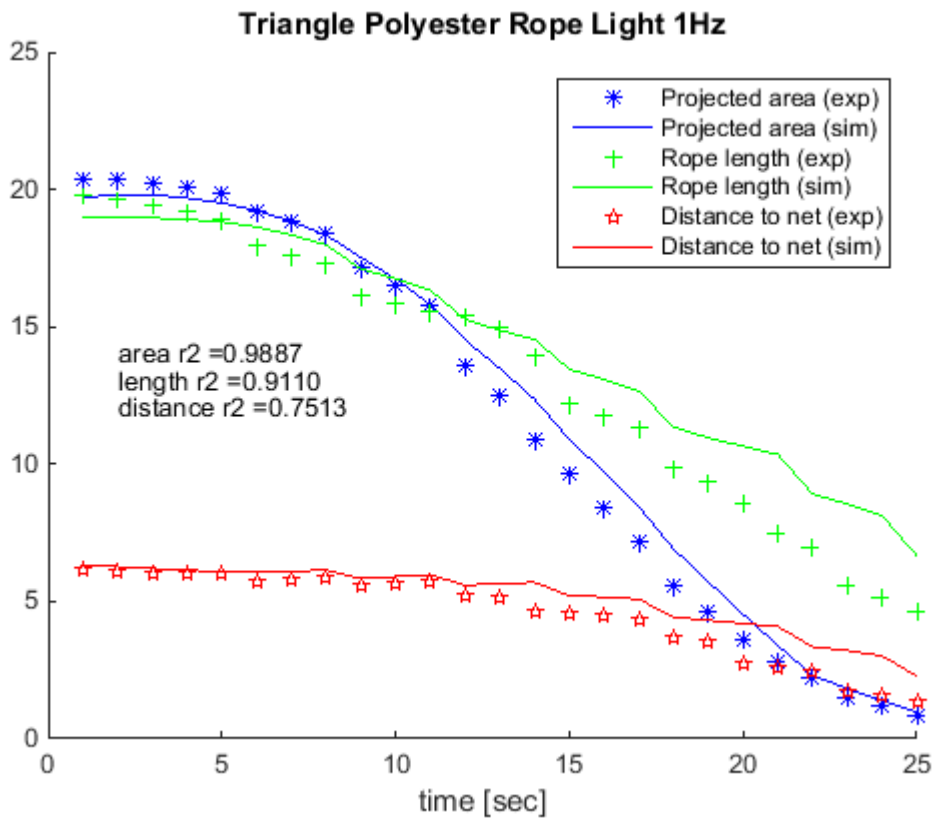
This section compares flume tank results to results from simulation for the polyester rope laid out in a triangle, using the light weight and the fast winch speed.

FIGURE 76 shows the seine rope geometry seen from above and from the side. The time step between the pictures is four seconds. The solid lines represent the simulated result. Diamond marks represent the flume tank result. The agreement between flume tank experiment and simulation is evident.



**FIGURE 76:** the geometry of the seine ropes seen from above and from the side. The six pictures are taken with four seconds interval. The diamond marks represent the flume tank results and the solid line the simulation.

FIGURE 77 plots respectively the projected area, the rope length and the distance to the net from the winch against the time.



**FIGURE 77:** shows the projected area [m<sup>2</sup>] encircled by the seine ropes, the seine rope length [m] and the distance [m] to the net from the winch plotted against time. The marks represent the flume tank results and the solid lines the simulation.

The agreement between flume tank experiment and simulation for the projected area, rope length and distance from winch to net is evident.

FIGURE 78 shows the rope length versus the projected area. The simulation results are presented by a solid line while the experimental data is shown by star marks.



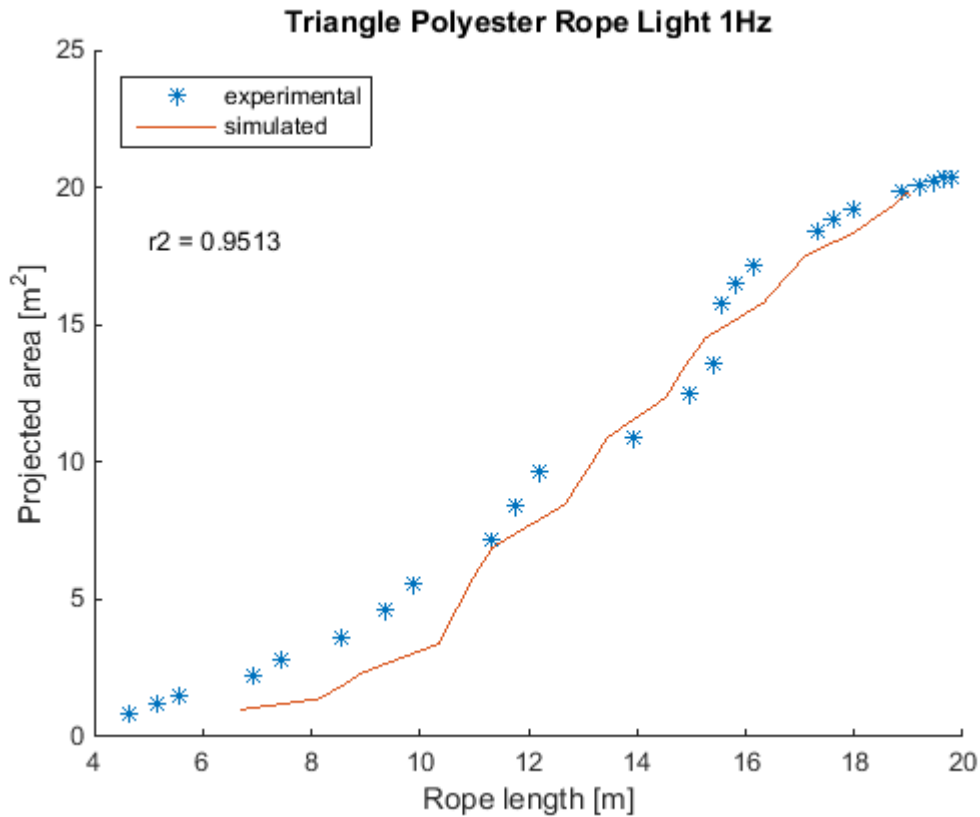


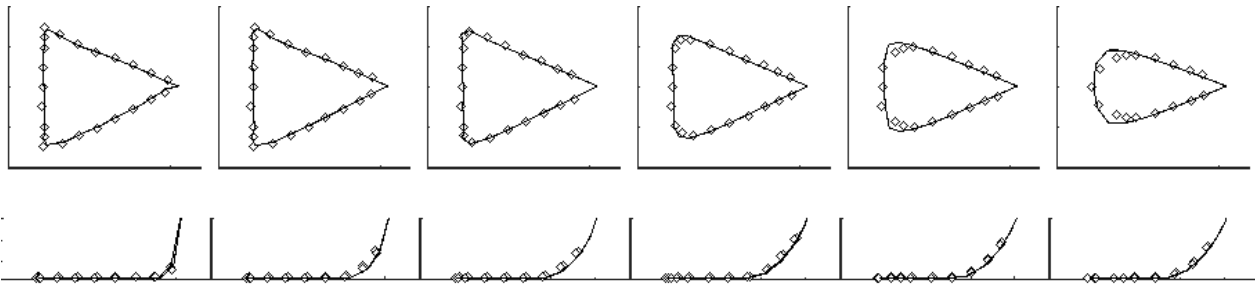
**FIGURE 78: projected area encircled by the seine ropes are plotted against the seine rope length. The star marks represent the flume tank results and the solid line the simulation.**

By using the rope length as the indicator for how far along the haul back procedure is we eliminate the effect of the experiment being imperfect (taking a small break in the hauling back). The  $R^2$  value is showing good agreement between experiment and simulation.

### 5.3.7 Polyester Rope; Heavy; Slow

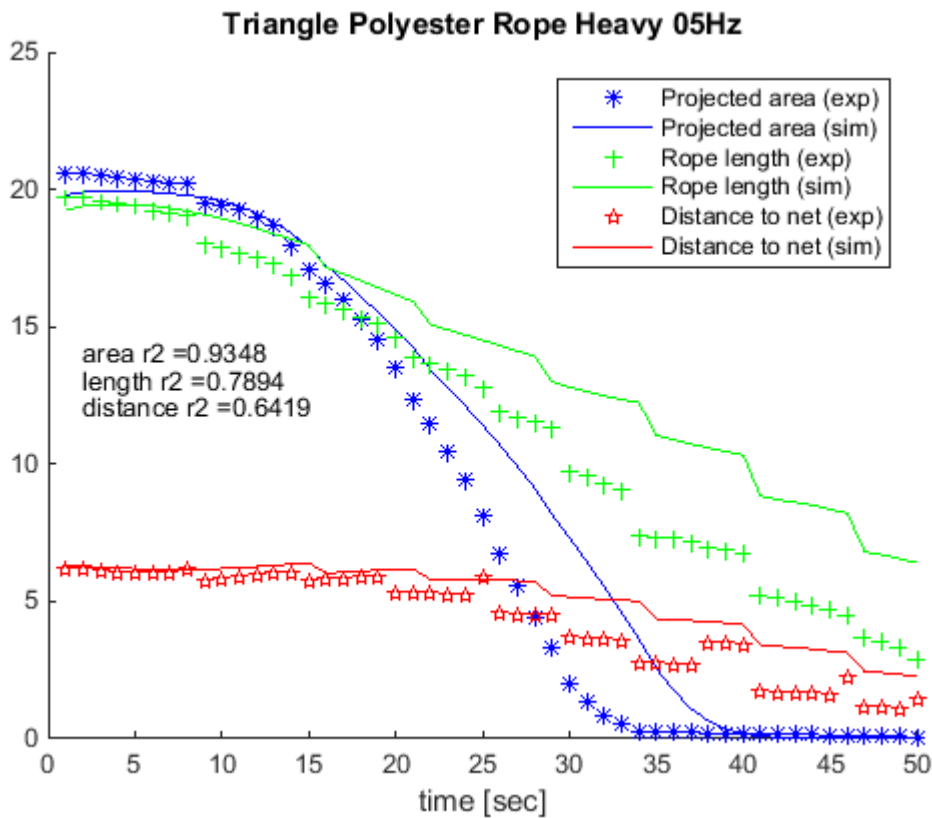
This section compares flume tank results to results from simulation for the polyester rope laid out in a triangle, using the light weight and the slow winch speed.

FIGURE 79 shows the seine rope geometry seen from above and from the side. The time step between the pictures is four seconds. The solid lines represent the simulated result. Diamond marks represent the flume tank result. The agreement between flume tank experiment and simulation is evident.



**FIGURE 79:** the geometry of the seine ropes seen from above and from the side. The six pictures are taken with four seconds interval. The diamond marks represent the flume tank results and the solid line the simulation.

FIGURE 80 plots respectively the projected area, the rope length and the distance to the net from the winch against the time.



**FIGURE 80:** shows the projected area [m<sup>2</sup>] encircled by the seine ropes, the seine rope length [m] and the distance [m] to the net from the winch plotted against time. The marks represent the flume tank results and the solid lines the simulation.

The agreement between flume tank experiment and simulation for the projected area, rope length and distance from winch to net is not evident. There seems to be synchronisation problems between the experimental haul back and the simulated haul back.

FIGURE 81 shows the rope length versus the projected area. The simulation results are presented by a solid line while the experimental data is shown by star marks.

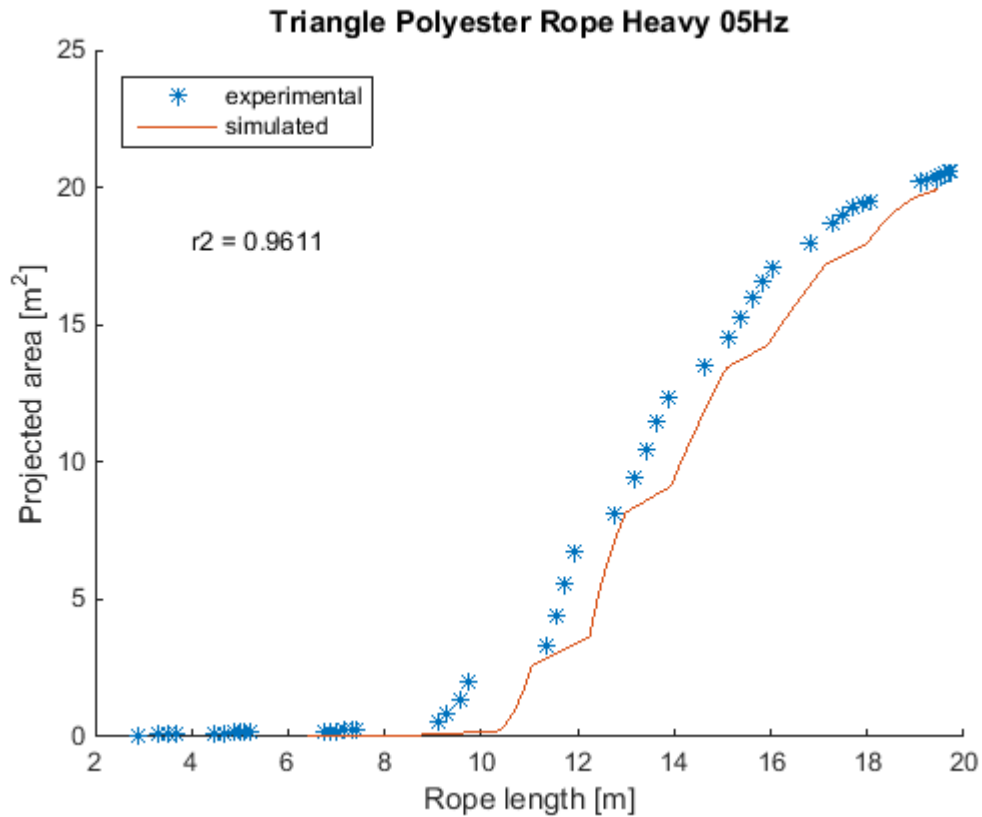


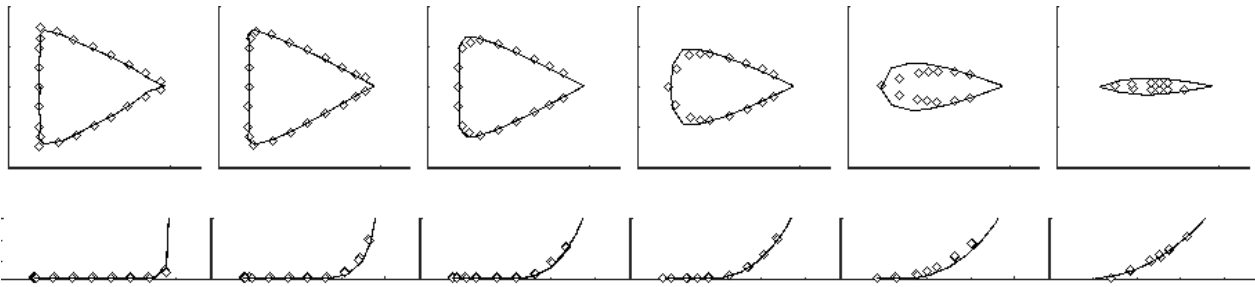
**FIGURE 81: projected area encircled by the seine ropes are plotted against the seine rope length. The star marks represent the flume tank results and the solid line the simulation.**

By using the rope length as the indicator for how far along the haul back procedure is we eliminate the effect of the experiment being imperfect (a discontinuity in the hauling back process). The  $R^2$  value is showing good agreement between experiment and simulation.

**5.3.8 Polyester Rope; Heavy; Fast**

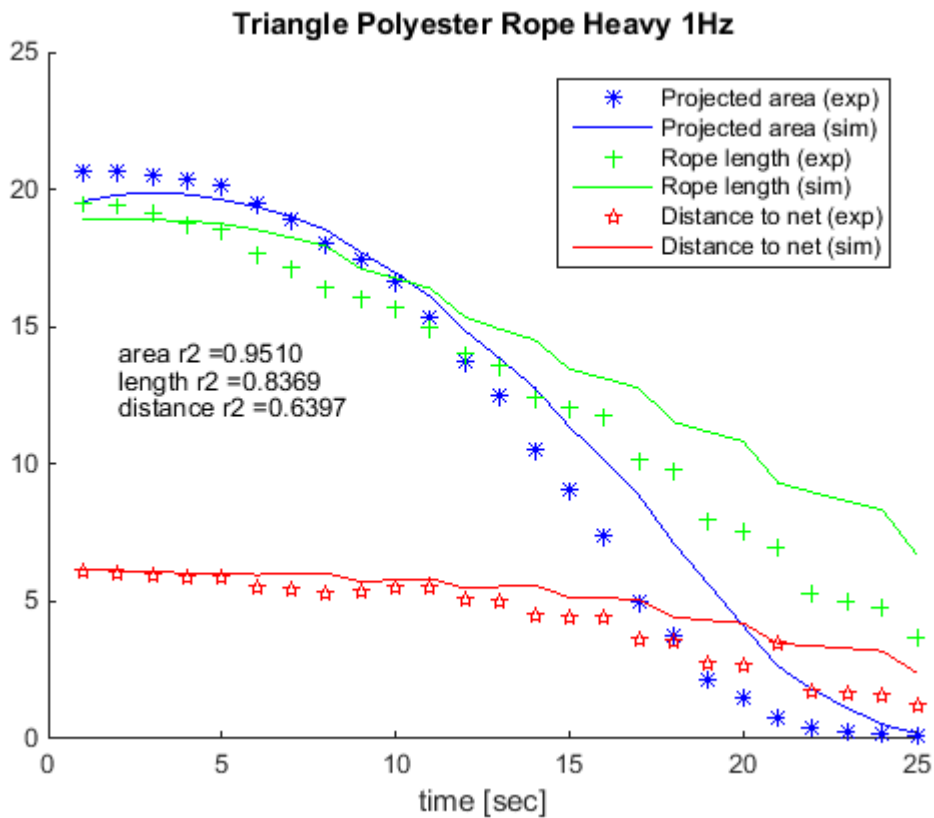
This section compares flume tank results to results from simulation for the polyester rope laid out in a triangle, using the heavy weight and the fast winch speed.

FIGURE 82 shows the seine rope geometry seen from above and from the side. The time step between the pictures is four seconds. The solid lines represent the simulated result. Diamond marks represent the flume tank result. The agreement between flume tank experiment and simulation is evident for the first part of the process, later the experimental results appear to run ahead of the simulation.



**FIGURE 82:** the geometry of the seine ropes seen from above and from the side. The six pictures are taken with four seconds interval. The diamond marks represent the flume tank results and the solid line the simulation.

FIGURE 83 plots respectively the projected area, the rope length and the distance to the net from the winch against the time.



**FIGURE 83:** shows the projected area [m<sup>2</sup>] encircled by the seine ropes, the seine rope length [m] and the distance [m] to the net from the winch plotted against time. The marks represent the flume tank results and the solid lines the simulation.

The agreement between flume tank experiment and simulation for the projected area, rope length and distance from winch to net is evident.

FIGURE 84 shows the rope length versus the projected area. The simulation results are presented by a solid line while the experimental data is shown by star marks.

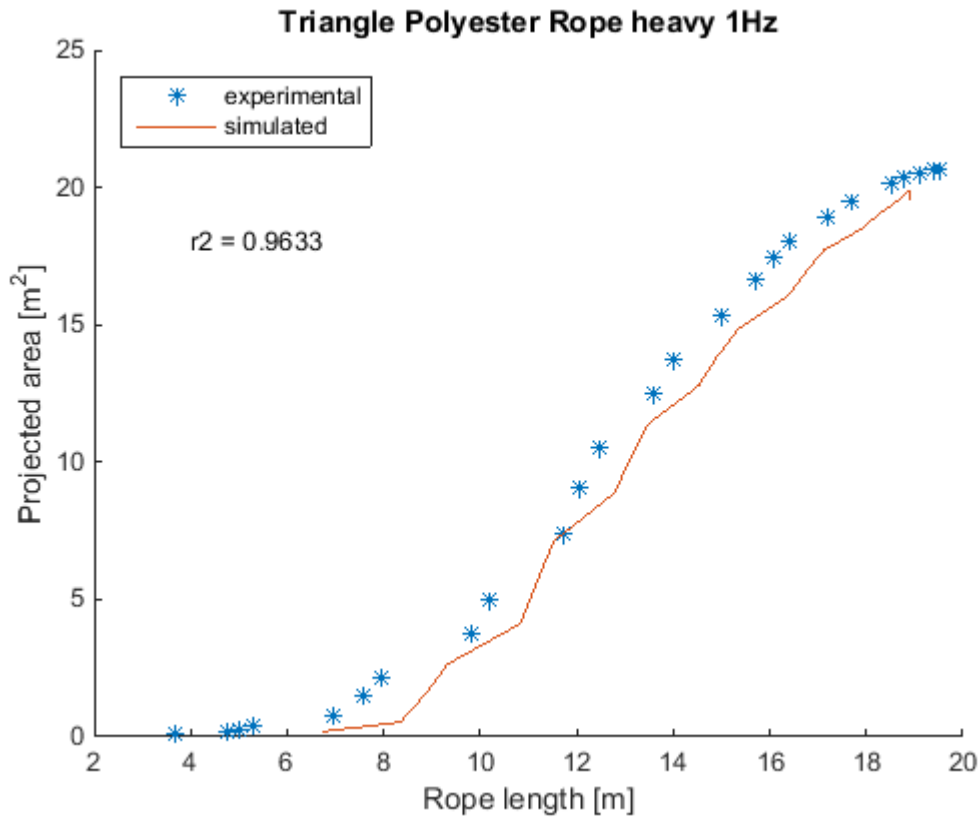


**FIGURE 84: projected area encircled by the seine ropes are plotted against the seine rope length. The star marks represent the flume tank results and the solid line the simulation.**

By using the rope length as the indicator for how far along the haul back procedure is we eliminate the effect of the experiment being imperfect (taking a small break in the hauling back). The  $R^2$  value is showing good agreement between experiment and simulation.

### 5.4 Overall Validation of the Simulation Model

Regarding the ability of the simulation model to predict the seine rope kinematics during the hauling procedure, sections 5.1 to 5.3 provided an examination for each of 24 experimentally cases conducted in the flume tank (section 4; TABLE 1) individually. The purpose of this section is to summarize all those results into an overall validation of the simulation model regarding its ability to predict seine rope kinematics. Overall most of the plots (FIGURE 13-84) in sections 5.1-5.3 did show a reasonable agreement between the flume tank results and the simulated when judged visually. This indicates that the simulation model should be fairly good at predicting the kinematics of seine ropes during haul back processes. In addition to this visual inspection we calculated the  $R^2$ -value for the ability of simulation model to predict how the size of the area encircled by the seine ropes on the seabed (flume tank floor) depends on respectively time in the haul back process and the amount of rope still not winched in at that point of the process. These  $R^2$ -values are summarized in TABLE 2.

**TABLE 2: R<sup>2</sup>-value for predicting the dependency of seine rope encircled area versus respectively time in the haul back process and respectively the length of the seine ropes not being winched in at that stage of the haul back process. R<sup>2</sup>-values are provided for each of the 24 experimental cases conducted in the flume tank.**

Layout	Rope type	Net Weight	Winch Speed	R <sup>2</sup> -value for area versus time: R <sup>2</sup> (t)	R <sup>2</sup> -value for area versus seine rope length: R <sup>2</sup> (l)
Square	Combination	light	slow	0.9978	0.9887
Square	Combination	heavy	slow	0.9844	0.9924
Square	Combination	light	fast	0.8473	0.9700
Square	Combination	heavy	fast	0.9894	0.9893
Square	Polyester	light	slow	0.9698	0.9887
Square	Polyester	heavy	slow	0.9724	0.9877
Square	Polyester	light	fast	0.9899	0.9927
Square	Polyester	heavy	fast	0.9846	0.9830
Diamond	Combination	light	slow	0.9541	0.8789
Diamond	Combination	heavy	slow	0.9793	0.8992
Diamond	Combination	light	fast	0.9558	0.9203
Diamond	Combination	heavy	fast	0.9440	0.9869
Diamond	Polyester	light	slow	0.9845	0.8216
Diamond	Polyester	heavy	slow	0.9439	0.9747
Diamond	Polyester	light	fast	0.9942	0.8746
Diamond	Polyester	heavy	fast	0.7822	0.9802
Triangle	Combination	light	slow	0.9702	0.9245
Triangle	Combination	heavy	slow	0.9910	0.9770
Triangle	Combination	light	fast	0.9470	0.9686
Triangle	Combination	heavy	fast	0.9861	0.9454
Triangle	Polyester	light	slow	0.9700	0.9344
Triangle	Polyester	heavy	slow	0.9348	0.9611
Triangle	Polyester	light	fast	0.9887	0.9513
Triangle	Polyester	heavy	fast	0.9510	0.9633
Mean value				0.9589	0.9522

From TABLE 2 it is seen that the both mean R<sup>2</sup>-values with values at respectively 0.9589 (encircled area versus time in haul back process) and 0.9522 (encircled area versus length of seine rope un-winched) are very high. This implies that on average that more than 95% of the variation found in the experimental data for the seine rope encircled area versus respectively time in the haul back process and respectively amount of seine rope not yet being winched in are actually explained by the simulation model. Considering uncertainty in the flume tank experiments a level of explanation above 95% on average must be considered as a convincing overall validation for the simulation model. However, inspecting the individual R<sup>2</sup>-values in TABLE 2 reveals some variation in results since the values ranges from 0.7822 to 0.9942 for encircled area versus time in haul back process and from 0.8216 to 0.9924 for encircled area versus length of seine rope un-winched. Only two of the 24 results were below 0.93 in R<sup>2</sup>-value for encircled area versus time. For area versus length of seine rope un-winched four R<sup>2</sup>-values of the 24 are below 0.92. Particular for the direct modelling meaning area versus time the few low R<sup>2</sup>-values could be suspected to be due to problems keeping the winch in process completely uniform during the flume tank experiment. Therefore if it is related to such experimental problems then there should not be any trend in the R<sup>2</sup>-values with respect to layout pattern, rope type, "net weight" and winch in speed. On the other hand if the R<sup>2</sup>-values would show any dependency

on layout pattern, rope type, "net weight" or winch in speed then it could be an indication on that the simulation model would have less ability to predict seine rope behaviour for some situations which then would indicate a problem with the model. To investigate if there is any such indication in the obtained set of  $R^2$ -values we examine the dependency of the  $R^2$ -value for encircled area against process time on: layout pattern (square, diamond or triangle), rope type (combination or polyester), "net-weight" (light or heavy), hauling speed (slow or fast). This investigation is the subject of the next section.

The potential dependency of the  $R^2$ -value ( $R^2(t)$ ) for the encircled area versus time on layout pattern (square, diamond or triangle), rope type (combination or polyester), "net-weight" (light or heavy), hauling speed (slow or fast) was investigated using the `lm` function in the statistical package R (version 2.15.2; [www.r-project.org](http://www.r-project.org)) using the following linear model as starting point:

$$R^2(t) = R_0^2 + \Delta diamond \times dp + \Delta triangle \times tp + \Delta rope \times hr + \Delta net \times hn + \Delta speed \times fs \quad (18)$$

In Eqn. (18)  $R_0^2$  is the  $R^2$ -value for the square layout for the polyester rope with light "net-weight" and slow hauling speed.  $\Delta diamond$  and  $\Delta triangle$  quantifies the effect of shifting from the square layout to respectively the diamond and triangle layout.  $\Delta rope$  quantifies the effect of shifting from the polyester rope to the combination rope.  $\Delta net$  quantifies the effect of shifting from the light "net weight" to the heavy.  $\Delta speed$  quantifies the effect of shifting from the slow winching speed to the high. The factors  $dp$ ,  $tp$ ,  $hr$ ,  $hn$  and  $fs$  each and independent undertake the value 0 or 1 dependent on which of the 24 investigated case is described. TABLE 3 show the values for these factors for each of the cases. Based on the using the values for  $dp$ ,  $tp$ ,  $hr$ ,  $hn$  and  $fs$  (TABLE 3) together with the value for  $R^2(t)$  (TABLE 2) in Eqn. (18) by using the `lm` function in R we investigated the significance of each of the factors layout pattern, rope type, "net weight" and hauling speed on the obtained  $R^2$ -value  $R^2(t)$ . The starting point for this analysis was the full model described by Eqn. (18) and then using backward eliminations by in each step eliminating the least significant parameter and continuing this process until all remaining parameters are at least statistical significant on a 95 % confidence level ( $p$ -value  $< 0.05$ ).

TABLE 3: values for the model factors  $dp$ ,  $tp$ ,  $hr$ ,  $hn$  and  $fs$  for each of the seine rope haul back cases (see Eqn. 18).

Layout	Rope type	Net Weight	Winch Speed	Dp	Tp	hr	hn	fs
Square	Combination	Light	slow	0	0	1	0	0
Square	Combination	Heavy	slow	0	0	1	1	0
Square	Combination	Light	fast	0	0	1	0	1
Square	Combination	Heavy	fast	0	0	1	1	1
Square	Polyester	Light	slow	0	0	0	0	0
Square	Polyester	Heavy	slow	0	0	0	1	0
Square	Polyester	Light	fast	0	0	0	0	1
Square	Polyester	Heavy	fast	0	0	0	1	1
Diamond	Combination	Light	slow	1	0	1	0	0
Diamond	Combination	Heavy	slow	1	0	1	1	0
Diamond	Combination	Light	fast	1	0	1	0	1
Diamond	Combination	Heavy	fast	1	0	1	1	1
Diamond	Polyester	Light	slow	1	0	0	0	0
Diamond	Polyester	Heavy	slow	1	0	0	1	0
Diamond	Polyester	Light	fast	1	0	0	0	1
Diamond	Polyester	Heavy	fast	1	0	0	1	1
Triangle	Combination	Light	slow	0	1	1	0	0
Triangle	Combination	Heavy	slow	0	1	1	1	0
Triangle	Combination	Light	fast	0	1	1	0	1
Triangle	Combination	Heavy	fast	0	1	1	1	1
Triangle	Polyester	Light	slow	0	1	0	0	0
Triangle	Polyester	Heavy	slow	0	1	0	1	0
Triangle	Polyester	Light	fast	0	1	0	0	1
Triangle	Polyester	Heavy	fast	0	1	0	1	1

TABLE 4 to 9 document the results of applying the above described backward elimination procedure.

TABLE 4: parameter values and p-values for significance for parameters in full model (Eqn. 18).

Model parameter	Parameter value	p-value
$R_0^2$	0.9810	<2e-16
$\Delta_{diamond}$	-0.0247	0.348
$\Delta_{triangle}$	0.0004	0.988
$\Delta_{rope}$	0.0067	0.753
$\Delta_{net}$	-0.0105	0.622
$\Delta_{speed}$	-0.0243	0.261



TABLE 5: parameter values and p-values for significance for remaining parameters after first elimination compared to the full model. \* eliminated parameter.

Model parameter	Parameter value	p-value
$R_0^2$	0.9812	<2e-16
$\Delta diamond$	-0.0249	0.264
$\Delta triangle$	*	*
$\Delta rope$	0.0067	0.746
$\Delta net$	-0.0105	0.612
$\Delta speed$	-0.0243	0.247

TABLE 6: parameter values and p-values for significance for remaining parameters after second elimination compared to the full model. \* eliminated parameter.

Model parameter	Parameter value	p-value
$R_0^2$	0.9812	<2e-16
$\Delta diamond$	-0.0249	0.253
$\Delta triangle$	*	*
$\Delta rope$	*	*
$\Delta net$	-0.0105	0.604
$\Delta speed$	-0.0243	0.236

TABLE 7: parameter values and p-values for significance for remaining parameters after third elimination compared to the full model. \* eliminated parameter.

Model parameter	Parameter value	p-value
$R_0^2$	0.9846	<2e-16
$\Delta diamond$	-0.0249	0.244
$\Delta triangle$	*	*
$\Delta rope$	*	*
$\Delta net$	*	*
$\Delta speed$	-0.0243	0.228

TABLE 8: parameter values and p-values for significance for remaining parameters after fourth elimination compared to the full model. \* eliminated parameter.

Model parameter	Parameter value	p-value
$R_0^2$	0.9710	<2e-16
$\Delta diamond$	*	*
$\Delta triangle$	*	*
$\Delta rope$	*	*
$\Delta net$	*	*
$\Delta speed$	-0.0243	0.232

TABLE 9: parameter values and p-values for significance for remaining parameters after fifths (last) elimination compared to the full model. \* eliminated parameter.

Model parameter	Parameter value	p-value
$R_0^2$	0.9589	<2e-16
$\Delta diamond$	*	*
$\Delta triangle$	*	*
$\Delta rope$	*	*
$\Delta net$	*	*
$\Delta speed$	*	*

As can be seen from the backward elimination process, TABLE 4 to 9, we end up with a model for  $R^2(t)$  only containing the intercept parameter  $R_0^2$ . This means the data does not show any evidence for dependency on the ability for the simulation model to predict the kinematic behaviour of the seine ropes during haul back on which experimental case is investigated. Based on the considerations above this means that combined with the very high mean  $R^2$ -value at 0.9589 we can be confident in the ability of the simulation model at predicting the seine rope kinematics.

## 6 Discussion & Conclusions

The purpose of the project "Danish Seine: Computer based Development and Operation" is to develop software tools to investigate Demersal Seine fishing. As part of this project this report has described a model for the physical behaviour of seine ropes for demersal seining; described the implementation of the model into a set of software tools that together enable simulation of seine rope kinematics for demersal fishing operations; and finally validated of the simulation toolbox predictions against flume tank experiments.

The dynamics of the demersal seine gear is dominated by the behaviour of the seine ropes. Hence, the numeric simulation model described in section 2.1 was developed using two cables modelling the seine ropes, attached to a weight representing the seine net. The model implemented has the cable dynamics formulated as a collection of hinged rigid bodies. A discretized cable can then be constructed by applying a constraint which imposes continuity between the endpoint, but a constraint equation will not remain satisfied as time progresses. The error of the constraint equation was eliminated by introduction of a control law, which guarantees global asymptotic stability (see section 2.1).

The model formulation for the seine ropes behaviour was implemented in the FhSim simulation framework [10]. The cables were connected to the weight at one end, representing the seine net, and to a winch at the other. The orientation of the catenary curve of the seine ropes was smoothly bended from vertical to horizontal near the bottom to avoid initializing cable segments beneath the bottom. The lump weight used to model a simple seine net was modelled as a capsule geometry and initialized at the average end point of the cables. The simulation model used an existing bottom contact model implemented in FhSim [10], which calculates a reaction force normal to the bottom from an overlap between element cylinder geometry and the flat bottom surface. Time integration was performed using a simple forward Euler scheme [11] and a time-step of  $1e-3s$ .

The rigid body implementation of the cable assumes that each element consists of a homogenous and isotropic material. This assumption is violated by the weaved structure of seine ropes and the large difference between bending and axial stiffness observed was introduced in the model by a scaling of the material stiffness. The effective material stiffness in bending was scaled linearly from the axial stiffness.

In section three the software tools implementing the seine rope model was presented.

24 cases with seine rope haul back processes, corresponding to the experiments performed in the flume tank in the autumn 2014 [13], were simulated using the model. Visual comparisons between experimental results and the corresponding simulated showed in general good agreement.  $R^2$ -values for the similarity between experimental results and the simulated were calculated for each case individually. The obtained mean  $R^2$ -values were very high ( $> 0.95$ ) meaning that on average did the predicted seine rope kinematic behaviour show excellent agreement with the results obtained during flume tank testing. Further a detailed analysis based on the obtained  $R^2$ -values was carried out to examine whether the ability of the model to predict seine rope kinematic indicated any dependency of which experimental case investigated. This analysis did not indicate any such dependency and therefore we can have confidence in using the model to predict kinematics for seine ropes during haul back procedure in general. The simulation model has therefore been validated with a positive result.

## 7 References

- [1] Norges Råfisklag 2014, "Norges Råfisklag," Available at <http://www.raafisklaget.no>, (accessed June 2014).
- [2] Sainsbury, J.C., 1996, "Commercial fishing methods - An Introduction to vessels and gears," Fishing News Books, Wiley.
- [3] Herrmann, B., Larsen, R.B., Sistiaga, M., Madsen, N.A.H., Aarsæther, K.G., Grimaldo, E., Ingolfsson, O.A., 2015, "Predicting size selection of cod (*Gadus morhua*) in square mesh codends for demersal seining: A simulation-based approach," *Fish. Res.* , DOI:10.1016/j.fishres.2015.07.015
- [4] Zienkiewicz, O. C., Taylor, R. L., Fox, D.D., 2013, "The Finite Element Method for Solid and Structural Mechanics, Seventh Edition," Butterworth-heinemann, ISBN-10: 1856176347.
- [5] Priour, D., 2015, "FEM modeling of flexible structures made of cables, bars and nets," *Maritime Transportation and Exploitation of Ocean and Coastal Resources Guides*, Soares, Garbatov and Fonseca (eds) Taylor and Francis Group, London, ISBN 0 415.39036: 2.
- [6] Driscoll, F. R. and Lueck, R. G. and Nahon, M., 2000, "Development and validation of a lumped-mass dynamics model of a deep-sea ROV system," *Applied Ocean Research*, Volume 22, Issue 3, Pages 169–182, DOI: 10.1016/S0141-1187(00)00002-X
- [7] Ramez, K., Priour, D., and Billard, J.Y., 2013, "Cable length optimization for trawl fuel consumption reduction," *Ocean Engineering* 58, pages 167-179, volume 58, DOI:10.1016/j.oceaneng.2012.10.001
- [8] Reite, K. J. 2006 "Modeling and control of trawl systems." PhD thesis, ISBN 82-471-8023-5, NTNU.
- [9] Johansen V., 2007, "Modelling of Flexible Slender Systems for Real-Time Simulation and Control Application," PhD thesis, ISBN 978-82-471-4915-7, NTNU.
- [10] Reite K. J., Føre, M., Aarsæther, K.G., Jensen, J., Rundtop, P., Kyllingstad, L. T., Endresen, P.C., Kristiansen, D., Johansen, V. and Fredheim, A., 2014, "Fhsim - Time Domain Simulation of Marine Systems." In ASME 2014 33rd International Conference on Ocean, Offshore and Arctic Engineering, volume 8A: Ocean Engineering. Ocean, Offshore and Arctic Engineering Division
- [11] Egeland, O., Gravdahl, J. T., 2002, "Modeling and simulation for automatic control," *Marine Cybernetics*, Trondheim, Norway, ISBN 82-92356-00-2.
- [12] Timoshenko, S.P., Goodier, J.N., 1982, "Theory of Elasticity," McGraw-Hill, ISBN: 07-085805-5.
- [13] Madsen, N. A.H., Herrmann B., Hansen K., Aarsæther K.G., 2014. Estimating the Physical Behaviour of Seine Ropes for Evaluating Demersal Seine Fishing. Sintef report no SINTEF A26520 ISBN 978-82-14-05775-1.



Technology for a better society

[www.sintef.no](http://www.sintef.no)